

18.353: Nonlinear Dynamics and Chaos

Prof. Matthew Durey

notes by **nambrath**

Contents

1 September 1, 2020	6
1.1 Flows on the line: 1D systems	6
2 September 3, 2020	12
2.1 Linear stability analysis	12
2.2 Potentials	15
2.3 Numerical methods	16
2.3.1 Euler's methods	16
2.3.2 Trapezium rule	17
2.3.3 Improved Euler method	17
2.3.4 Fourth order Runge-Kutta method	18
2.4 Existence and uniqueness theorem	18
3 September 8, 2020	19
3.1 Saddle-node bifurcation	20
3.1.1 Bifurcation diagrams	21
3.1.2 A more general equation	21
3.2 Transcritical bifurcation	23
4 September 10, 2020	26
4.1 Supercritical pitchfork bifurcation	26
4.2 Subcritical pitchfork bifurcation	30
4.3 A mechanical example	31
5 September 15, 2020	35
5.1 Imperfect bifurcations and catastrophes	35
6 September 17, 2020	41

6.1	Ghosts and bottlenecks	44
7	September 22, 2020	47
8	September 24, 2020	52
8.1	Complex eigenvalues	55
8.2	Regime diagram	56
9	September 29, 2020	57
9.1	Numerical implementation	57
9.2	Fixed points and linearization	59
10	October 1, 2020	63
10.1	Conservative systems	66
10.2	Reversible systems	70
11	October 6, 2020	72
11.1	The index of a closed curve	72
11.1.1	Properties of the index of a curve	74
11.2	Index of a fixed point	75
12	October 8, 2020	78
12.1	Ruling out limit cycles	81
12.1.1	Lyapunov functions	83
12.1.2	Dulac's criterion	84
12.2	Poincaré–Bendixson theorem	85
13	October 13, 2020	86
13.1	Liénard's theorem	89
13.2	Relaxation oscillators	91
13.3	Weakly nonlinear oscillators	93

14 October 20, 2020	94
14.1 Weakly damped van der Pol oscillator	97
14.2 Bifurcations in 2D systems	98
14.2.1 Saddle-node bifurcations	98
15 October 22, 2020	101
15.1 Global bifurcations	106
15.2 Generic scaling laws	108
16 October 27, 2020	109
16.1 Analyzing the Lorenz equations	111
16.2 Sensitivity to initial conditions	113
17 October 29, 2020	115
17.1 Synchrony of chaotic systems	119
18 November 3, 2020	121
19 November 5, 2020	128
19.1 Period doubling	130
19.2 Lyapunov exponent	131
19.3 Universality	133
20 November 10, 2020	134
20.1 Feigenbaum's observations	135
20.2 Feigenbaum's approach	136
21 November 12, 2020	140
21.1 Countable and uncountable sets	140
21.2 The Cantor set	142
21.3 Dimension of self-similar fractals	144

21.4 Similarity dimension	145
22 November 17, 2020	146
22.1 Cantor set – abstraction	146
22.2 Box dimension	146
22.3 Pointwise and correlation dimension	148
22.4 Strange attractors	150
23 November 19, 2020	151
24 December 1, 2020	155
24.1 Attractor reconstruction	155
24.2 Practical issues	157
24.3 Non-autonomous systems	159
25 December 3, 2020	162

1 September 1, 2020

Linear ODEs are relatively straightforward. Nonlinear equations on the other hand, are more complicated:

$$m \frac{d^2x}{dt^2} + b \left(\frac{dx}{dt} \right)^2 + kx = F(t)$$

Here the drag is dependent on the square of the speed.

Chaotic dynamics: “when the present determines the future, but the approximate present does not approximately determine the future” according to E. Lorenz.

In other words, when the long-term dynamics of a system are highly sensitive to the initial conditions. All chaotic systems are described by nonlinear equations, but not all nonlinear equations yield chaotic dynamics.

1.1 Flows on the line: 1D systems

We'll be looking at equations of the form:

$$\frac{dx}{dt} = f(x(t)), \quad x(0) = x_0$$

$x(t)$ must be real-valued, and $f(x)$ must be smooth and real.

A word on notation: \dot{x} means a time derivative.

This equation is an **autonomous** system, because it has no explicit time-dependence. (If it did, the RHS should have been $f(x(t), t)$).

Example.

Consider a Newtonian system described by the following second order ODE: $m\ddot{x} + b\dot{x} = F(x)$

The LHS is inertia and drag, and on the RHS is some applied force on the particle. We assume that inertia is small compared to the drag: $|m\ddot{x}| \ll |b\dot{x}|$.

Then we can neglect inertia, and we get the “**overdamped**” approximation:

$$\dot{x} = \frac{F(x)}{b}$$

This is a first-order ODE, so we see the motivation for studying 1D flows.

Canonical system: $\dot{x} = f(x)$, $x = x(t)$, and $x(0) = x_0$.

If $f(x)$ is linear, like $f(x) = x + 1$, this is a straightforward equation to solve: $\dot{x} - x = 1$.

But we are interested in the *nonlinear* case. Let's try: $f(x) = \sin(x)$.

Then we have:

$$\frac{dx}{dt} = \sin(x(t))$$

How do you solve this? One option is to use separation of variables. You get:

$$t(x) = \log \left| \frac{\csc(x_0) + \cot(x_0)}{\csc(x(t)) + \cot(x(t))} \right|$$

Nominally this is correct, but it's also incredibly hard to interpret its dynamics!

Let's try a graphical method. See Fig. 1.

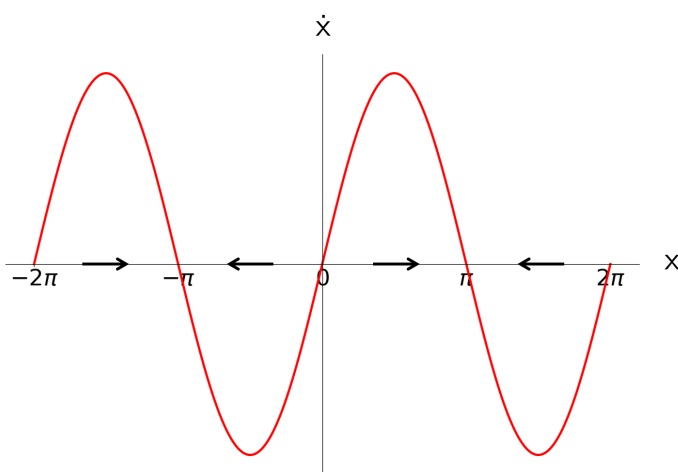


Figure 1: x and \dot{x}

For $0 < x < \pi$, \dot{x} is positive. This means that x is increasing over time. This is also the case for $-2\pi < x < -\pi$.

For $-\pi < x < 0$ and $\pi < x < 2\pi$, $\dot{x} < 0$. So x is decreasing with time and the flow is to the left.

At x_* at which $\sin(x_*) = 0$, we have $\dot{x} = 0$. These are **equilibrium or fixed points** of the dynamical system. In this case, if you start near the fixed point $x_* = 0$ (on either side), you can see from the graph that you will be propelled away from it. This makes $x_* = 0$ a **repelling fixed point**. By periodicity, $x = 0, \pm 2\pi, \pm 4\pi, \dots$ are all repelling fixed points. You can see from the diagrams that the **attracting fixed points** are $x = \pm\pi, \pm 3\pi, \dots$

Repelling fixed points are also called **unstable**, and attracting fixed points are called **stable**.

How does this system evolve in time? Let's try another graphical approach (Fig. 2).

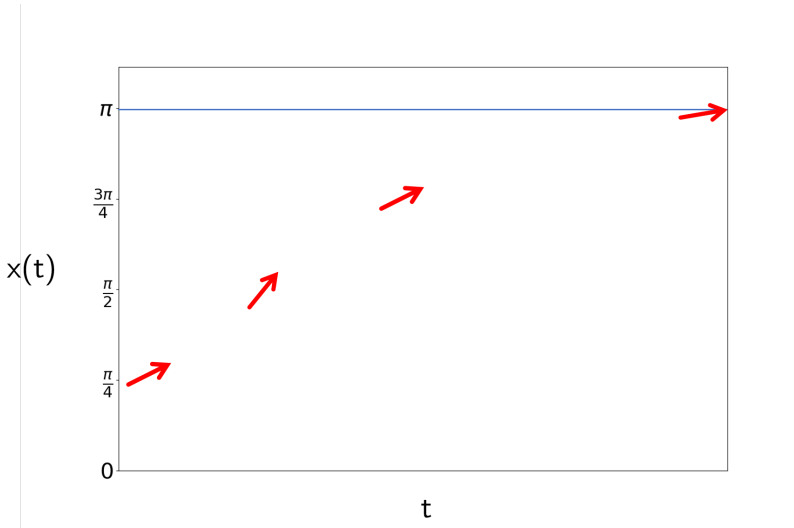


Figure 2: A trajectory.

Since π is an attracting fixed point, at large t the system will approach π .

At the start, $x_0 = \pi/4$. The slope there is $\dot{x} = \sin(\pi/4) \sim 0.7$. When $x = \pi/2$, the slope is 1. So it gets steeper there. At $x = 3\pi/4$, the slope is ~ 0.7 again. We can fill in the curve to get an idea of the shape.

This doesn't give us any information about the times at which any of these changes occur, though.

Example.

Is it possible for trajectories to intersect?

Let's define intersection (at some $t = t_0$) more mathematically:

$$x_1(t_0) = x_2(t_0) \quad \dot{x}_1(t_0) \neq \dot{x}_2(t_0)$$

Well, $\dot{x}_1 = f(x_1)$, and $\dot{x}_2 = f(x_2)$ – but the RHS are both the same at $t = t_0$. This means the LHS are equal, and $\dot{x}_1 = \dot{x}_2$. This is a contradiction: **trajectories cannot cross**.

Example.

$$\dot{x} = f(x) = x^2 - 1 = (x - 1)(x + 1)$$

We have fixed points at $f(x_*) = 0$, so our fixed points are $x_* = \pm 1$.

See Fig. 3 for a plot of x and \dot{x} .

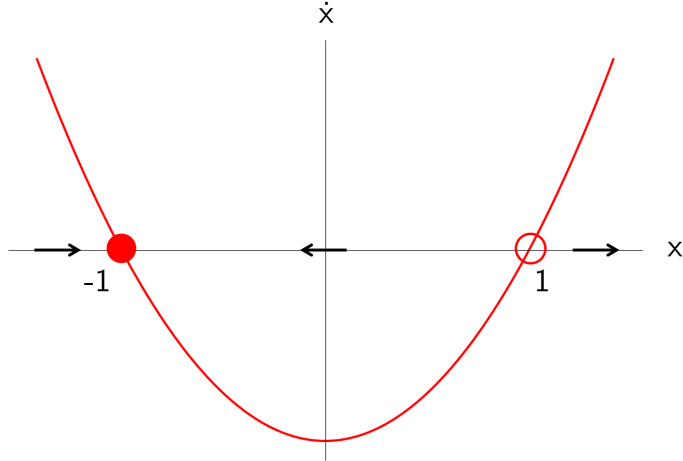


Figure 3: x and \dot{x} .

A word on notation. Filled-in circle: stable/attracting, open circle: unstable/repelling.

When $x > 1$, \dot{x} is positive so x is increasing. Between -1 and 1 , \dot{x} is negative so x is decreasing. For $x < -1$, x is increasing. We can see that $x = -1$ is *stable* and $x = 1$ is *unstable*.

Example.

$$\dot{x} = f(x) = x - \cos(x)$$

We need to find the fixed points: $f(x_*) = 0 \implies x_* = \cos(x_*)$. This needs a numerical solution, we can't do it analytically.

We're going to plot some slightly different things this time: $y = x$ and $y = \cos(x)$. Where they intersect, we have a fixed point. Where one curve is above/below the other, we can decide which direction the flow goes in. See Fig. 4.

The fixed point is pretty clear as the intersection of the two curves. For $x > x_*$, $x > \cos(x)$ so \dot{x} is positive and the flow is to the right. For $x < x_*$, the opposite is true and the flow is to the left. So the fixed point is *unstable*.

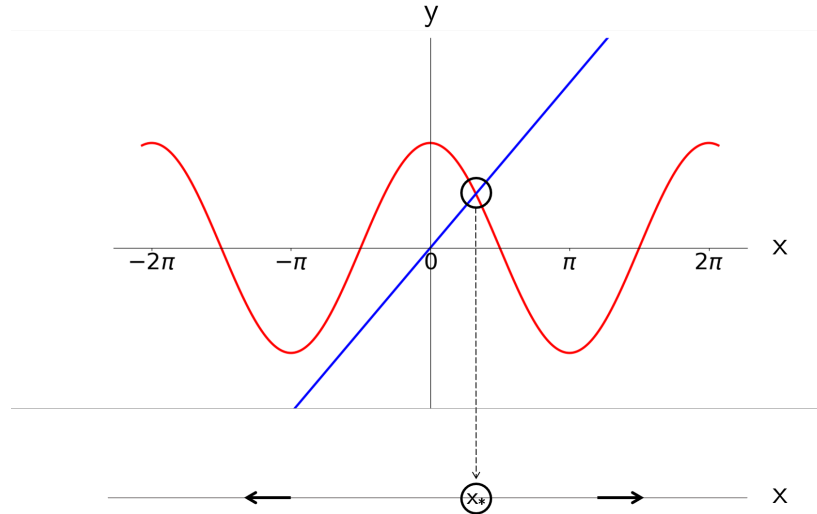


Figure 4: y and x , and what it means for 1D flow in x .

Example.

$$\dot{x} = f(x) = 1 - x$$

See Fig. 5.

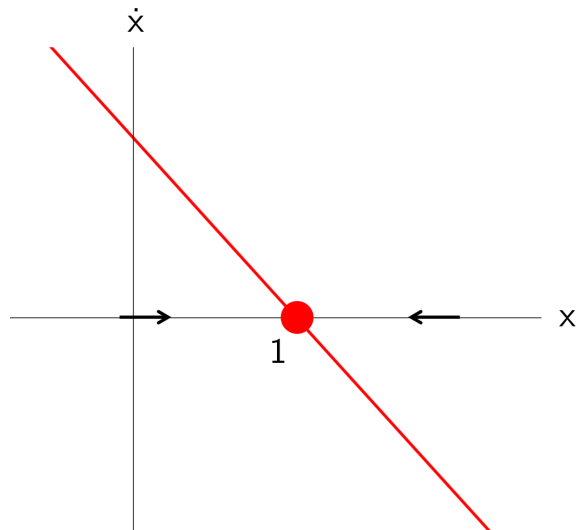


Figure 5: x and \dot{x} .

Our fixed point is $x = 1$. For $x > 1$, the flow is to the left, and for $x < 1$, the flow is to the right – $x_* = 1$ is *stable*.

This is an example with **global stability**. No matter what point you start at, all trajectories approach $x_* = 1$ as $t \rightarrow \infty$.

Example.

Application to population models (**logistic growth**).

Our criteria:

- $N(t) \geq 0$ population
- For small populations: $dN/dt = rN$, where r is the growth rate.
- For larger populations, we have a “carrying capacity” K
- We want $\dot{N} < 0$, $N > K$ and $\dot{N} > 0$, $N < K$.

Consider a simple model:

$$\frac{dN}{dt} = rN \left(1 - \frac{N}{K}\right) = f(N)$$

For $N \ll K$, the second term in the parentheses vanishes and we get exponential growth, basically. For larger N , that term becomes much more significant.

See Fig. 6 for a plot.

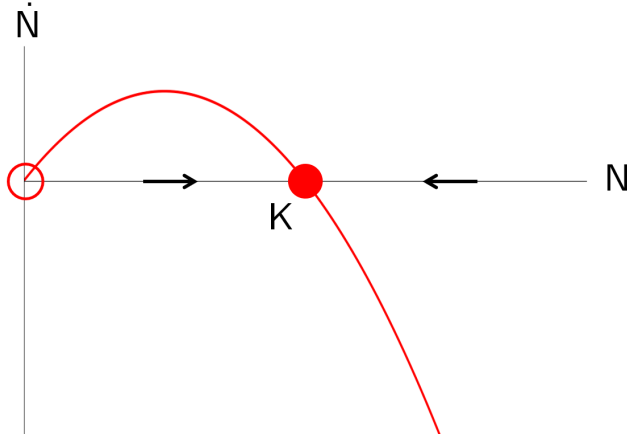


Figure 6: x and \dot{x} .

Our fixed points are at $N_1 = K$ and $N_0 = 0$. Since $f(N)$ is a negative quadratic, the curve is easy to draw. For $0 < N < K$, N is increasing. For $N > K$, N is decreasing. So $N_1 = K$ is a *stable fixed point*, and $N_0 = 0$ is *unstable*.

When is the population growing the fastest? From the plot, we can see that \dot{N} is largest at $K/2$, so the population is growing at the highest rate then.

We can try to plot some more trajectories, see Fig. 7.

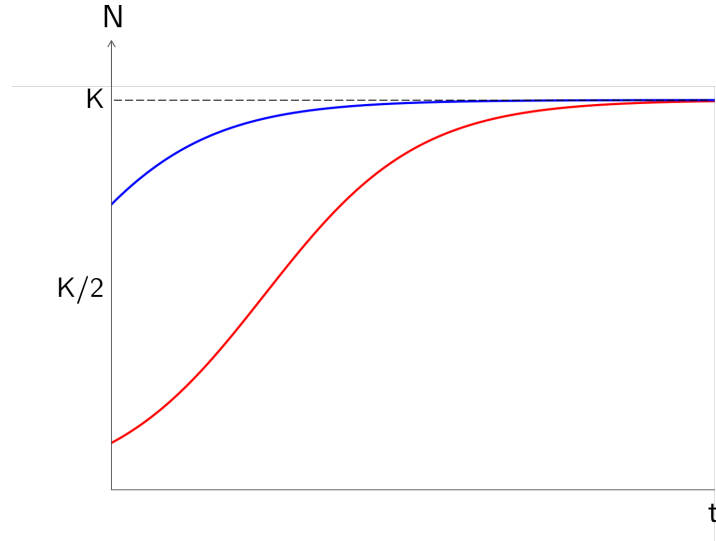


Figure 7: $N(t)$ trajectories.

2 September 3, 2020

Prof. Durey emphasizes that even though his t-shirt says otherwise, he's often wrong.

Last time we looked at graphical approaches. Today we're doing to try to get some quantitative information about flows on a line.

We left off last time with logistic growth. For small populations, we have exponential growth. As the population grows larger, the nonlinear term dominates. The plot of \dot{N} and N contains a **velocity field** and a **phase portrait**. The velocity field is essentially the arrows we're drawing on the axis to show the direction of flow, while the phase portrait shows us trajectories in $\dot{N} - N$ space.

We've established what the fixed points are for this system, but we don't really know what things look like near the fixed points. In order to gain some insights into those nearby trajectories, we can zoom in without having to solve the entire differential equation.

2.1 Linear stability analysis

We want to gain quantitative information about trajectories $x(t)$ in the vicinity of a fixed point x_* . A reminder of the canonical form: $\dot{x} = f(x)$.

Suppose that for some $f(x)$, we can find what the fixed point x_* is. At x_* , the velocity is 0 so $f(x_*) = 0$.

Consider $x(t) = x_* + \eta(t)$, where $\eta \ll 1$ is a small perturbation. We can substitute this into the canonical differential equation:

$$\frac{d}{dt}(x_* + \eta(t)) = f(x_* + \eta(t))$$

Well, x_* is a constant, so when we differentiate we get:

$$\dot{\eta} = f(x_* + \eta)$$

Now we can Taylor expand, since we know η is small.

$$\dot{\eta} \simeq f(x_*) + \eta f'(x_*) + O(\eta^2)$$

The quadratic error terms can then be neglected, since they're small. We also have $f(x_*) = 0$, so

$$\dot{\eta} \simeq \eta f'(x_*)$$

This gives us an approximation that is a *linear* equation:

$$\dot{\eta} = r\eta, \quad r = f'(x_*)$$

Solving this is straightforward, and we get

$$\eta(t) = \eta(0)e^{rt}$$

Why did we start all this? We want to find out if the fixed point is stable or unstable.

- If $r < 0$, then $\eta(t) \rightarrow 0$, and x_* is attracting. Then x_* is a **linearly stable fixed point**.
- If $r > 0$, then $\eta(t)$ blows up, and x_* is repelling. Then x_* is a **linearly unstable fixed point**.

Our approximation for η is pretty good for $r < 0$, because the higher-order terms get smaller and smaller. But for $r > 0$, the error terms get huge with time, and the approximation becomes invalid.

There's one case we haven't yet considered: $r = 0$. In that case, $\eta(t)$ seems like it's constant. What's going on here? Well, the equation we're actually solving in this case is $\dot{\eta} = O(\eta^2)$, so we need to worry about the quadratic terms and we no longer have a linear equation. This method doesn't work, and we would need a different approach.

Example.

$$\text{Logistic growth: } f(N) = rN \left(1 - \frac{N}{K}\right)$$

Looking at Figure 6, we see that f' near $x_* = 0$ is positive, so it's an unstable fixed point. Similarly, near $x_* = K$, we see that f' is negative, so it's a stable fixed point.

The benefit of the linear stability analysis here is that $\frac{1}{|r|}$ defines a timescale for growth/decay of perturbations.

Example.

(Linear stability fails.)

1. $f(x) = x^3$

2. $f(x) = x^2$

In the first case, $f'(0) = 0$ so we have a fixed point at the origin. We can solve this graphically, but because $r = 0$, we have no information about the timescale. See Figure 8.

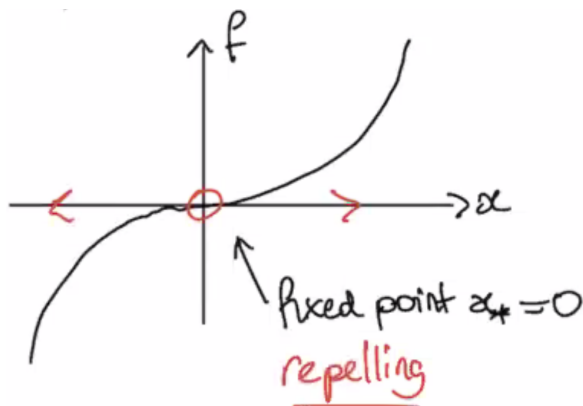


Figure 8: Case 1.

In the second case, we have really essentially the same thing. But the nature of the fixed point is different: it's **half-stable**. See Figure 9.

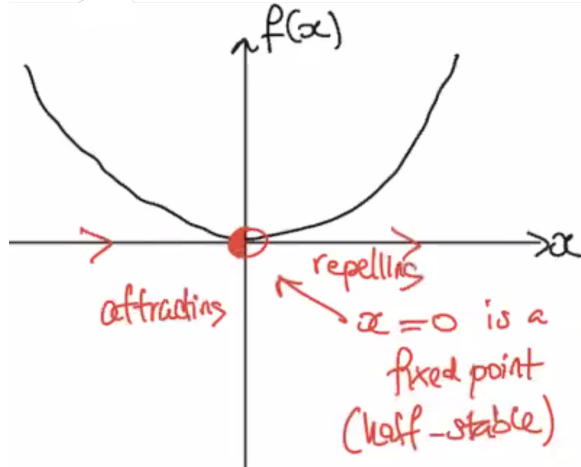


Figure 9: Case 2.

2.2 Potentials

Now we consider special cases of f . Define a **potential function** $V(x)$ to satisfy

$$f(x) = -\frac{dV}{dx}(x)$$

Note: Once we have found a V for a given f , we may always add a constant to V and there is no change in the dynamics.

$$\dot{x} = f(x(t)) \rightarrow \dot{x}(t) = -V'(x(t))$$

(The prime means d/dx .)

How does $V(x(t))$ change along trajectories? Consider $\frac{d}{dt}V(x(t))$, the time derivative of V . Time for chain rule shenanigans!

$$\frac{d}{dt}V(x(t)) = \frac{dV}{dx}(x(t)) \frac{dx}{dt}(t) = V'(x(t)) \dot{x}(t)$$

Using the definition above of the equation, this is equal to $-\dot{x}^2(t)$

So the time derivative of V is ≤ 0 for all time, and equal to 0 only at fixed points. This means that the particle goes “downhill” on the potential, giving us the dynamics in Figure 10. At the bottom of the potential is our fixed point $x = x_*$, and $V'(x_*) = 0$. It is a stable fixed point.

Figure 11 shows the double-well potential. It has two stable fixed points and one unstable fixed point, shown in Figure 11.

Can we have oscillations in a potential? If you have gradient-driven motion, where the motion is driven by the slope of the potential, it turns out that you *cannot* have oscillations. Remember, oscillations require going up the

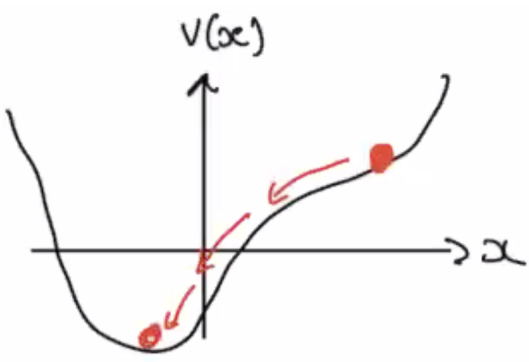


Figure 10: Going downhill.

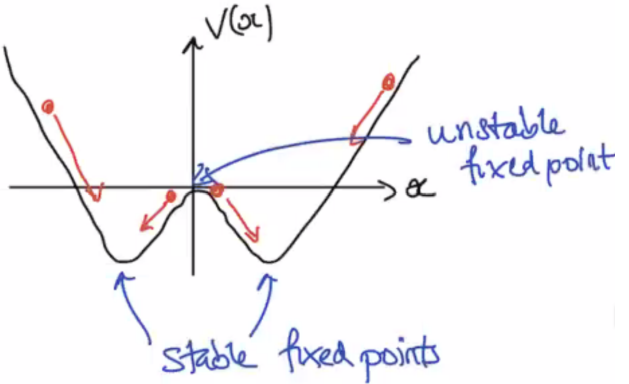


Figure 11: The double well.

well past the fixed point, but potentials restrict us to downhill motion. So there's some intuition there.

2.3 Numerical methods

Consider our equation $\dot{x} = f(x(t))$, $x(0) = x_0$. In order to things numerically, we introduce a timestep $h > 0$ ($h \rightarrow 0$). Define $t_n = nh$.

We want to approximate our solution at these times t_n , because computationally we can't do it continuously. We want $x(t_n) \approx x_n$ – we're looking for a **numerical approximation**.

2.3.1 Euler's methods

From calculus, we have

$$\int_{t_n}^{t_{n+1}} dt \implies x(t_{n+1}) - x(t_n) = \int_{t_n}^{t_{n+1}} f(x(t)) dt$$

We're looking for the area under a curve like in Figure 12.

We'll approximate this area as $hf(x(t_n))$. The **explicit scheme** is

$$x_{n+1} = x_n + hf(x_n)$$

We call it explicit because it uses information only about x_n .

The **implicit scheme** uses information from the future:

$$\int_{t_n}^{t_{n+1}} f(x(t)) dt \approx hf(x(t_{n+1})) \implies x_{n+1} = x_n + hf(x_{n+1})$$

This is complicated, because x_{n+1} is dependent on information about itself.

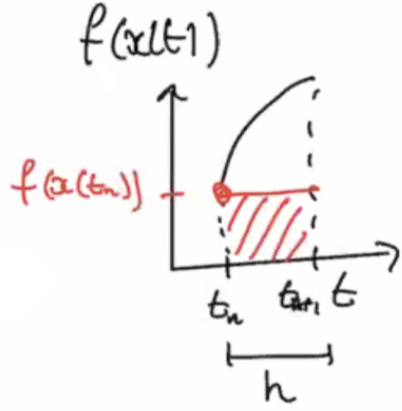


Figure 12: The explicit scheme.

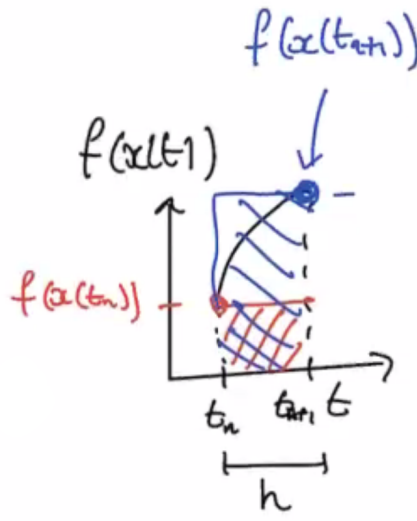


Figure 13: The implicit scheme.

As $h \rightarrow 0$, these two schemes need to converge. They both have $O(h)$ accuracy, meaning if you halved your timestep you would also halve your error. So error $\propto h$.

2.3.2 Trapezium rule

These approximations both use rectangles. We can improve the approximation with a trapezoid. The **trapezium rule**:

$$\int_{t_n}^{t_{n+1}} f(x(t)) dt \approx \frac{h}{2} [f(x(t_n)) + f(x(t_{n+1}))]$$

$$x_{n+1} = x_n + \frac{h}{2} [f(x_n) + f(x_{n+1})]$$

This is a much better approximation, with $O(h^2)$ accuracy. Halving the timestep gives a factor of 4 improvement in error. However, the trapezium rule is still an implicit scheme, because it's also dependent on x_{n+1} .

2.3.3 Improved Euler method

This motivates a predictor-corrector method. The idea is to predict x_{n+1} using an explicit Euler scheme, and then correct it using the trapezium rule. This has two stages, and is part of a class of **Runge-Kutta** methods.

- *Explicit Euler.* $\bar{x}_{n+1} = x_n + hf(x_n)$.
- *Trapezium rule.* $x_{n+1} = x_n + \frac{h}{2} [f(x_n) + f(\bar{x}_{n+1})]$

This is an explicit method, which is nice, and it also has $O(h^2)$ accuracy!

2.3.4 Fourth order Runge-Kutta method

This is also a predictor-corrector approach, but with four stages. The stages are chosen cleverly to give us an $O(h^4)$ method.

Let's define four quantities:

$$\begin{aligned}k_1 &= hf(x_n) \\k_2 &= hf\left(x_n + \frac{k_1}{2}\right) \\k_3 &= hf\left(x_n + \frac{k_2}{2}\right) \\k_4 &= hf(x_n + k_3)\end{aligned}$$

Then:

$$x_{n+1} = x_n + \frac{1}{6}[k_1 + 2k_2 + 2k_3 + k_4]$$

The Süli and Mayers book goes over a derivation of this and why its accuracy is so good.

2.4 Existence and uniqueness theorem

Consider the problem $\frac{dx}{dt} = f(x(t))$, $x(0) = x_0$.

Suppose that $f(x)$ and $f'(x)$ are continuous on the open interval R where $x_0 \in R$, as shown in Figure 14. Then the problem has a solution on some interval $t \in (-\tau, \tau)$ and the solution is unique.

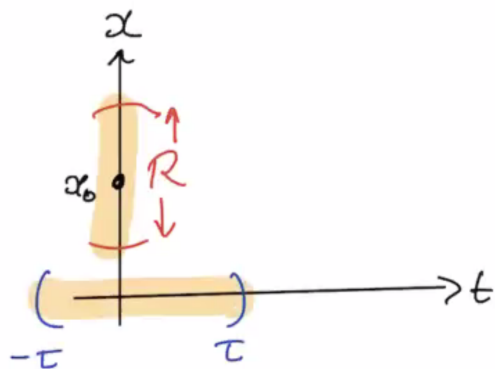


Figure 14: The setup

Let's look at some examples where the theorem doesn't work – where the function isn't nice enough.

Example.

(Non-uniqueness.) Consider $\dot{x} = x^{1/3}$, $x(0) = 0$.

$x(t) = 0$ is the trivial solution, but separation of variables also gives us $x(t) = (2t/3)^{3/2}$. In fact, there are infinitely many solutions to this equation.

Why aren't we guaranteed uniqueness here? Well, $x^{1/3}$ is continuous about $x = 0$, but $f'(x) = \frac{1}{3}x^{-2/3}$ which has an asymptote at $x = 0$. So there's a discontinuity in $f'(x)$, so we don't satisfy the conditions for the theorem.

Example.

(Finite-time existence.) Consider $\dot{x} = -\frac{1}{2x}$, $x(0) = x_0 \neq 0$.

Solving this,

$$\begin{aligned} 2x\dot{x} &= -1 \\ \frac{d}{dt}(x^2) &= -1 \\ x^2(t) &= x_0^2 - t \\ x(t) &= x_0 \sqrt{1 - \frac{t}{x_0^2}} \end{aligned}$$

This is greater than 0 for $t < x_0^2$, but when $t = x_0^2$ we get $\dot{x} = -\infty$. We can't solve the equation any more, because the theorem only guarantees a solution on some interval. The derivative blows up in finite time, so we don't have a solution everywhere.

3 September 8, 2020

We want to determine the qualitative changes in the system dynamics (the form of the vector field) as we vary a **control parameter** (i.e a coefficient in the differential equation). What changes are we considering?

- creation/destruction of fixed points
- change in stability of a fixed point

Think of pushing something across a table. As you increase the force, the object changes from not moving to sliding. This is a clear example of a varying parameter leading to different dynamics.

3.1 Saddle-node bifurcation

The **saddle-node bifurcation** is also referred to as the turning point bifurcation, the fold bifurcation, or the blue sky bifurcation.

This is associated with the creation/destruction of a pair of fixed points as the parameter varies.

Here is the “normal form” or “prototypical example”. Let $x(t)$ be our variable, and r be the (real) parameter.

$$\dot{x} = r + x^2$$

We want to see how r varies the stability and existence of fixed points.

If we want two fixed points, we need $\dot{x} = 0$, so $r < 0$. If $r = 0$, we have a pair of fixed points at $r = 0$. If $r > 0$, we can't have any fixed points.

Let's draw the vector field for these three cases. See Figure 15.

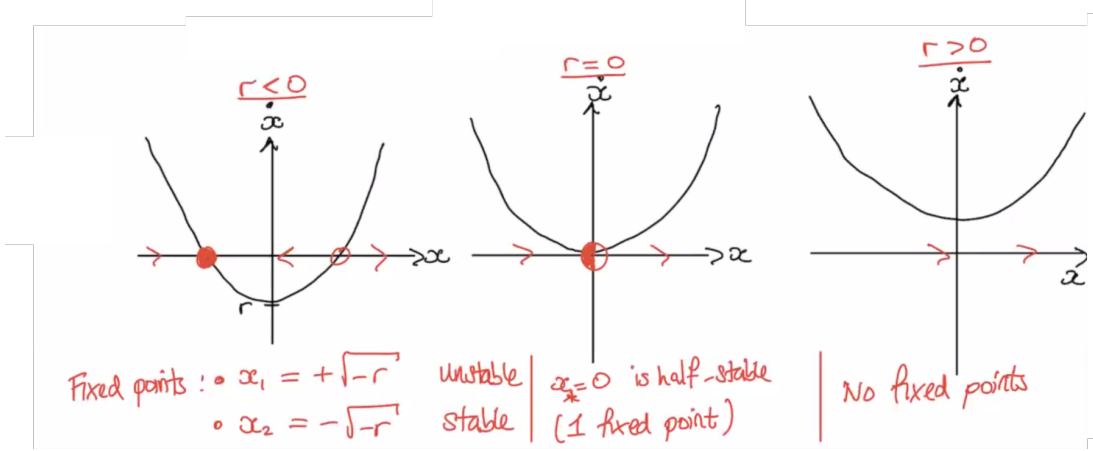


Figure 15: Vector fields.

When $r < 0$, we have a positive parabola and the y -intercept is negative, so we have two fixed points. The negative fixed point $x_1 = -\sqrt{-r}$ is stable, and the other at $x_2 = \sqrt{-r}$ is unstable.

When $r = 0$, the parabola passes through the origin. Linear stability analysis fails for this example, but considering it graphically, we have $\dot{x} > 0$ always, so the flow is always to the right. This gives us semi-stability for the fixed point at $x_* = 0$.

When $r > 0$, the parabola is always above the x -axis and we have no fixed points. Flow is always to the right.

3.1.1 Bifurcation diagrams

Now let's explore the qualitative change at $r = 0$. As we increase r , we see that the two fixed points collide and annihilate each other. For this, we use a **bifurcation diagram**, shown in Figure 16.

We plot r on the horizontal axis, and the fixed points x_* on the vertical axis. We use a dashed line for unstable fixed points, and a solid line for stable fixed points.

We can supplement the bifurcation diagram with flow arrows (drawn in green), to show the direction of the flow as we vary r .

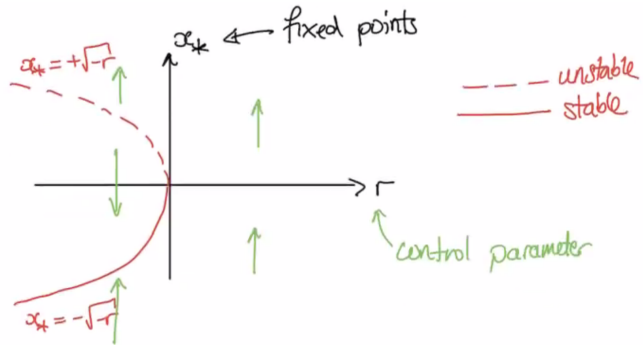


Figure 16: Bifurcation diagram.

3.1.2 A more general equation

Consider $\dot{x} = f(x; r)$. (The semicolon means that r is a parameter.) Figure 17 shows an example of one such f .

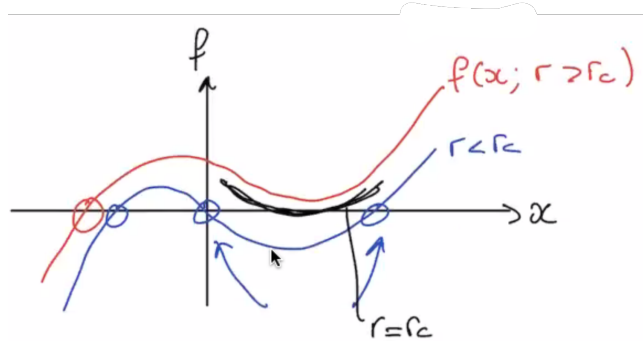


Figure 17: A general example.

We only have one fixed point when $r > r_c$. When we vary $r < r_c$, we see that two new fixed points are created. This is exemplary of a saddle-node. Between the two examples is $r = r_c$ (drawn in black). In the neighborhood of r_c when f touches the axis, the function can be Taylor expanded as a parabola and we can recover the canonical form discussed above. So this is quite a general tool.

Example.

$$\dot{x} = f(x; r) = r - x - e^{-x}$$

Find $r = r_c$ at which we have a saddle-node bifurcation.

Let us plot two functions: $y = r - x$ and $y = e^{-x}$. The intersections of the two curves are the fixed points. See Figure 18 for the vector field for different values of r .

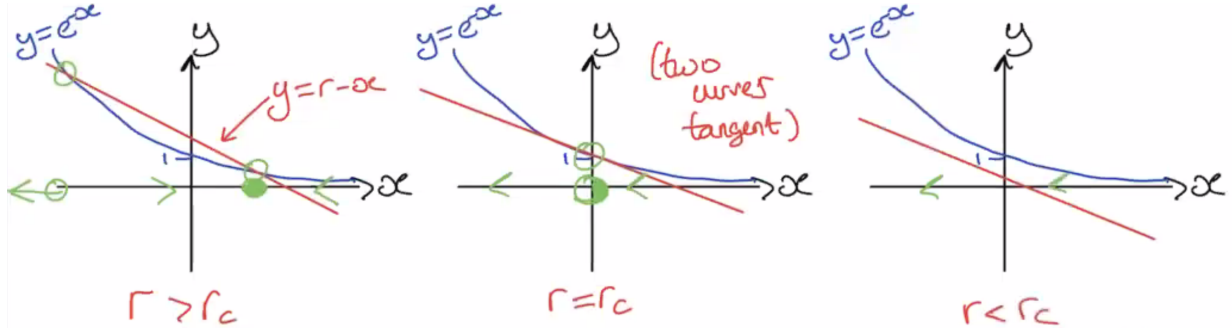


Figure 18: Vector fields.

For $r > r_c$, we have two fixed points. At large x , the blue curve is above the red curve so \dot{x} is negative. Between the fixed points, the flow is to the right. As $x \rightarrow -\infty$, the flow is to the left. So the positive fixed point is stable, and the negative fixed point is unstable.

As we decrease r , at some point the straight line will be tangent to the blue curve – when $r = r_c$. Then we only have one fixed point, which will be semi-stable. Since \dot{x} is negative everywhere, the flow is to the left.

For $r < r_c$, we have no fixed points and the flow is always to the left.

To find r_c , we need $y = r - x$ and $y = e^{-x}$ to intersect tangentially at x_* . We want:

1. $r_c - x_* = e^{-x_*}$
2. $\frac{d}{dx}(r_c - x)|_{x=x_*} = \frac{d}{dx}(e^{-x})|_{x=x_*}$

The second requirement is for the tangent requirement. We can solve:

$$\begin{aligned} -1 &= -e^{-x_*} \\ \implies 1 &= e^{-x_*} \iff x_* = 0 \end{aligned}$$

Next we must solve for r_c . The first requirement gives:

$$\begin{aligned} r_c &= x_* + e^{-x_*} \\ r_c &= 0 + 1 \\ r_c &= 1 \end{aligned}$$

So we have a saddle-node bifurcation at $r = 1$. For $r > 1$ there are two fixed points. At $r = 1$ there is one half-stable fixed point. For $r < 1$ there are no fixed points.

3.2 Transcritical bifurcation

This situation involves an interchange of stability between two fixed points at $r = r_c$.

The normal form here is

$$\dot{x} = rx - x^2$$

Note that we can write this as $x(r - x)$, so our fixed points are $x_0 = 0$ and $x_1 = r$ for all values of r .

Let's consider some cases again. See Figure 19.

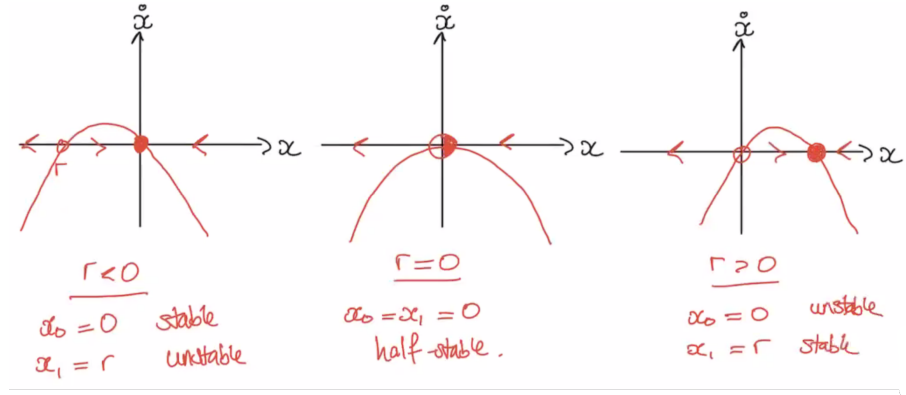


Figure 19: Vector fields.

When $r < 0$, the fixed point at $x_0 = 0$ is stable and the other is unstable. When $r = 0$, the fixed point at $x_0 = x_1 = 0$ is half-stable. When $r > 0$, the fixed point at $x_0 = 0$ is unstable and the other is stable.

As we went through $x_0 = 0$, we had an exchange of stability. We can draw a bifurcation diagram for this. See Figure 20.

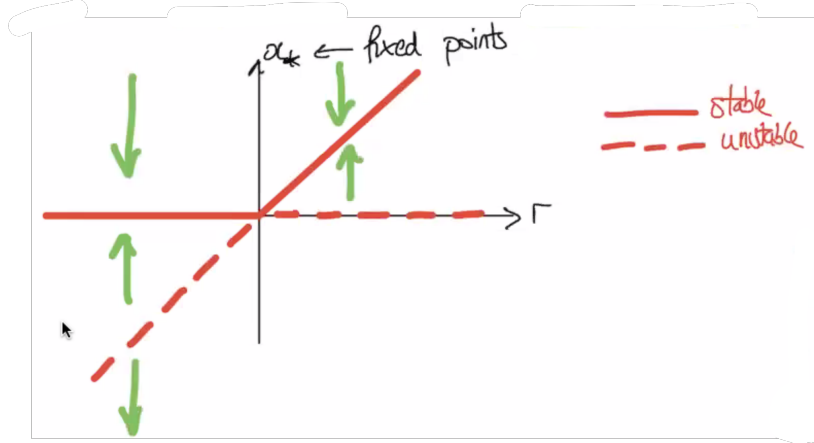


Figure 20: Bifurcation diagram.

Example.

$$\dot{x} = r \log(x) + x - 1$$

Observe that for any value of r , $x_0 = 1$ is a fixed point.

If we were to have a transcritical bifurcation, we expect that the exchange of stability will happen around $x_0 = 1$. Let's zoom in around $x = 1$.

Consider $x = 1 + u$, with $|u| \ll 1$.

Substitute this into the original equation.

$$\frac{d}{dt}x = \frac{d}{dt}(1 + u) = \dot{u} = r \log(1 + u) + u$$

We can Taylor expand the logarithm around 1.

$$\begin{aligned}\dot{u} &= r \left[u - \frac{1}{2}u^2 + O(u^3) \right] + u \\ &= (1 + r)u - \frac{r}{2}u^2 + \text{cubic terms}\end{aligned}$$

We will ignore the cubic terms. We keep the quadratic terms in order to apply the transcritical bifurcation work.

In the normal form above, r was on the linear term but not the quadratic term. Here we have r on the quadratic term as well. So to get around this, we rescale u and the small perturbation. We use

$$u = \alpha X(t)$$

where α is to be determined. We can substitute this in to get

$$\alpha \dot{X} \approx (1 + r) \alpha X - \frac{r\alpha^2}{2} X^2$$

We can cancel out factors of α , and we are left with

$$\dot{X} = (1 + r) X - \frac{r\alpha}{2} X^2$$

We are getting close to the canonical form because we can choose α to be whatever we want. We can choose it so that the quantity $r\alpha/2 = 1$, i.e $\alpha = 2/r$.

Then we can define $R = r + 1$. Finally, we have

$$\dot{X} \approx RX - X^2$$

and this is the approximate canonical form of a transcritical bifurcation at $R = 0$. So $r = -1$ is the critical value.

Example.

$$\dot{x} = x(r - e^x)$$

There is clearly a fixed point at $x_0 = 0$. The other fixed point is at $x_1 = \log(r)$ when $r > 0$.

Note: at $r = 1$, $x_1 = x_0 = 0$.

We can now draw a bifurcation diagram. As $x \rightarrow \infty$, then $\dot{x} \sim -xe^x < 0$. As $x \rightarrow -\infty$, then $\dot{x} \sim rx > 0$. So the flow is always towards the origin.

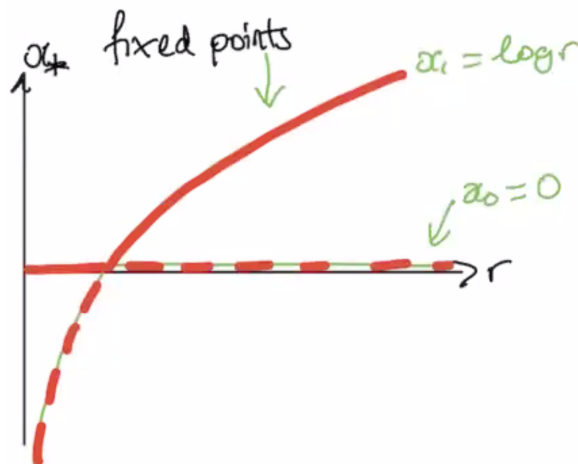


Figure 21: Bifurcation diagram.

4 September 10, 2020

Today we're going to be looking at **pitchfork bifurcations**, which are associated with systems that possess symmetry. There are two kinds we'll look at today: the **supercritical** bifurcation, and the **subcritical** bifurcation.

4.1 Supercritical pitchfork bifurcation

The normal form here is

$$\dot{x} = rx - x^3$$

where r is a real parameter. This is symmetric because if you swap x to $-x$, you recover the same thing.

When r goes from negative to positive, we expect a change – without the nonlinear term we'd see a transition from exponential growth to decay.

First let's consider $r < 0$ (Figure 22). There will only be one real root, so we'll get a negative cubic curve with one stable fixed point at $x = 0$.

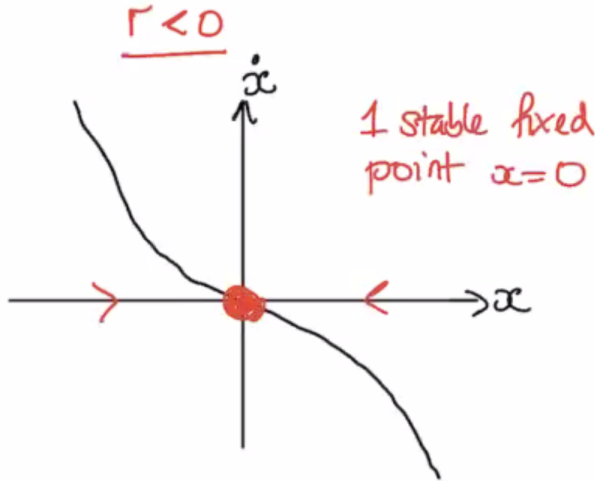


Figure 22: $r < 0$.

When $r = 0$, we still only have one fixed point, but the curve is flatter near the origin. See Figure 23.

When $r > 0$, we add two more fixed points. The flow changes direction between fixed points, so $x = 0$ is unstable, and the new fixed points at $\pm\sqrt{r}$ are stable.

Note that we've gone from 1 to 3 fixed points (not 0 to 2, as in the saddle-node case), and that the fixed points are symmetric.

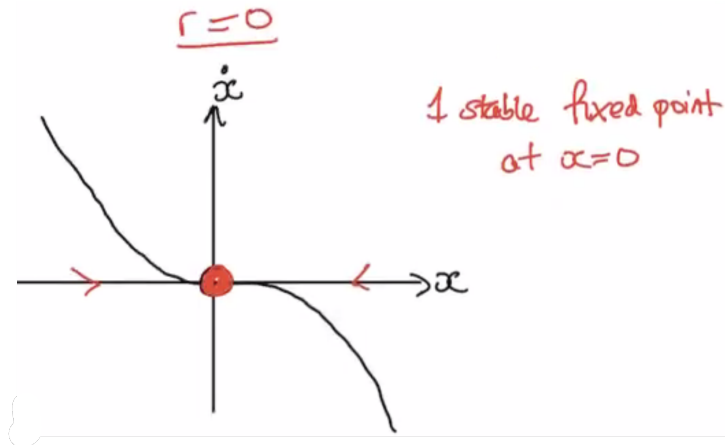


Figure 23: $r = 0$.

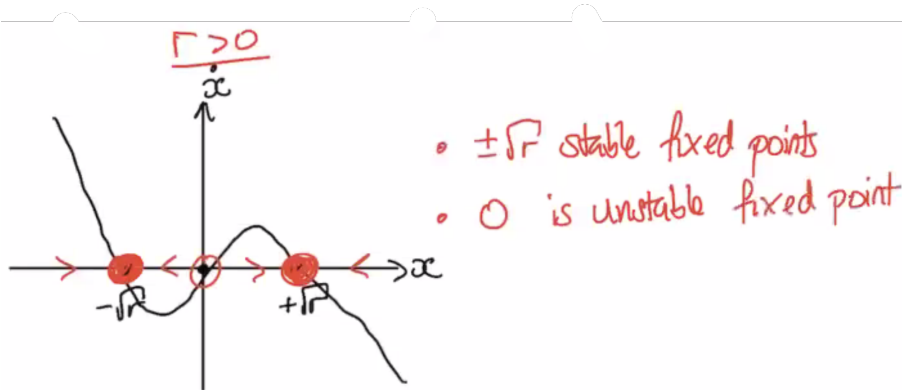


Figure 24: $r > 0$.

We can draw a bifurcation diagram for this. See Figure 25. It's pretty clear why it's called a pitchfork bifurcation.

Example.

$$\dot{x} = -x + \beta \tanh(x), \text{ where } \tanh(x) = \frac{\sinh(x)}{\cosh(x)} = \frac{e^x - e^{-x}}{e^x + e^{-x}}.$$

Remember that $\tanh(x)$ is odd, so \dot{x} is an odd function of x . Then we have the same x to $-x$ symmetry that we did with the cubic above.

Some properties of \tanh :

- $\frac{d}{dx} \tanh(x) = 1 - \tanh^2(x)$, so $\frac{d}{dx} \tanh(x) |_{x=0} = 1$

- $\tanh(x) \rightarrow \pm 1$ as $x \rightarrow \pm\infty$

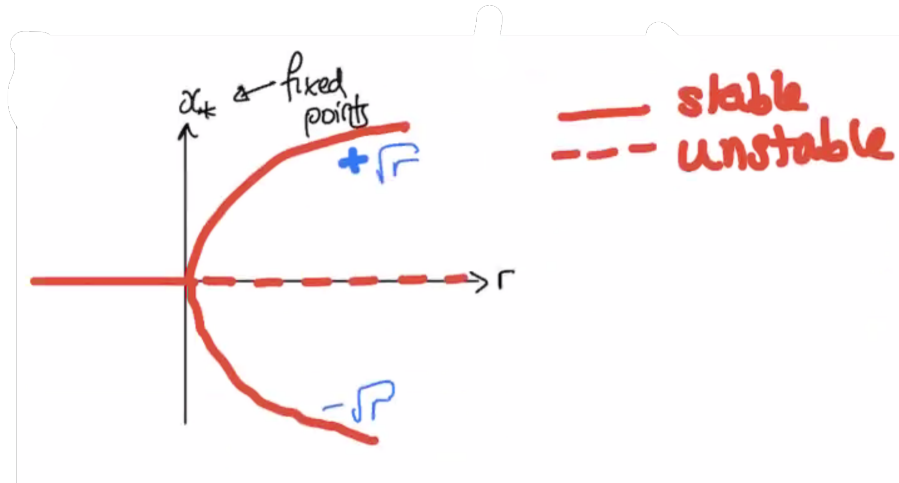


Figure 25: Bifurcation diagram for the cubic normal form.

Let's rewrite the equation as

$$\dot{x} = \beta \left[\tanh(x) - \frac{x}{\beta} \right]$$

Let's look at $y = \tanh(x)$ and $y = x/\beta$.

As usual, we'll look at a few different cases. We'll look at $\beta < 1$, $\beta = 1$, and $\beta > 1$. We use 1 because that's the slope of the tanh curve at the origin, so that's where we expect the tangent point to be for the two y curves.

When $\beta < 1$, the slope of the line $y = x/\beta$ is steeper than $\tanh(x)$, so we only have one intersection (i.e fixed point) at the origin. This fixed point is stable. See Figure 26.

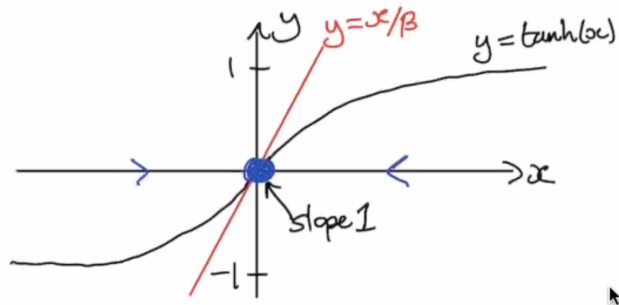


Figure 26: $\beta < 1$.

When $\beta = 1$, the two curves have the same slope. We have essentially the same situation, only the x/β curve is tangent at the origin instead of so steep.

When $\beta > 1$, the straight line is shallower and we have three intersections

between the straight line and the $\tanh(x)$ curve. Two more fixed points emerge. At large x , the linear term dominates and flow is to the left. The flow direction alternates as we go through each fixed point, so we can fill in the flow to get the result shown in Figure 27. The fixed point at the origin is unstable, and the other two fixed points $\pm x_*$ are stable.

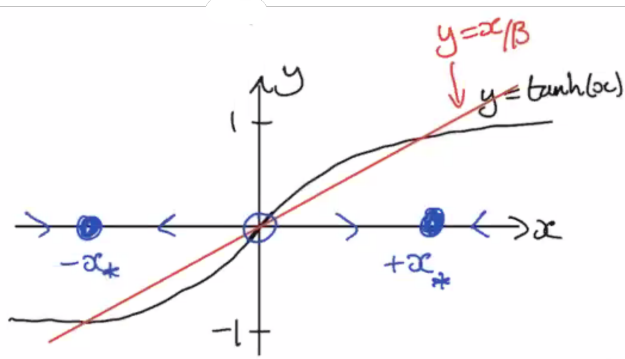


Figure 27: $\beta > 1$.

We can expand the fixed points $\pm x_*$ using a Taylor expansion for $\beta = 1 + \epsilon$. This gives us the square root shape near the bifurcation, giving the pitchfork form near $\beta = 1$. We have our equation $\dot{x} = -x + \beta \tanh(x)$, so $x_* = \beta \tanh(x_*)$. Instead of some complicated root-finding methods, we can plot

$$\beta(x_*) = \frac{x_*}{\tanh(x_*)}$$

As $x_* \rightarrow \infty$, this quantity is about x_* and we have a linear relationship. So we get the curve in Figure 28.

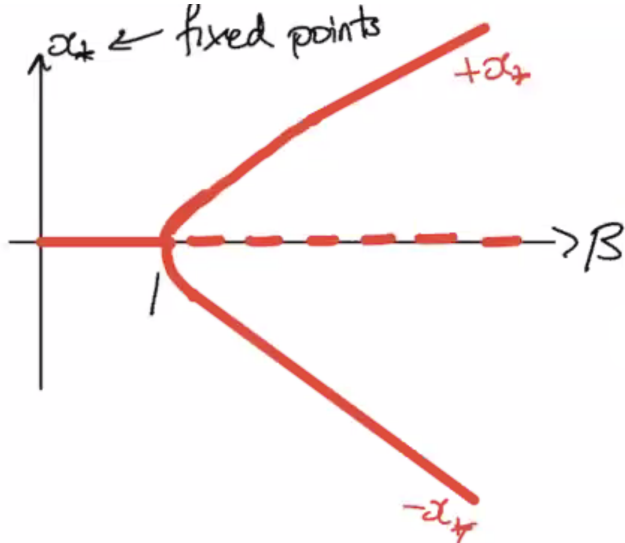


Figure 28: Bifurcation diagram for $\tanh(x)$ example.

There's a supercritical pitchfork bifurcation at $\beta = 1$.

4.2 Subcritical pitchfork bifurcation

The normal form is

$$\dot{x} = rx + x^3$$

The cubic term is no longer stabilizing! The change in sign means it is now destabilizing. When x is positive, \dot{x} is positive and we get growth.

Skipping past the details, we can draw a bifurcation diagram. We don't get the new fixed points when r is positive, but rather when it is negative. The fixed point at the origin behaves the same, but the pitchfork is flipped. See Figure 29.

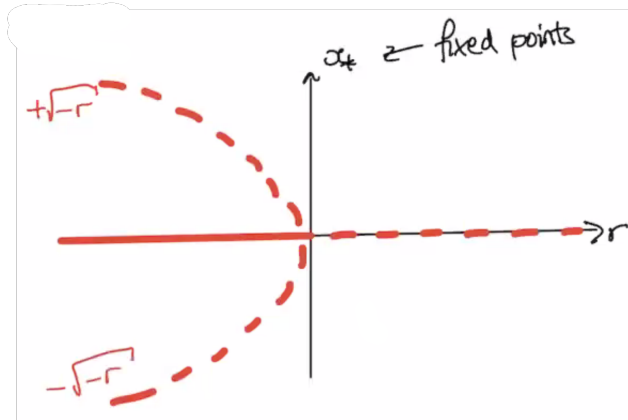


Figure 29: Subcritical pitchfork bifurcation.

Strogatz describes this as the two unstable fixed points “squeezing” the stable one as r increases.

In finite time, $x \rightarrow \infty$. This blow-up is unphysical. To fix this, we modify the normal form to add a stabilizing term.

$$\dot{x} = rx + x^3 - x^5$$

The x^5 term keeps the symmetry that characterizes these systems while adding a stabilizing effect.

Let's draw the bifurcation diagram for this. We can rewrite the normal form as $x(r + x^2 - x^4)$. The nonzero fixed points satisfy

$$r(x_*) = x_*^4 - x_*^2 = x_*^2(x_*^2 - 1) = x_*^2(x_* - 1)(x_* + 1)$$

We can plot $r(x_*)$ instead of trying to find the actual fixed points.

Nothing changes for the origin, really – the cubic term was already small, and the quintic term is even smaller. The overall shape is a sideways “W” (because $r(x_*)$ has a quadratic shape).

Around $x = 0$, we expect the cubic term to dominate, so we have the left-facing unstable pitchfork from the subcritical case. But as r becomes more negative, the quintic term becomes more important and we have a turning point at some critical r_c . There's a saddle-node bifurcation when it turns around – two new fixed points appear – and there is a change in stability!

Take a look at Figure 30.

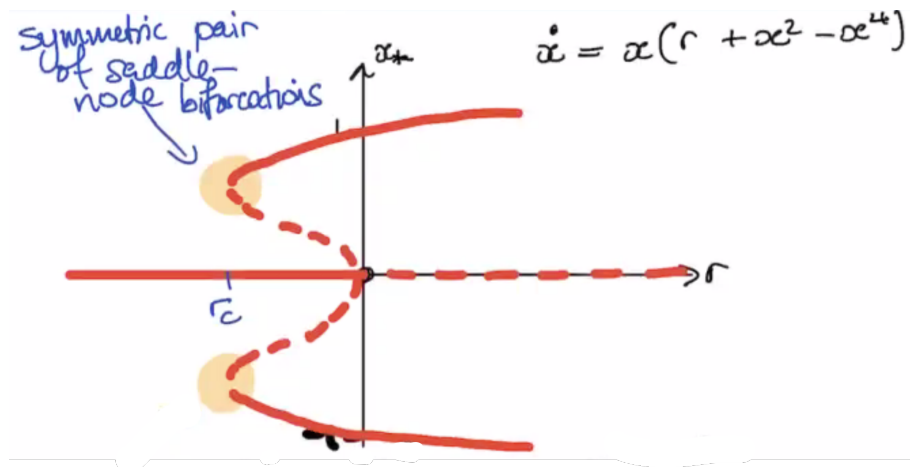


Figure 30: The hysteresis loop pitchfork bifurcation.

This is called a **hysteresis loop**. Increasing r will send x from 0 to one of the saddle-node fixed points, because those are the only stable ones. As we dial r down to r_c , we'll see that x jumps from the upper branches back to the origin. So it's not reversible! The jump happens at 0 and r_c , depending on which direction you're changing r .

4.3 A mechanical example

Example.

Consider an overdamped bead on a rotating hoop.

Figure 31 is a diagram to visualize the situation. The hoop of radius r is rotating at some angular frequency ω . The bead makes an angle ϕ with the center of the hoop.

The bead is being acted on by gravity, so that's a force of mg . There's some friction acting on the bead, acting as a linear drag proportional to the angular velocity. The friction has a magnitude of $b\dot{\phi}$, and is tangential to the hoop.

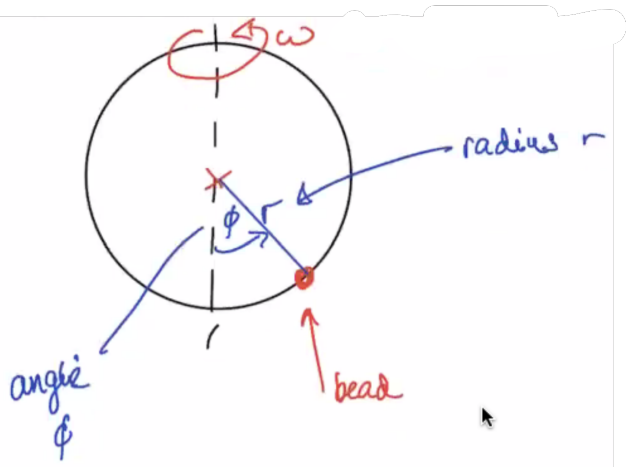


Figure 31: A diagram of the hoop.

The last force is an outwards centrifugal force of magnitude $m\rho\omega^2$, where $\rho = r \sin \phi$ is the radius of the spinning. We need to project the centrifugal force onto the line tangential to the hoop. That component of the force is $m\rho\omega^2 \cos \phi$.

Similarly, we can project gravity along this line. The component tangent to the hoop is $mg \sin \phi$.

See Figure 32 for a force diagram with all of these.

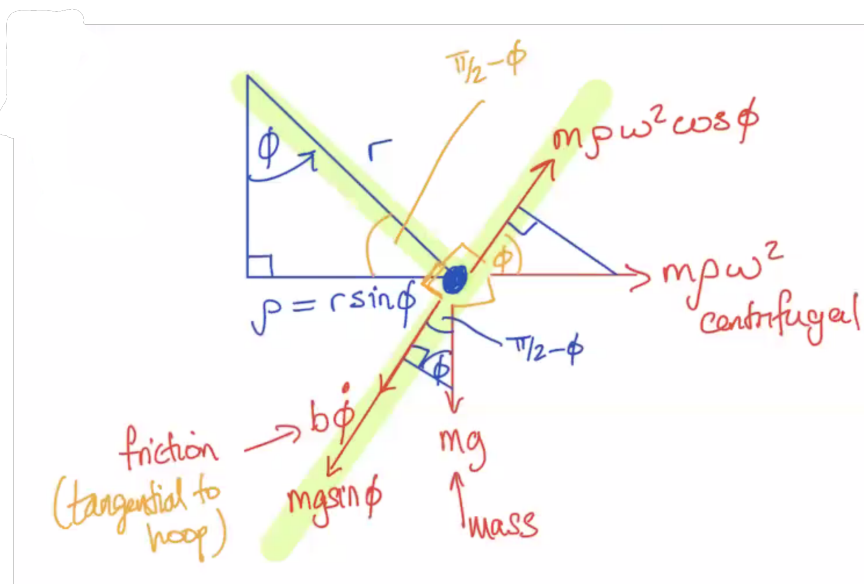


Figure 32: A force diagram for the bead.

Now we can use Newton's second law to write an equation.

$$\begin{aligned} mr\ddot{\phi} &= -b\dot{\phi} - mg \sin \theta + m\rho\omega^2 \cos \phi \\ &= -b\dot{\phi} - mg \sin \phi + mr\omega^2 \sin \phi \cos \phi \end{aligned}$$

Now we'll consider the "overdamped limit" – the regime in which inertia is weak compared to drag. Then,

$$b\dot{\phi} = mg \sin \phi \left[\frac{r\omega^2}{g} \cos \phi - 1 \right]$$

Let's define a parameter γ .

$$\gamma = \frac{r\omega^2}{g} \quad \gamma \text{ is dimensionless acceleration}$$

What are the fixed points of this system? For all $\gamma > 0$, we have $\phi = 0, \pi$ as fixed points.

When $\gamma > 1$, the entire term in brackets can be cancelled, so there are fixed points $\pm\phi_*$ that satisfy $\cos \phi_* = 1/\gamma$. There are two because \cos is an even function of ϕ .

We can plot $y = 1/\gamma$ and $y = \cos \phi$ to see what's going on here. See Figure 33.

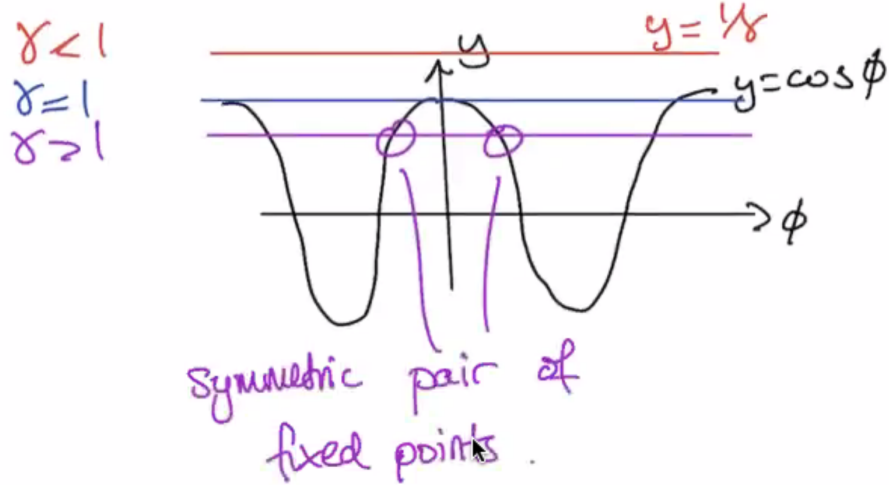


Figure 33: A symmetric pair of fixed points.

As $\gamma \rightarrow \infty$, the fixed points approach $\pm\pi/2$. So as we get faster and faster, the bead moves further up the sides, approaching the equator of the hoop.

We can do a linear stability analysis on the fixed points, and after working through that we get a bifurcation diagram, shown in Figure 34.

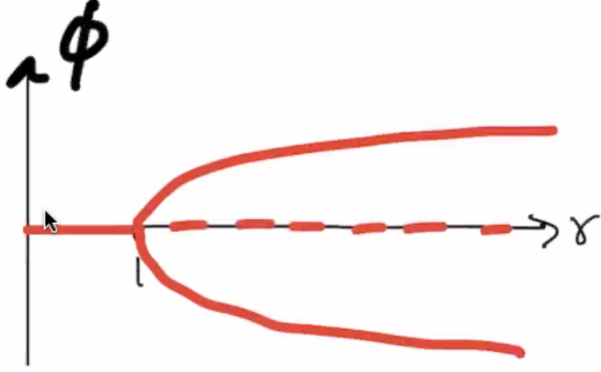


Figure 34: Rotation destabilizes the state $\phi = 0$.

The only thing missing from this diagram is the unstable fixed points at $\phi = \pm\pi$. The supercritical pitchfork bifurcation is at $\gamma = 1$.

The last thing we'll do today is justify the choice of the overdamped approximation. To do this, we'll nondimensionalize. We'll use a characteristic time scale T (to be determined), and use it to define a dimensionless time

$$\tau = \frac{t}{T}$$

We want to introduce T in a clever way. We'll write equations in terms of τ , not t . For this we need the chain rule, which says

$$\frac{d}{dt} = \frac{d\tau}{dt} \frac{d}{d\tau} = \frac{1}{T} \frac{d}{d\tau}$$

We can substitute this into the equation of motion.

$$\begin{aligned} mr \frac{d^2\phi}{dt^2} + b \frac{d\phi}{dt} &= mg \sin \phi [\gamma \cos \phi - 1] \\ \frac{mr}{T^2} \frac{d^2\phi}{d\tau^2} + \frac{b}{T} \frac{d\phi}{d\tau} &= mg \sin \phi [\gamma \cos \phi - 1] \\ \frac{mr}{Tb} \frac{d^2\phi}{d\tau^2} + \frac{d\phi}{d\tau} &= \frac{Tmg}{b} \sin \phi [\gamma \cos \phi - 1] \end{aligned}$$

We will choose $T = \frac{b}{mg}$ to balance drag and the gravity/centrifugal forces.

Define $\epsilon = \frac{mr}{Tb} = \frac{m^2 gr}{b^2}$. The overdamped approximation is valid when

(i) $\epsilon \ll 1$

(ii) $\left| \frac{d^2\phi}{d\tau^2} \right| = O(1)$

So we can neglect inertia on this timescale.

5 September 15, 2020

Here's a paradox from last time: we went from a second-order equation with two initial conditions to a first-order equation:

$$\frac{d\phi}{d\tau} = \sin \phi [\gamma \cos \phi - 1]$$

How do we account for both original initial conditions?

This leads us to a **single perturbation problem**. We establish a fast time scale to deal with the initial stages of the dynamics, $\tau = \epsilon\sigma$. Here, τ is the “slow” time, and σ is the fast time. Let $\sigma = O(1)$ and $\epsilon \ll 1$.

We can use the chain rule on the equation to get it in terms of σ .

$$\frac{d^2\phi}{d\sigma^2} + \frac{d\phi}{d\sigma} + \epsilon \sin \phi [1 - \gamma \cos \phi] = 0$$

Note that this is a second order system! The first two terms balance inertia and drag, and the last term is small so we neglect it.

This gives us initial speed damping on the fast σ -timescale initially. Inertia is important only over an initial transient.

5.1 Imperfect bifurcations and catastrophes

These systems violate symmetry on a supercritical pitchfork bifurcation.

$$\dot{x} = h + rx - x^3$$

Here, h is the **imperfection parameter**.

Let's look at a case where we fix r and vary h . Note that we can write the system as $\dot{x} = h - (x^3 - rx)$. We can plot $y = h$ and $y = x(x^2 - r)$.

In the case where $r \leq 0$, we get the results in Figure 35. We can calculate $h_c(r)$, the critical values of h , and the fixed points $x_{\pm}(r)$. To find x_{\pm} , we want

$$\begin{aligned} \frac{d}{dx}(x^3 - rx) |_{x=x_{\pm}} &= 0 \\ \implies 3x_{\pm}^2 - r &= 0 \\ \implies x_{\pm} &= \pm \sqrt{\frac{r}{3}} \end{aligned}$$

So there's one stable fixed point for all values of h .

When $r > 0$, we have either 3 fixed points or 1 fixed point, depending on the value of h . The critical values h_c exist wherever tangential intersections

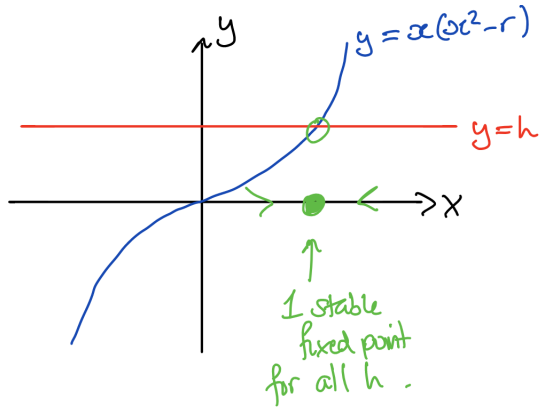


Figure 35: When $r \leq 0$.

are between $y = x(x^2 - r)$ and $y = h$. When $-h_c < h < h_c$, we have three fixed points (one unstable, two stable). When $|h| > h_c$, we have one stable fixed point.

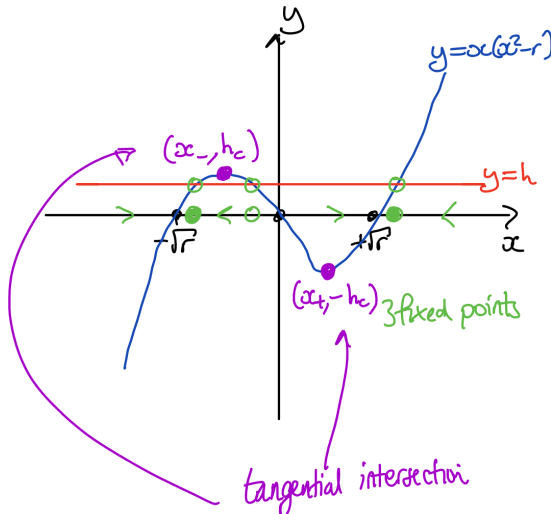


Figure 36: When $r > 0$.

We can calculate h_c :

$$h_c(r) = (x^3 - rx) |_{x=x_-} \implies h_c(r) = \frac{2r}{3} \sqrt{\frac{r}{3}}$$

We can draw a bifurcation diagram for this system, and we get another hysteresis loop. See Figure 37.

Let's introduce a new type of plot here – a **stability plot**. Here we plot h against r . One region of the plot contains dynamics with three fixed points, and another region contains plots with one fixed point. See Figure 38.

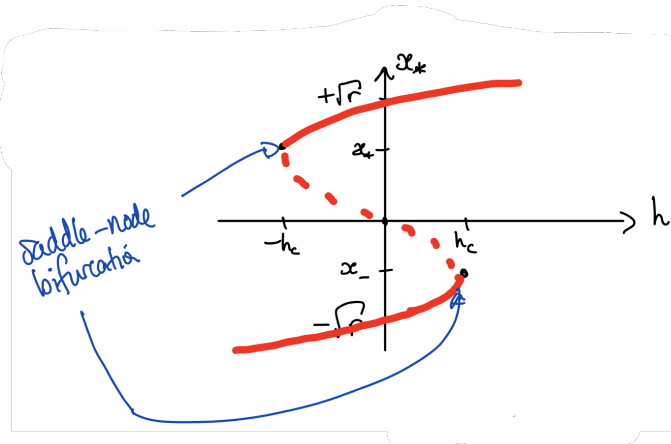


Figure 37: Bifurcation diagram.

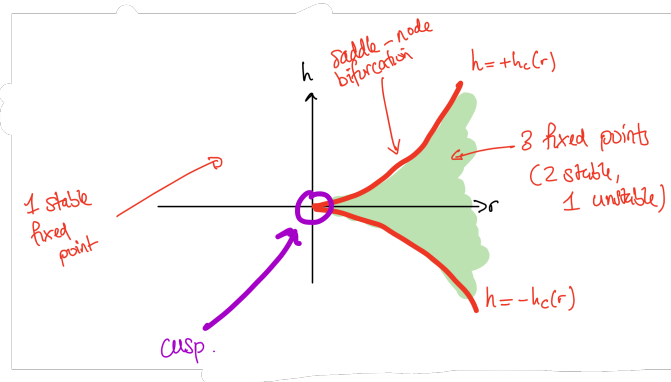


Figure 38: Stability plot.

Example.

A spruce budworm outbreak. The worms attack leaves on the balsam fir tree. Upon outbreak, budworms kill most of the trees.

Some observations: there are two timescales. There's a fast timescale (months) where we see the evolution of the budworm population. Then there's a slow timescale (decades) for the growth of trees.

We will look at this under a quasi-static approximation, where we treat the forest variables as constant.

Let $N(t)$ be the budworm population at time t . Then we can write

$$\dot{N} = RN \left(1 - \frac{N}{K}\right) - p(N)$$

where $p(N)$ is the death rate due to predation.

We use a candidate predation function:

$$p(N) = \frac{BN^2}{A^2 + N^2}$$

where the parameters $A, B > 0$. See Figure 39.

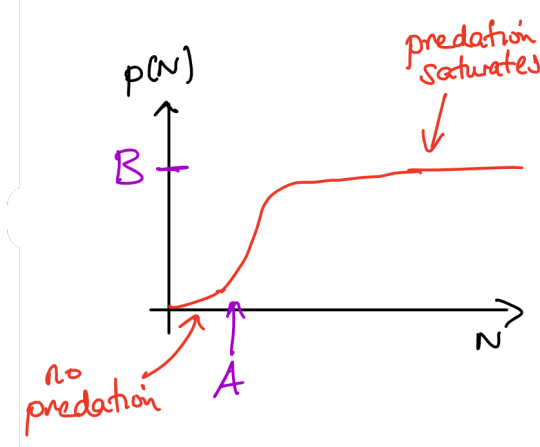


Figure 39: The candidate function.

Our first task will be to nondimensionalize the population. So we introduce a timescale T , where $t = T\tau$. Then our dimensionless time is τ , and our dimensionless population is given by

$$x(\tau) = \frac{N(t)}{A}$$

We can substitute this into the model:

$$\begin{aligned} \frac{A}{T} \frac{dx}{d\tau} &= RAx \left(1 - \frac{A}{K}x\right) - \frac{Bx^2}{1+x^2} \\ \frac{dx}{d\tau} &= RTx \left(1 - \frac{A}{K}x\right) - \frac{BT}{A} \frac{x^2}{1+x^2} \end{aligned}$$

We then choose our timescale T so that $BT/A = 1$, i.e $T = A/B$.

Let's define some more dimensionless parameters, $r, k > 0$.

$$r = RT \quad k = \frac{K}{A}$$

Then our final dimensionless model is

$$\frac{dx}{d\tau} = rx \left(1 - \frac{x}{k}\right) - \frac{x^2}{1+x^2}$$

We can see that $x_0 = 0$ is a fixed point for this system. If we linearize the equation, we see that $x_0 = 0$ is an unstable fixed point.

The other fixed points satisfy

$$r \left(1 - \frac{x}{k}\right) = \frac{x}{1+x^2}$$

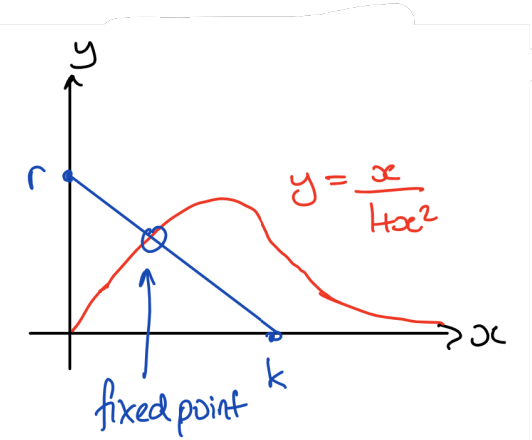


Figure 40: Finding fixed points.

We can use our usual plotting method to identify the fixed points. See Figure 40.

If we fix k and vary r , we see that we can find up to 3 nonzero fixed points.

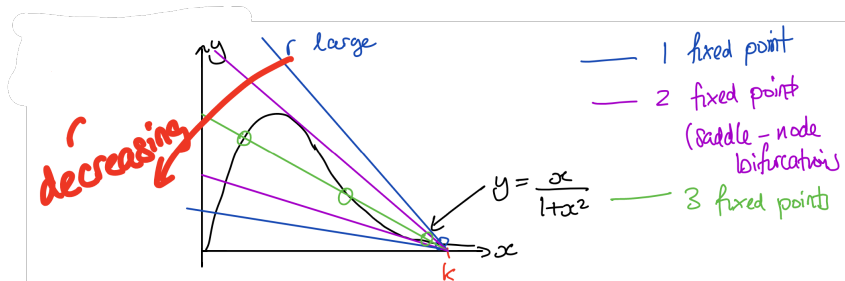


Figure 41: Different fixed point configurations.

If we have three fixed points besides $x_0 = 0$, we find that two are stable and one, in between, is unstable. The lower fixed point, closer to $x_0 = 0$, is the “refuge level”, where budworms are under control. The upper fixed point is the outbreak level. We can draw a bifurcation diagram for the situation. See Figure 42.

For the stability plot, we want to find the saddle-node bifurcations. We need a tangential intersection of $y = r(1 - x/k)$ and $y = x/(1 + x^2)$. This gives us two conditions to work with.

$$1. \quad r \left(1 - \frac{x}{k}\right) = \frac{x}{1 + x^2}$$

$$2. \quad \frac{d}{dx} \left[r \left(1 - \frac{x}{k}\right) \right] = \frac{d}{dx} \left[\frac{x}{1 + x^2} \right]$$

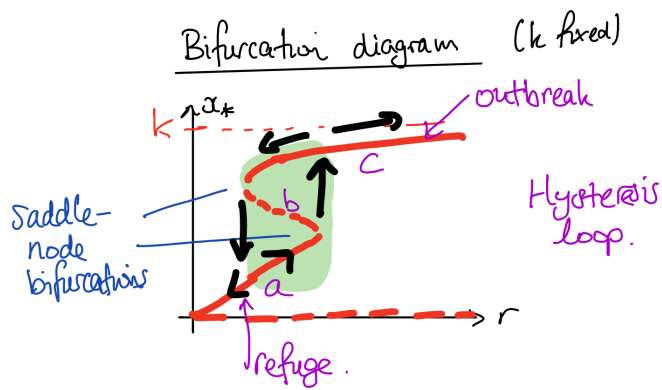


Figure 42: Bifurcation diagram.

Then,

$$-\frac{r}{k} = \frac{1-x^2}{(1+x^2)^2}$$

After a bunch of algebra we can parametrize $r(x)$ and $k(x)$ to get

$$r(x) = \frac{2x^3}{(1+x^2)^2}$$

$$k(x) = \frac{2x^3}{x^2 - 1} \quad x > 1$$

Note that as $x \rightarrow \infty$, $r(x) \sim 2/x$ and $k(x) \sim 2x$. So $r \sim 4/k$ as $x \rightarrow \infty$.

As $x \rightarrow 1^+$, $r(x) \sim 1/2$ and $k(x) \sim 1/(x-1)$.

This lets us draw the stability diagram.

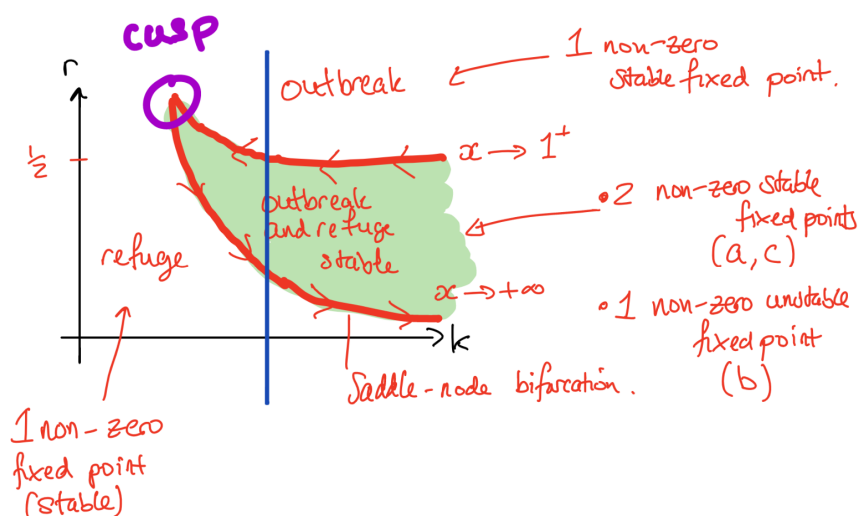


Figure 43: Stability diagram.

6 September 17, 2020

So far we've talked about $\dot{x} = f(x)$, flows along a line. Now we'll talk about flows on a circle.

$$\dot{\theta} = f(\theta)$$

Here, periodicity requires that $f(\theta)$ is 2π -periodic, namely $f(\theta+2\pi) = f(\theta)$ for all $\theta \in \mathbb{R}$. Note that we also need f to be sufficiently smooth for existence and uniqueness to be satisfied. The periodicity here allows for systems to oscillate.

Example.

Flow on a circle: $\dot{\theta} = \sin \theta$

Let's consider $\theta \in (-\pi, \pi]$. Then the fixed points are $\theta_* = 0$ and $\theta_* = \pi$. The first one is unstable, and the second is stable.

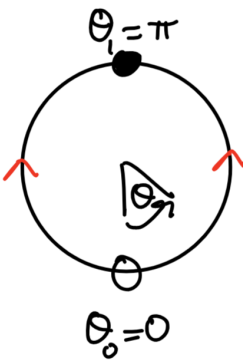


Figure 44: Flow on a circle.

Example.

A uniform oscillator $\dot{\theta} = \omega$.

Here, $\theta(t) = \omega t + \theta_0$. The initial angle is θ_0 , and ω is the angular frequency. The period is $T = 2\pi/\omega$.

Example.

Two joggers, Speedy and Pokey, run at a constant pace around a circular track. Speedy takes T_1 time to do a lap, and Pokey takes T_2 time, with $T_1 < T_2$. How long does it take for Speedy to lap Pokey once?

Speedy is going at $\dot{\theta}_1 = \omega_1 = 2\pi/T_1$, and Pokey is going at $\dot{\theta}_2 = \omega_2 = 2\pi/T_2$. This gives us a **beat phenomenon** where two independent oscillators periodically go in and out of phase.

There is a phase difference $\phi = \theta_1 - \theta_2$. How long until ϕ increases by 2π ?

$$\dot{\phi} = \dot{\theta}_1 - \dot{\theta}_2 = 2\pi \left[\frac{1}{T_1} - \frac{1}{T_2} \right]$$

So then for the period, we have

$$T = \frac{2\pi}{\omega} = \left[\frac{1}{T_1} - \frac{1}{T_2} \right]^{-1}$$

Example.

Consider an overdamped pendulum with constant torque. The equation governing this is

$$mL^2\ddot{\theta} + b\dot{\theta} + mgL \sin \theta = \Gamma$$

where Γ is the torque.

To determine the conditions under which inertia is negligible, we nondimensionalize $t = T\tau$ so that τ is dimensionless time. We need to find T , the characteristic time. Let $\phi(\tau) = \theta(t)$. Then,

$$\frac{mL^2}{T^2} \frac{d^2\phi}{d\tau^2} + \frac{b}{T} \frac{d\phi}{d\tau} + mgL \sin \phi = \Gamma$$

We want to balance the drag term and the pendulum term.

$$\frac{mL^2}{Tb} \frac{d^2\phi}{d\tau^2} + \frac{d\phi}{d\tau} + \frac{mgLT}{b} \sin \phi = \frac{\Gamma T}{b}$$

We can define some constants, and choose a timescale for T .

$$\begin{aligned} T &= \frac{b}{mgL} \\ \epsilon &= \frac{mL^2}{Tb} = \frac{m^2gL^3}{b^2} = gL \left(\frac{mL}{b} \right)^2 \\ \gamma &= \frac{\Gamma T}{b} = \frac{\Gamma}{mgL} \end{aligned}$$

Then we can write the equation as

$$\epsilon \frac{d^2\phi}{d\tau^2} + \frac{d\phi}{d\tau} + \sin \phi = \gamma$$

For $\epsilon \ll 1$, the dynamics are well-approximated by the singular limit

$$\frac{d\phi}{d\tau} = \gamma - \sin \phi$$

following an initial transient. Here, γ is the ratio of applied torque to maximum gravitational torque.

We can try to find the fixed points. We need to find ϕ_* to satisfy $\gamma = \sin \phi_*$.

For $\gamma > 1$, the pendulum will overturn and there are no fixed points.

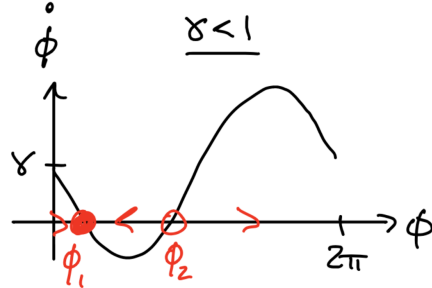


Figure 45: Vector field for $0 < \gamma < 1$.

Therefore fixed points exist only for $\gamma < 1$ (recall $\gamma > 0$). So at $\gamma_c = 1$, there's a saddle-node bifurcation. We have $\phi_1 = \phi_2 = \pi/2$.

As γ decreases past $\gamma_c = 1$, we have a saddle-node bifurcation with fixed points emerging around $\phi = \pi/2$. In this case, there is a pair of fixed points ϕ_1, ϕ_2 .

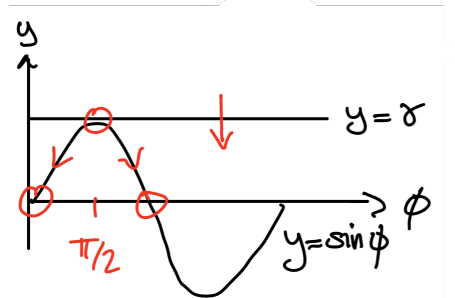


Figure 46: Vector field for $0 < \gamma < 1$.

The fixed points move apart as γ decreases, with $\phi_* = 0, \pi$ at $\gamma = 0$ (like a normal pendulum).

Using linear stability analysis, we find that $\phi_* = \arcsin \gamma$. We can define ϕ_{\pm} such that $\sin \phi_{\pm} = \gamma$ and $\cos \phi_{\pm} = \pm \sqrt{1 - \gamma^2}$. Then, $f'(\phi_{\pm}) = \mp \sqrt{1 - \gamma^2}$.

Therefore, for $0 < \gamma < 1$, we have ϕ_+ as a stable fixed point and ϕ_- as an unstable fixed point.

Note that ϕ_+ approaches 0 as $\gamma \rightarrow 0$, and ϕ_- approaches π as $\gamma \rightarrow 0$.

We can also calculate the oscillation period. For $\gamma > 1$, there are no fixed points and so we expect oscillatory solutions. The time taken for $\phi(\tau)$ to change by 2π is

$$\tau_* = \int_0^{2\pi} \frac{d\tau}{d\phi} d\phi = \int_0^{2\pi} \frac{1}{\gamma - \sin \phi} d\phi = \dots = \frac{2\pi}{\sqrt{\gamma^2 - 1}}$$

Note that $\tau_* \rightarrow \infty$ as $\gamma \rightarrow 1^+$.

Let $\gamma = 1 + \epsilon$ for $\epsilon \ll 1$. Then $\gamma^2 - 1 = 2\epsilon + \epsilon^2$. So as $\epsilon \rightarrow 0$,

$$\tau_* = \frac{2\pi}{\sqrt{(\gamma-1)(\gamma+1)}} = \frac{2\pi}{\sqrt{\epsilon}\sqrt{2+\epsilon}} \sim \frac{\sqrt{2}\pi}{\sqrt{\epsilon}}$$

6.1 Ghosts and bottlenecks

The square root scaling law we just derived turns out to be a very general feature of systems that are close to a saddle-node bifurcation.

Recall $\dot{\phi} = \gamma - \sin \phi$. For $\gamma > 1$, $\dot{\phi}$ is still small for $\phi \approx \pi/2$.

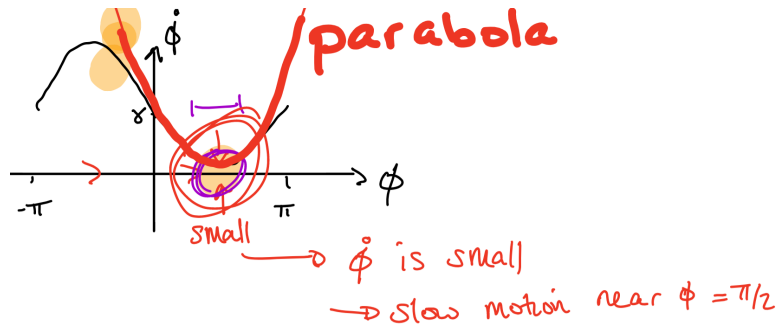


Figure 47: $\dot{\phi}$ is small near $\pi/2$.

The effect of the nearby saddle-node bifurcation is felt as a **ghost**, leading to a **bottleneck**. This influences the dynamics as the flow is then very slow.

To derive a scaling law for the time to pass through a bottleneck, we note that only $\dot{\phi}$ is needed near its minimum, i.e. $\phi \approx \pi/2$. Typically, $\dot{\phi}$ is parabola-like near its minimum. We Taylor expand ϕ about $\pi/2$, namely $\phi = \frac{\pi}{2} + \psi$, for $|\psi| \ll 1$.

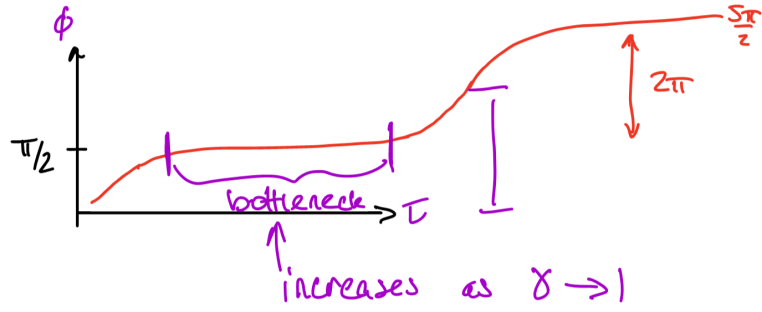


Figure 48: Bottleneck dynamics.

So,

$$\begin{aligned}\dot{\psi} &= \gamma - \sin\left(\psi + \frac{\pi}{2}\right) \\ &= \gamma - \left(\sin\frac{\pi}{2} + \psi \cos\frac{\pi}{2} - \frac{\psi^2}{2} \sin\frac{\pi}{2} + O(\psi^4)\right) \\ &= \gamma - 1 + \frac{\psi^2}{2} + O(\psi^4)\end{aligned}$$

Let $\psi = a\Psi$. Then,

$$\begin{aligned}\dot{\psi} &\simeq \frac{\gamma - 1}{a} + \frac{\alpha}{2}\Psi^2 && \text{so set } \alpha = 2 \text{ and } r = \frac{\gamma - 1}{\alpha} \\ \dot{\Psi} &\simeq r + \Psi^2 + O(\Psi^4)\end{aligned}$$

This gives us an approximate normal form.

We can calculate τ_+ from this.

$$\begin{aligned}\tau_+ &\approx \int_{-\infty}^{\infty} \frac{d\tau}{d\Psi} d\Psi \\ &= \int_{-\infty}^{\infty} \frac{1}{r + \Psi^2} d\Psi \\ &= \frac{\pi}{\sqrt{r}} \\ &= \frac{\sqrt{2}\pi}{\sqrt{\gamma - 1}}\end{aligned}$$

This gives us $\frac{1}{\sqrt{r}}$ scaling.

Example.

An application to synchronization: fireflies.

Male fireflies gather in trees at night and flash on and off in unison to attract females. The fireflies do not start off in synchrony – they influence each other and the synchrony builds up over time.

Model: consider one firefly and its response to a periodic stimulus.

The stimulus is $\dot{\Theta} = \Omega$, and $\Theta = 0$ is the flash of the stimulus.

The firefly model is $\dot{\theta} = \omega + A\sin(\Theta - \theta)$, where $A > 0$. The firefly's natural frequency is ω . If Θ is ahead of θ , then $\dot{\theta} > \omega$, i.e the firefly speeds up!

We can define a phase difference $\phi = \Theta - \theta$, so

$$\dot{\phi} = \dot{\Theta} - \dot{\theta} = (\Omega - \omega) - A\sin\phi$$

We nondimensionalize by scaling $\tau = At$ and $\mu = \frac{\Omega - \omega}{A}$. (Here, μ is a measure of the frequency difference relative to the resetting strength.) Then

$$\frac{d\phi}{d\tau} = \mu - \sin\phi$$

We can draw a bifurcation diagram.

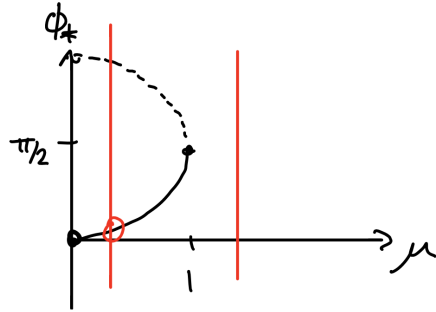


Figure 49: Bifurcation diagram.

When $\mu = 0$, $\phi_* = 0$ is a stable fixed point, so we obtain zero phase difference after a long time.

When $\mu \in (0, 1)$, $\phi_* > 0$ is stable, so we approach a constant difference and the firefly is phase-locked to the stimulus. So the frequency is the same, but the flash is not in unison. As $\phi_* > 0$, the stimulus flashes slightly ahead of the firefly.

For $\mu > 1$, there is no synchrony and there are no fixed points. There's phase drift until $\phi = 2\pi$, when the oscillators are briefly in phase again.

The phase drift period for $\mu > 1$ is the time for ϕ to change by 2π , namely

$$\tau_{\text{drift}} = \int_0^{2\pi} \frac{d\tau}{d\phi} d\phi = \int_0^{2\pi} \frac{1}{\mu - \sin\phi} d\phi = \frac{2\pi}{\sqrt{\mu^2 - 1}}$$

Back in dimensional variables,

$$T_{\text{drift}} = \frac{2\pi}{\sqrt{(\Omega - \omega)^2 - A^2}}$$

7 September 22, 2020

Recall that earlier in the course we looked at a damped oscillator,

$$m\ddot{x} + b\dot{x} + kx = 0$$

in the overdamped limit, where inertial effects were small compared to damping effects ($m\ddot{x} \ll b\dot{x}$) so we neglected inertia.

Now we'll consider systems where inertia is appreciable, and we have a second order differential equation. More generally, we could consider a system with coupled linear equations.

$$\begin{aligned}\dot{x} &= ax + by \\ \dot{y} &= cx + dy\end{aligned}$$

We could write this in a matrix form:

$$\frac{d}{dt} \begin{pmatrix} x \\ y \end{pmatrix} = \begin{pmatrix} a & b \\ c & d \end{pmatrix} \begin{pmatrix} x \\ y \end{pmatrix}$$

The vector-matrix form in general is $\dot{\vec{x}} = A\vec{x}$.

To go from second-order differential equations to first-order systems, we take an equation like $m\ddot{x} + b\dot{x} + kx = 0$. We then define the velocity, $v = \dot{x}$. Then we can write

$$\begin{aligned}\dot{x} &= v \\ \dot{v} &= \ddot{x} = -\frac{1}{m}(bv + kx)\end{aligned}$$

Then this can be written in vector-matrix form.

$$\frac{d}{dt} \begin{pmatrix} x \\ v \end{pmatrix} = \begin{pmatrix} 0 & 1 \\ -\frac{k}{m} & -\frac{b}{m} \end{pmatrix} \begin{pmatrix} x \\ v \end{pmatrix}$$

The matrix here is usually referred to as the **companion matrix**. It accompanies higher-order differential equations.

We will use linear systems to develop methodologies for tackling nonlinear systems (stay tuned for next week).

Just a reminder on terminology: a system is **linear** if x and y are both solutions then $c_1x + c_2y$ is also a solution.

The vector field for an undamped harmonic oscillator ($b = 0$) can be obtained in this way. The equations we have are

$$\begin{aligned}m\ddot{x} + kx &= 0 \\ \implies \dot{x} &= v \\ \implies \dot{v} &= -\frac{k}{m}x\end{aligned}$$

We can define $\omega = \sqrt{\frac{k}{m}}$ as the angular frequency, and our equation is then $\ddot{x} + \omega^2 x = 0$.

To get the vector field, we draw an arrow pointing in $(\dot{x}, \dot{v}) = (v, -\omega^2 x)$ in the x - v plane.

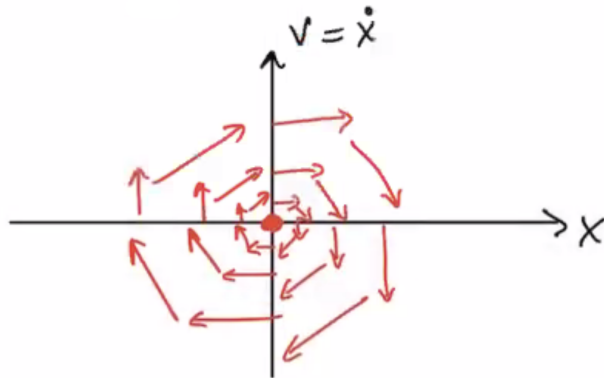


Figure 50: Vector field. Arrows determined by (\dot{x}, \dot{v}) .

If $x = 0$, $(\dot{x}, \dot{v}) = (v, 0)$. If $v = 0$, $(\dot{x}, \dot{v}) = (0, -\omega^2 x)$.

Now we turn to the phase portrait. These are sample trajectories in the (x, v) -phase space. The axes are still x and v . Later we'll prove that trajectories are elliptical in this example.

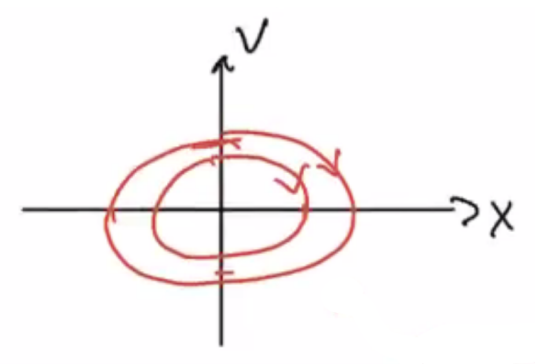


Figure 51: The arrows denote flow direction.

The “size” of the ellipse is determined by the initial condition $(x(0), v(0))$.

When $v = 0$ and $x > 0$, the oscillator is fully extended. This is the positive x -intercept of the ellipse. Then the oscillator compresses, and as it passes through equilibrium v is at its minimum and $x = 0$, so we're at the negative v -intercept. Then the oscillator reaches full compression, so $v = 0$ and $x < 0$ so we're at the negative x -intercept. So we have a picture of the trajectory in this ellipse.

Why are trajectories here ellipses? Along the trajectories we have

$$\frac{dv}{dx} = \frac{dv}{dt} \frac{dt}{dx} = \frac{\dot{v}}{\dot{x}} = \frac{-\omega^2}{v}x \implies v \frac{dv}{dx} = -\omega^2 x$$

We can integrate both sides over x to get

$$\frac{1}{2}v^2 = -\frac{\omega^2}{2}x^2 + C$$

Rearranging,

$$\frac{1}{2}v^2 + \frac{\omega^2}{2}x^2 = C$$

So the trajectories are ellipses, and C is determined by initial conditions.

On an overdamped system, we'd reach $x = 0$ and stop. The inertial term gives us “inertial overshoot” past the equilibrium, leading to oscillatory behavior.

Example.

Consider the following coupled system.

$$\dot{x} = ax$$

$$\dot{y} = -y$$

This gives us $x(t) = x_0 e^{at}$ and $y(t) = y_0 e^{-t}$. Note that we have a fixed point then at

$$\begin{pmatrix} \dot{x} \\ \dot{y} \end{pmatrix} = \begin{pmatrix} 0 \\ 0 \end{pmatrix} \implies \begin{pmatrix} x \\ y \end{pmatrix} = \begin{pmatrix} 0 \\ 0 \end{pmatrix}$$

When $a < -1$, we get $x(t) \rightarrow 0$ as $t \rightarrow \infty$ and $y(t) \rightarrow 0$ as $t \rightarrow \infty$. But $x(t)$ will decay faster than $y(t)$. We can look at the ratio to learn more (assuming $x_0, y_0 \neq 0$).

$$\frac{y(t)}{y_0} = e^{-t} \quad \frac{x(t)}{x_0} = e^{at} = (e^{-t})^{-a} = \left(\frac{y(t)}{y_0}\right)^{-a}$$

Let's draw the phase portrait. We get trajectories that approach the fixed point at the origin along parabolic paths. This is called a **stable node**. Since $x(t)$ decays faster, the trajectory approaches $x = 0$ much faster than $y = 0$. So the trajectories go towards the y -axis faster than the x -axis. The trajectories approach the fixed point tangential to the slowest-decaying direction. See Figure 52.

In the case where $a = -1$, the ratio $x(t)/x_0$ is the same as $y(t)/y_0$. Then the trajectories are straight lines. This is called a **star**. See Figure 53.

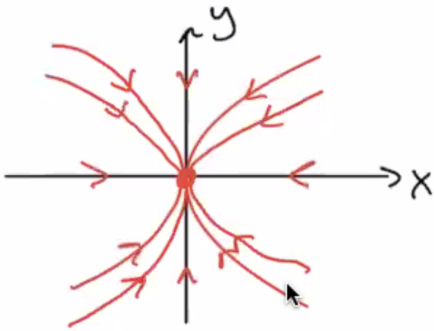


Figure 52: Phase portrait for $a < -1$.

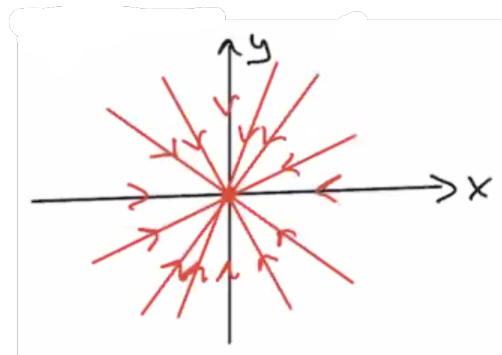


Figure 53: Phase portrait for $a = -1$.

When $-1 < a < 0$, we have $y(t) \rightarrow 0$ as $t \rightarrow \infty$ faster than $x(t) \rightarrow 0$. So we get parabolic trajectories, but pointing the “right” way. This is also a stable node, but the shape is different because $x(t)$ is decaying slowest now. See Figure 54.

When $a = 0$, $\dot{x} = 0$ and $\dot{x} = x_0$ for all t . So the trajectories are vertical lines. We don’t just have a single fixed point, the entire line $y = 0$ is fixed points. This is a system with **non-isolated fixed points**. See Figure 55.

One last case: $a > 0$. We have $x(t) = x_0 e^{at}$, so $|x| \rightarrow \infty$ as $t \rightarrow \infty$ and $|x| \rightarrow 0$ as $t \rightarrow -\infty$. The trajectories approach the x -axis as $t \rightarrow \pm\infty$. At times near 0, the trajectory is near the y -axis. The fixed point at the origin here is called a **saddle**. See Figure 56.

Some terminology! Let x_* be a fixed point, and $x(t)$ be a trajectory.

1. If $x(t) \rightarrow x_*$ as $t \rightarrow \infty$ for $x(0)$ “sufficiently close” to x_* , then we say that x_* is an **attractor**.
2. If $x(t) \rightarrow x_*$ as $t \rightarrow \infty$ for *any* $x(0)$, then x_* is a **global attractor**.
3. (New!) If $x(t)$ is “sufficiently close” to x_* for all $t > 0$, then x_* is **Lyapunov stable**.

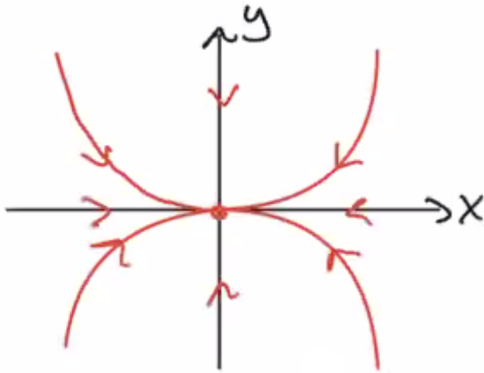


Figure 54: Phase portrait for $-1 < a < 0$.

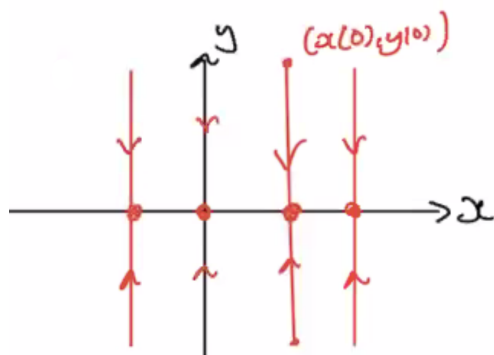


Figure 55: Phase portrait for $a = 0$.

The important difference between an attractor and Lyapunov stability is that the trajectory is near x_* for all time. For example, in the harmonic oscillator, we had elliptical trajectories. If the trajectory is close to the origin (the fixed point) at $t = 0$, it will remain close to the origin for all time $t > 0$. So in this case, the harmonic oscillator has $(x, \dot{x}) = (0, 0)$ as a Lyapunov stable fixed point. Note that it is *not* an attractor.

Here's another example: flow on a circle, with $\dot{\theta} = 1 - \cos \theta$. There is a half-stable fixed point at $\theta = \pi/2$. This is an attractor, because trajectories approach the fixed point as $t \rightarrow \infty$. However it is not Lyapunov stable because trajectories might start close to the fixed point but go far away before approaching it again.

If x_* is Lyapunov stable *and* an attractor, the fixed point is stable or asymptotically stable.

If x_* is neither attracting or Lyapunov stable, then x_* is unstable.

A word on notation: an unstable fixed point will be drawn with an open circle, and Lyapunov stable fixed point or attractor with a filled circle.

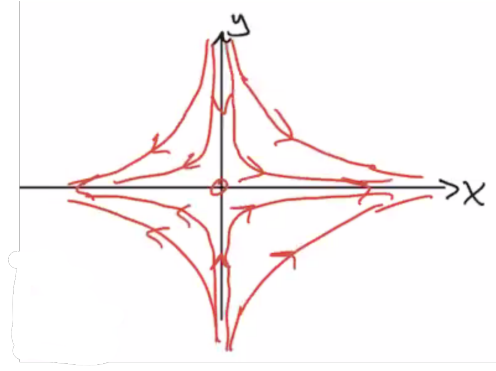


Figure 56: Phase portrait for $a > 0$.

8 September 24, 2020

We are looking at linear systems of the form

$$\begin{aligned}\dot{x} &= ax + by \\ \dot{y} &= cx + dy\end{aligned}$$

which we can write as

$$\frac{d}{dt} \begin{pmatrix} x \\ y \end{pmatrix} = \begin{pmatrix} a & b \\ c & d \end{pmatrix} \begin{pmatrix} x \\ y \end{pmatrix}$$

The fixed points are $\dot{x} = \dot{y} = 0$, where the stability types include nodes, saddles, and spirals.

We need to solve $\dot{x} = Ax$. In one dimension, this looks like $\dot{x} = ax$ and $x = e^{\lambda t}$. We are looking for solutions of the form

$$x(t) = ve^{\lambda t}$$

We can substitute this in, and we get $\lambda ve^{\lambda t} = Ave^{\lambda t}$ for all t . Then $Av = \lambda v$, so $v \neq 0$ is an eigenvector.

So our solutions are of the form

$$x(t) = c_1 v_1 e^{\lambda_1 t} + c_2 v_2 e^{\lambda_2 t}$$

where (λ_1, v_1) and (λ_2, v_2) are eigenpairs.

Note: we have assumed that v_1 and v_2 are linearly independent (which is guaranteed if $\lambda_1 = \lambda_2$).

We can compute eigenvalues. If $Av = \lambda v$ with $v \neq 0$, then $\det(A - \lambda \mathbb{1})v = 0$.

So for a matrix

$$A = \begin{pmatrix} a & b \\ c & d \end{pmatrix}$$

we can compute the eigenvalues.

$$\det(A - \lambda \mathbb{1}) = (a - \lambda)(d - \lambda) - bc = \lambda^2 - \lambda(a + d) + (ad - bc)$$

Note that the trace of A is $a + d$ and the determinant is $ad - bc$.

So the eigenvalues have to satisfy $\lambda^2 - T\lambda + D = 0$.

$$\lambda_{\pm} = \frac{1}{2} [T \pm \sqrt{T^2 - 4D}]$$

Example.

Solution to $\dot{x} = Ax$, where

$$A = \begin{pmatrix} 1 & 1 \\ 4 & -2 \end{pmatrix}$$

The eigenvalues satisfy $\lambda^2 + \lambda - 6 = 0$, so we have $\lambda_1 = 2$ and $\lambda_2 = -3$. We can find the corresponding eigenvectors to get the solution,

$$x(t) = c_1 e^{2t} \begin{pmatrix} 1 \\ 1 \end{pmatrix} + c_2 e^{-3t} \begin{pmatrix} 1 \\ -4 \end{pmatrix}$$

where c_1, c_2 are arbitrary real constants.

Let's sketch the phase portrait. Each eigenvector defines its own solution, which we can draw on the phase portrait.

$$x_1 = e^{2t} \begin{pmatrix} 1 \\ 1 \end{pmatrix} \quad x_2 = e^{-3t} \begin{pmatrix} 1 \\ -4 \end{pmatrix}$$

x_1 corresponds to $y = x$. As t increases, x and y increase, so the flow along the v_1 direction is away from the origin. The second solution defines $y = -4x$, with an inward flow.

We can write our coupled equations from the matrix definition.

$$\begin{aligned} \dot{x} &= x + y \\ \dot{y} &= 4x - 2y \end{aligned}$$

Now we'll add in **nullclines**, curves where either $\dot{x} = 0$ or $\dot{y} = 0$. These are useful because when $\dot{x} = 0$, the flow is vertical. When $\dot{y} = 0$, the flow is horizontal. The $\dot{x} = 0$ nullcline is the line $y = -x$, and for $\dot{y} = 0$ we

have $y = 2x$. Note that nullclines are not trajectories! But we can use them to identify where the trajectories flow (drawn in grey).

As $t \rightarrow \infty$, the flow in $x_1(t)$ dominates. As $t \rightarrow -\infty$, the $x_2(t)$ term dominates. So we can fill in our phase portrait. As the trajectories cross the nullclines, we know the flow must be either entirely horizontal or vertical. We end up with a picture for a saddle.

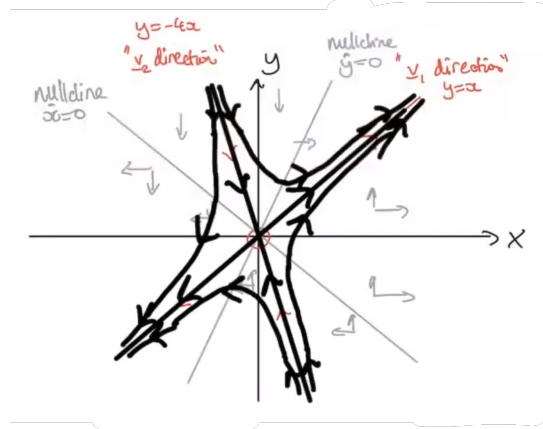


Figure 57: Saddle phase portrait.

The trajectories along the eigenvectors are either towards or away from the saddle. These curves are called **manifolds**. The **stable manifold** is $x(t) \rightarrow x_* = 0$ as $t \rightarrow \infty$. The **unstable manifold** is $x(t) \rightarrow x_* = 0$ as $t \rightarrow -\infty$. The definition of stability is based on the flow relative to the saddle. Note that there are trajectories which start near the stable manifold and approach the unstable manifold. So the definition of stability is not about the trajectories.

Consider the general trajectory

$$x(t) = c_1 v_1 e^{\lambda_1 t} + c_2 v_2 e^{\lambda_2 t}$$

where λ_1, λ_2 are real eigenvalues, and v_1, v_2 are the eigenvectors of A .

The example we just looked at is one positive eigenvalue and one negative eigenvalue, which gave us a saddle.

Case: $\lambda_2 < \lambda_1 < 0$. The origin is then a stable fixed point. We'll draw another phase portrait. Both manifolds are stable, towards the origin. As $t \rightarrow \infty$, the v_2 direction decays to the origin faster than the v_1 direction, so the v_1 direction dominates. As $t \rightarrow -\infty$, the v_2 direction dominates.

What about when $0 < \lambda_1 < \lambda_2$? We get the same picture but the arrows are swapped.

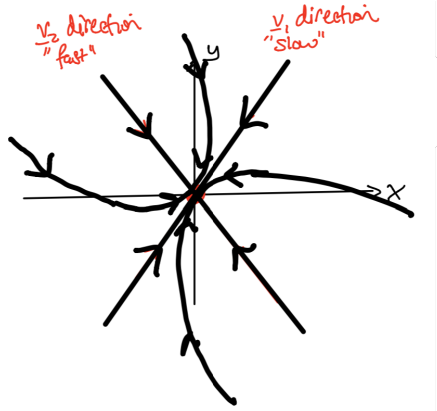


Figure 58: Two negative eigenvalues.

8.1 Complex eigenvalues

Remember the definition of the eigenvalues.

$$\lambda_{\pm} = \frac{1}{2} [T \pm \sqrt{T^2 - 4D}]$$

If $T^2 - 4D > 0$, then λ_{\pm} are real. If $T^2 - 4D < 0$, the eigenvalues $\lambda_{\pm} = \alpha + i\omega$ where $\alpha = T/2$ and $\omega = \frac{1}{2}\sqrt{|T^2 - 4D|}$. So,

$$e^{\lambda_{\pm}t} = e^{(\alpha \pm i\omega)t} = e^{\alpha t} e^{\pm i\omega t}$$

So as t increases, we get growth if $\alpha > 0$ and decay if $\alpha < 0$. For the complex term, Euler's formula gives us sines and cosines so we get oscillations in time.

This means we can have spirals in time. If $\alpha < 0$, these are stable. If $\alpha > 0$, they are unstable.

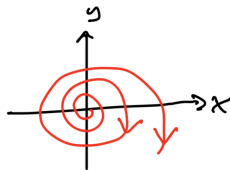


Figure 59: An unstable spiral.

So we can update our definition of general solutions:

$$x(t) = c_1 v_1 e^{(\alpha+i\omega)t} + c_2 v_2 e^{(\alpha-i\omega)t}$$

where c_1, c_2 are arbitrary complex constants.

Note that for a real A and $\lambda_1 = \lambda_2^*$, $v_1 = v_2^*$. So we can write

$$x(t) = e^{\alpha t} (c_1 v_1 e^{i\omega t} + c_2 v_2 e^{-i\omega t})$$

For real $x(t)$, we need $x = x^*$, so we need to find $c_1 = c_2^*$. Then

$$\begin{aligned} x(t) &= e^{\alpha t} (c_1 v_1 e^{i\omega t} + c_1^* v_1^* e^{-i\omega t}) \\ &= 2e^{\alpha t} \operatorname{Re}[c_1 v_1 e^{i\omega t}] \end{aligned}$$

So this is the general real solution.

8.2 Regime diagram

The eigenvalues are given by

$$\lambda_{\pm} = \frac{1}{2} [T \pm \sqrt{T^2 - 4D}]$$

where T is the trace and D is the determinant.

What happens when $D < 0$? Then $\sqrt{T^2 - 4D} > T$ so we have that $\lambda_+ > 0$ and $\lambda_- < 0$. Then we have a saddle (like the earlier example).

For $D > 0$, let's draw the parabola $T^2 - 4D = 0$. When we are above the parabola and $T^2 - 4D > 0$ and $D > 0$, $T^2 - 4D < T$. We have two real eigenvalues of the same sign. If $T > 0$, both eigenvalues will be positive and we'll have an unstable node. If $T < 0$, we have two negative eigenvalues and a stable node.

When $T^2 - 4D < 0$ and $D > 0$, we have complex-conjugate pairs as the eigenvalues, where $\operatorname{Re}(\lambda_{\pm}) = T/2$. When $T > 0$ we have an unstable spiral, and when $T < 0$ we have a stable spiral.

When $T = 0$, we have no growth or decay and we just have ellipses in phase space. This is called a **center**.

When $D = 0$, our eigenvalues are $\lambda_+ = T$ and $\lambda_- = 0$. Then we have a line of fixed points (non-isolated) on the v_- direction.

The last remaining case is the parabola boundary itself, when $T^2 - 4D = 0$. We get $\lambda_{\pm} = T/2$, a repeated eigenvalue of algebraic multiplicity 2. There are two possibilities here. One, that λ has geometric multiplicity 2, so we could find two linearly independent eigenvectors. Then, working from the general solution,

$$\begin{aligned} x(t) &= c_1 e^{\lambda t} v_1 + c_2 e^{\lambda t} v_2 \\ &= e^{\lambda t} (c_1 v_1 + c_2 v_2) \\ &= ue^{\lambda t} \end{aligned}$$

for $u \in \mathbb{R}^2$ as v_1, v_2 form a basis for \mathbb{R}^2 . This gives us a star, which would be stable for $T < 0$ and unstable for $T > 0$.

The other case is that $\lambda = T/2$ has geometric multiplicity 1 (i.e, rank $A = 1$). Then we only have one linearly independent eigenvector v . We get solutions of the form $ve^{\lambda t}$ and $tve^{\lambda t}$. We end up getting a degenerate node (stable if $T < 0$, unstable otherwise).

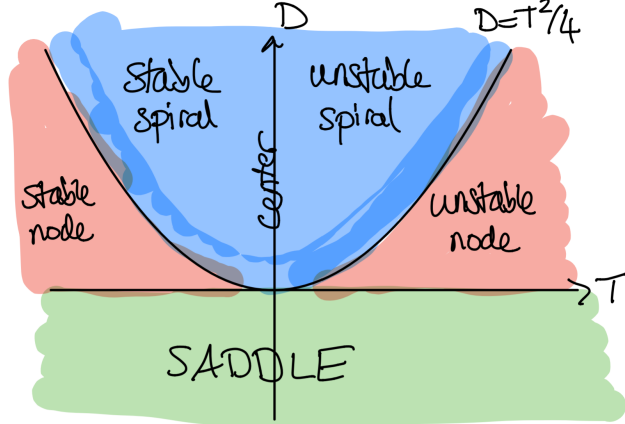


Figure 60: The regime diagram.

9 September 29, 2020

We will investigate nonlinear systems of the form

$$\begin{aligned}\dot{x}_1 &= f_1(x_1, x_2) \\ \dot{x}_2 &= f_2(x_1, x_2)\end{aligned}$$

so we have some $\dot{x} = f(x)$ where all of these are vectors.

$$x = \begin{pmatrix} x_1 \\ x_2 \end{pmatrix} \quad f = \begin{pmatrix} f_1 \\ f_2 \end{pmatrix}$$

We'll look at the results in phase space, when we plot x_1 against x_2 .

We'll explore the qualitative behavior of these systems. We're interested in fixed points, where x_* satisfy $f(x_*) = \vec{0}$. We'll also look at closed orbits, i.e periodic trajectories through phase space. We're also interested in the behavior near fixed points (i.e stability).

9.1 Numerical implementation

We'll use a 4th-order Runge-Kutta method. We'll use some timestep $h > 0$, so the times are given by $t_n = nh$. The initial condition is $\vec{x}_0 = \vec{x}(0)$, so $\vec{x}_n \approx \vec{x}(t_n)$.

The iteration process is given by

$$\vec{x}_{n+1} = \vec{x}_n + \frac{1}{6} [\vec{k}_1 + 2\vec{k}_2 + 2\vec{k}_3 + \vec{k}_4]$$

where

$$\begin{aligned}\vec{k}_1 &= h\vec{f}(\vec{x}_n) \\ \vec{k}_2 &= h\vec{f}\left(\vec{x}_n + \frac{1}{2}\vec{k}_1\right) \\ \vec{k}_3 &= h\vec{f}\left(\vec{x}_n + \frac{1}{2}\vec{k}_2\right) \\ \vec{k}_4 &= h\vec{f}(\vec{x}_n + \vec{k}_3)\end{aligned}$$

Example.

Solve: $\dot{x} = x + e^{-y}$ $\dot{y} = -y$

The fixed points satisfy $\dot{x} = 0$ and $\dot{y} = 0$.

$$x_* + e^{-y_*} = 0 \quad -y_* = 0$$

So $y_* = 0$, and then $x_* = -1$. So we have $(-1, 0)$ as a fixed point.

Note that $y(t) = y_0 e^{-t} \rightarrow 0$ as $t \rightarrow \infty$. Therefore at large t , $\dot{x} \approx x + 1$. Note then that $|x| \rightarrow \infty$ as $t \rightarrow \infty$.

Let's do the phase portrait. The nullclines are the curves along which $\dot{x} = 0$ or $\dot{y} = 0$. So,

$$\dot{x} = x + e^{-y} \quad x = -e^{-y}, \quad y = -\log(-x)$$

We can draw in this nullcline (shown in red). We can use this to determine that the flow in the x direction is away from the nullcline. If $x > -e^{-y}$, $\dot{x} > 0$.

The other nullcline (drawn in blue) is just $y = 0$. Note that no trajectories can cross this curve, so we call it a **separatrix**. The only way to cross would be to have some nonzero \dot{y} , but by definition of the nullcline that's not possible. Above the curve, $y > 0$ so $\dot{y} < 0$, and vice versa for below it.

The intersection of the nullclines gives us our fixed point $(-1, 0)$. Given the flow directions, we can see that it's an unstable fixed point.

Now we can start to draw in some trajectories. See Figure 61.

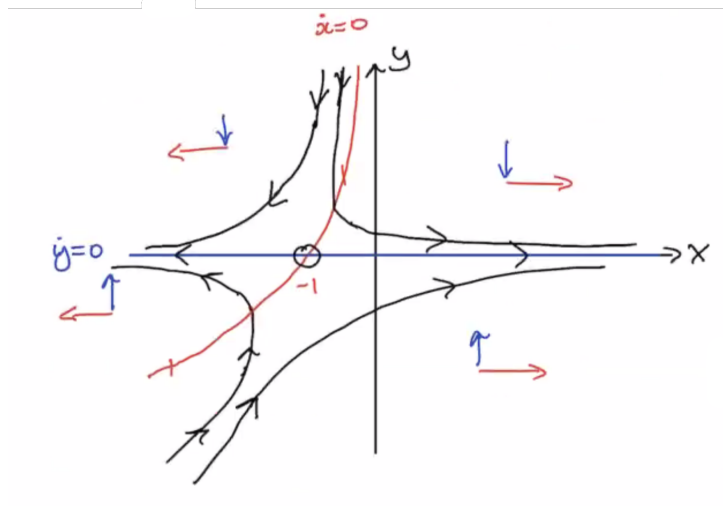


Figure 61: Trajectories.

The fixed point appears to be a saddle, but we need linear stability analysis to show this rigorously.

Like in 1D, we have an existence/uniqueness theorem (everything works well when \vec{f}) is sufficiently smooth.

Can trajectories cross? Suppose they do. Then $\vec{x}_1 = \vec{x}_2$ at $t = t_*$, but $\dot{\vec{x}}_1 \neq \dot{\vec{x}}_2$ at $t = t_*$. But then $\vec{f}(\vec{x}_1) \neq \vec{f}(\vec{x}_2)$. So we have a contradiction, as $\vec{x}_1 = \vec{x}_2$ by assumption. So no crossing!

9.2 Fixed points and linearization

We're going to do local analysis about a fixed point (x_*, y_*) to determine asymptotic linear stability.

Consider the system

$$\begin{aligned}\dot{x} &= f(x, y) \\ \dot{y} &= g(x, y)\end{aligned}$$

where a fixed point (x_*, y_*) satisfies $f(x_*, y_*) = g(x_*, y_*) = 0$.

Consider a small perturbation $x(t) = x_* + u(t)$ and $y(t) = y_* + v(t)$. Here, u and v are the small perturbations, with $0 < |u| \sim |v| \ll 1$.

We can do a two-dimensional Taylor expansion.

$$\begin{aligned}\frac{d}{dt}(x_* + u) &= f(x_* + u, y_* + v) \\ &\sim f(x_*, y_*) + u \frac{\partial f}{\partial x}(x_*, y_*) + v \frac{\partial f}{\partial y}(x_*, y_*) + O(u^2, v^2, |uv|)\end{aligned}$$

Since we have a fixed point at (x_*, y_*) , the first term is 0. We also know that $\frac{d}{dt}x_* = 0$. Then,

$$\dot{u} \sim u \frac{\partial f}{\partial x}(x_*, y_*) + v \frac{\partial f}{\partial y}(x_*, y_*) + \text{h.o.t.}$$

Everything on the right, except the higher order terms (h.o.t.) are constant.

We can play the same game with the y terms, and we get

$$\dot{v} \sim u \frac{\partial g}{\partial x}(x_*, y_*) + v \frac{\partial g}{\partial y}(x_*, y_*) + \text{h.o.t.}$$

We can write this system in vector form to get the **Jacobian matrix**.

$$J = \begin{pmatrix} \frac{\partial f}{\partial x} & \frac{\partial f}{\partial y} \\ \frac{\partial g}{\partial x} & \frac{\partial g}{\partial y} \end{pmatrix}$$

We can now write

$$\frac{d}{dt} \begin{pmatrix} u \\ v \end{pmatrix} = J(x_*, y_*) \begin{pmatrix} u \\ v \end{pmatrix} + \text{h.o.t.}$$

We can linearize this to obtain

$$\frac{d}{dt} \begin{pmatrix} u \\ v \end{pmatrix} = A \begin{pmatrix} u \\ v \end{pmatrix} \quad A = J(x_*, y_*)$$

So the local behavior of trajectories can be inferred from the solution for u, v , provided that the neglected quadratic terms are not important.

Example.

Solve the system:

$$\dot{x} = -x + x^3 = -x(1-x)(1+x)$$

$$\dot{y} = -2y$$

This is a somewhat artificial example because the system decouples, but we'll go through it.

The fixed points are at $(0,0), (1,0), (-1,0)$.

Note that the system has symmetry under $x \mapsto -x$ and/or $y \mapsto -y$.

Let's do our linear stability analysis. The Jacobian is given by

$$J(x, y) = \begin{pmatrix} 3x^2 - 1 & 0 \\ 0 & -2 \end{pmatrix}$$

At the fixed point (0,0),

$$J(0, 0) = \begin{pmatrix} -1 & 0 \\ 0 & -2 \end{pmatrix}$$

The eigenvalues are -1 and -2, so we have a stable node.

At the fixed point ($\pm 1, 0$),

$$J(\pm 1, 0) = \begin{pmatrix} 2 & 0 \\ 0 & -2 \end{pmatrix}$$

We can consider these simultaneously because of the symmetry. The eigenvalues are 2 and -2, so we have a saddle point.

Let's plot these. Along $x = 1$ we have a stable manifold. Since $\dot{y} = -2y$, the flow is towards $(1, 0)$. Along $y = 0$ we have an unstable manifold. See Figure 62.

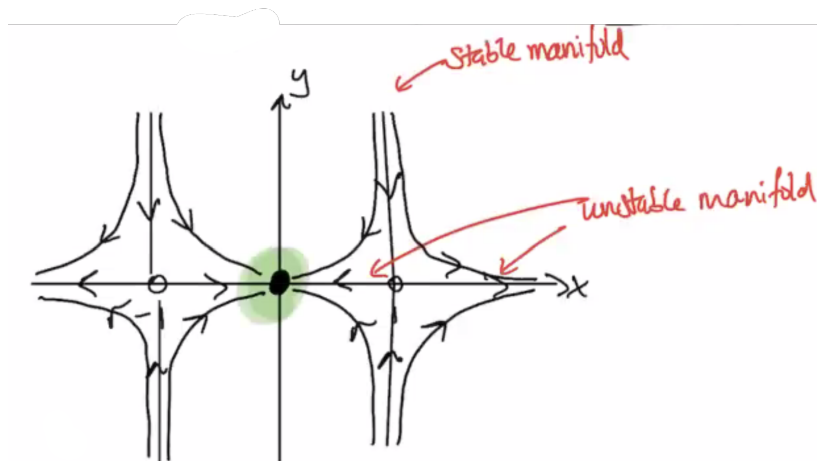


Figure 62: We can see the symmetry.

Example.

Let's see the effect of nonlinear terms for a center.

$$\begin{aligned}\dot{x} &= -y + ax(x^2 + y^2) \\ \dot{y} &= x + ay(x^2 + y^2)\end{aligned}$$

where a is a real parameter.

Note that $(0, 0)$ is a fixed point of the system. The linearized system is

$$\begin{aligned}\dot{x} &= -y \\ \dot{y} &= x\end{aligned}$$

This is the same as the harmonic oscillator. We can write

$$\frac{d}{dt} \begin{pmatrix} x \\ y \end{pmatrix} = \begin{pmatrix} 0 & -1 \\ 1 & 0 \end{pmatrix} \begin{pmatrix} x \\ y \end{pmatrix}$$

The trace is 0, and the determinant is $1 > 0$. So linear stability analysis predicts that we have a center.

But if we include the nonlinear terms, we get a different answer! To study this, we introduce polar coordinates $r(t)$ and $\theta(t)$.

$$x = r \cos \theta \quad y = r \sin \theta \quad x^2 + y^2 = r^2$$

We want differential equations for $r(t)$ and $\theta(t)$. If we differentiate the third equation above with respect to time, we get

$$r\dot{r} = x\dot{x} + y\dot{y}$$

We can substitute in the differential equations for \dot{x} and \dot{y} .

$$\begin{aligned}r\dot{r} &= x(-y + ax(x^2 + y^2)) + y(x + ay(x^2 + y^2)) \\ &= a(x^2 + y^2)^2 \\ &= ar^4 \\ \implies \dot{r} &= ar^3\end{aligned}$$

If $a > 0$ then r is growing. If $a < 0$, r is decaying.

Note that $\tan \theta = y/x$. So we can differentiate with respect to time:

$$(1 + \tan^2 \theta)\dot{\theta} = \frac{\dot{y}}{x} - \frac{\dot{x}y}{x^2} = \frac{xy - \dot{x}\dot{y}}{x^2}$$

We can multiply by x^2 to get

$$r^2\dot{\theta} = xy - \dot{x}\dot{y}$$

If we substitute in \dot{x} and \dot{y} , we get

$$\dot{\theta} = 1$$

(after a lot of algebra).

So our trajectory is always rotating in a counterclockwise direction. But depending on the value of a , the distance from the origin is either growing or decaying.

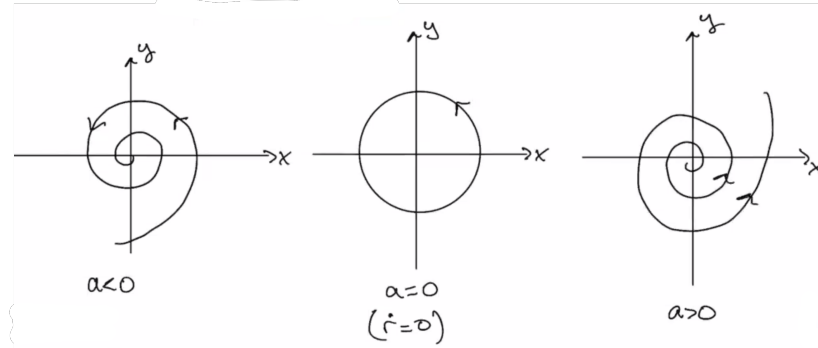


Figure 63: Trajectories after accounting for nonlinearity.

So we have something like in Figure 63. The only time we get a center is when $a = 0$. Otherwise, when $a < 0$, we have a stable spiral. When $a > 0$, it's an unstable spiral. So linearizing wasn't really the most accurate here!

Linear stability gives *robust* results when the fixed point is a node, spiral, or saddle (as predicted by the Jacobian).

But there are marginal cases (centers, non-isolated fixed points, etc) when linear stability analysis will give us spurious results. In these cases, we need nonlinear terms to accurately predict trajectories in the vicinity of a fixed point.

10 October 1, 2020

Today we'll be continuing with our study of phase space. Last time we saw we could apply linear stability analysis to some extent, but we had to watch out for centers and some other marginal cases.

Example.

Rabbits versus sheep.

Define $0 \leq x(t)$ as the rabbit population, and $0 \leq y(t)$ as the sheep population. We'll assume that we have a large enough population that a continuum model makes sense.

Here's our model.

$$\begin{aligned}\dot{x} &= 3x - x^2 - 2xy \\ \dot{y} &= 2y - y^2 - 3xy\end{aligned}$$

So we have logistic growth (the first two terms on the RHS) and a competition term (the last term on the RHS). This accounts for the (not entirely accurate) fact that if there are more sheep, there's less grass for rabbits, and the rabbits die.

Note that we can write this system as

$$\begin{aligned}\dot{x} &= x(3 - x - 2y) \\ \dot{y} &= y(2 - y - x)\end{aligned}$$

This allows us to identify fixed points. We have the trivial fixed point, $(x_*, y_*) = (0, 0)$. Then setting just one of x and y equal to 0, we get $(x_*, y_*) = (0, 2), (3, 0)$. We can also solve the parenthetical terms to get $(x_*, y_*) = (1, 1)$ as the last fixed point.

Let's calculate the Jacobian.

$$J(x, y) = \begin{pmatrix} 3 - 2x - 2y & -2x \\ -y & 2 - 2y - x \end{pmatrix}$$

We can work out the linear stability of each fixed point using this.

$$J(0, 0) = \begin{pmatrix} 3 & 0 \\ 0 & 2 \end{pmatrix}$$

The eigenvalues are 2 and 3, so we have an unstable node at the origin. Nodes are robust under linear stability approximations, so this holds for nonlinear dynamics too. The slow direction is given by the eigenvector corresponding to 2, which is $\vec{v} = (0, 1)^T$.

As trajectories leave $(0, 0)$, they'll go away from the vertical axis. We can also add in trajectories on the axes, because the $(0, 2)$ and $(3, 0)$ fixed points are stable at least for flow on a line. We showed this when we did logistic 1D growth.

Next fixed point:

$$J(0, 2) = \begin{pmatrix} -1 & 0 \\ -2 & -2 \end{pmatrix}$$

Eigenvalues are -1 and -2 , so we have a stable node. The slow-approaching direction corresponds to $\lambda = -1$, and that eigenvector is $\vec{v} = (1, -2)^T$. So the slow direction is along the line $y = -2x + 2$.

Fixed point $(3, 0)$:

$$J(3, 0) = \begin{pmatrix} -3 & -6 \\ 0 & -1 \end{pmatrix}$$

So the eigenvalues are -3 and -1 , so it's a stable node. The eigenvector for $\lambda = -1$ is the slow direction, so that's $\vec{v} = (3, -1)^T$. The direction is the line $y = -\frac{1}{3}(x - 3)$.

The last fixed point is (1,1).

$$J(1, 1) = \begin{pmatrix} -1 & -2 \\ -1 & -1 \end{pmatrix}$$

The determinant of J is $-1 < 0$, so we have a saddle. You could calculate the eigenvectors to get the stable and unstable manifold, but we'll try to do it with intuition.

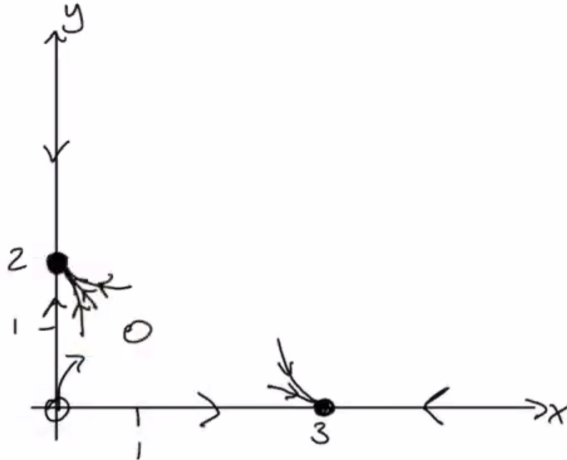


Figure 64: Progress so far.

We can start filling in trajectories. There should be trajectories out of the origin going to the other fixed points. The unstable manifold of the (1,1) saddle should be going towards the other stable nodes. The stable manifold should be coming in towards it from the top right. There are other trajectories approaching in that direction which then part along the unstable manifold towards the stable nodes.

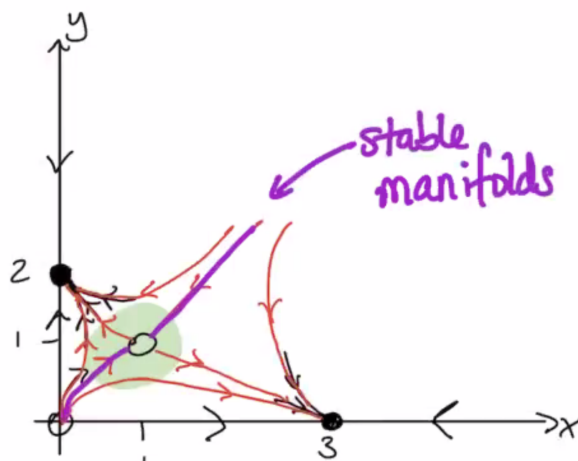


Figure 65: Trajectories drawn in.

Below the stable manifold, that entire region ends up getting directed to

$(3,0)$. We call this a **basis of attraction** of $(3,0)$. The other basis of attraction is above the stable manifold, for $(0,2)$. If you start in either basin, you end up going towards $(3,0)$ or $(0,2)$. *In this example*, the stable manifolds of the saddle point act as separatrices.

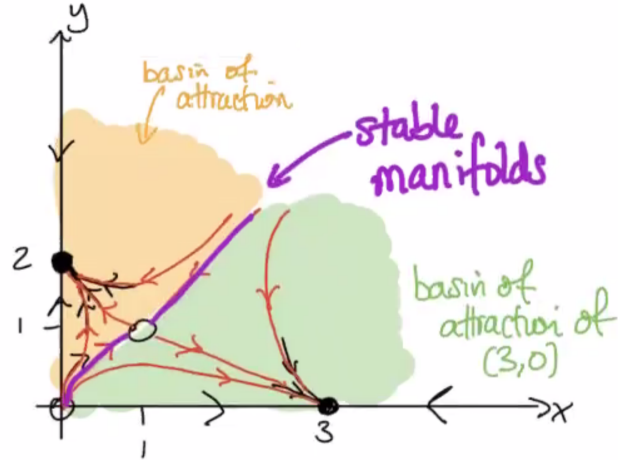


Figure 66: Basins of attraction.

One other ingredient which is useful to note here is that there are trajectories here linking fixed points. There are trajectories from the unstable node to the saddle, from the unstable node to the stable nodes, and from the saddle to the stable nodes.

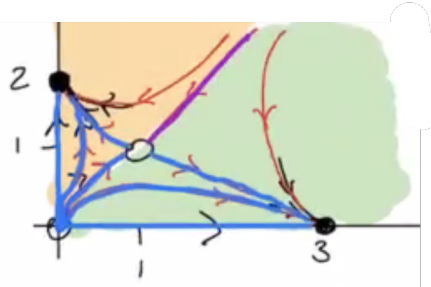


Figure 67: Zoom in on heteroclinic trajectories (in blue).

These are **heteroclinic trajectories**: they link two different fixed points as $t \rightarrow \pm\infty$.

10.1 Conservative systems

Newton's law tells us $m\ddot{x} = F(x(t))$, where F is some nonlinear force. We're going to construct a **potential** $V(x)$ so that

$$F(x) = -V'(x) = -\frac{dV}{dx}$$

Then Newton's second law becomes

$$m\ddot{x}(t) + V'(x(t)) = 0$$

If we multiply by $\dot{x}(t)$, we get

$$\begin{aligned} m\ddot{x}\dot{x} + \dot{x}V'(x(t)) &= 0 \\ \implies \frac{d}{dt} \left(\frac{1}{2}m\dot{x}^2 + V(x(t)) \right) &= 0 \\ \implies \frac{1}{2}m\dot{x}^2 + V(x(t)) &= E \end{aligned}$$

Note that the first term is **kinetic energy**, and the second is **potential energy**. The overall energy E is conserved! It is constant for all time.

This system is an example of a **conservative system**.

Let's motivate a more general setting (not linked to Newton's laws). In general, consider

$$\dot{\vec{x}} = \vec{f}(\vec{x}(t))$$

Definition.

A **conserved quantity** $E(\vec{x})$ (real, scalar) is a continuous function that is constant along trajectories. That is,

$$\frac{d}{dt}E(\vec{x}(t)) = 0$$

We preclude trivial cases where E is a constant value and independent of x on any open set of \mathbb{R}^2 .

Property.

A conservative system cannot have any attracting fixed points.

If there's an attracting fixed point x_* , it has some basin of attraction around it. Then all points in the basin of attraction have $E(x) = E(x_*)$, so E is constant in an open set of \mathbb{R}^2 . We just said that this isn't allowed, so it can't be possible.

We cannot have any attracting fixed points in a conservative system. But we can have saddles, centers, etc.

Example.

Consider $\ddot{x} + V'(x(t)) = 0$, where $V(x) = -\frac{1}{2}x^2 + \frac{1}{4}x^4$.

We have $\ddot{x} = x - x^3$, and a double-well potential.

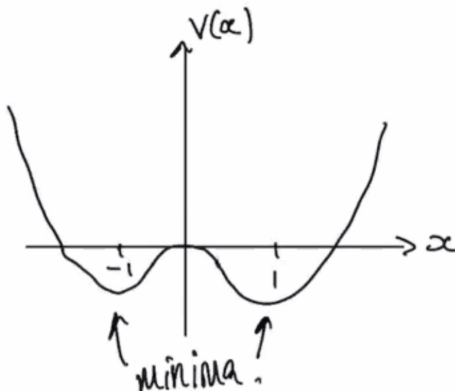


Figure 68: Double well potential.

We can write this in a phase-space formulation.

$$\begin{aligned}\dot{x} &= y \\ \dot{y} &= x - x^3 = x(1 - x)(1 + x)\end{aligned}$$

The fixed points will be the origin and the minima: $(0,0)$, $(\pm 1,0)$.

Let's calculate the Jacobian.

$$J(x,y) = \begin{pmatrix} 0 & 1 \\ 1 - 3x^2 & 0 \end{pmatrix}$$

At the origin,

$$J(0,0) = \begin{pmatrix} 0 & 1 \\ 1 & 0 \end{pmatrix}$$

The determinant is negative, so we have a saddle.

At the minima,

$$J(\pm 1,0) = \begin{pmatrix} 0 & 1 \\ -2 & 0 \end{pmatrix}$$

The determinant is positive. The trace is 0, so we have a linear center.

This should set off some alarm bells because we've used nonlinear theory to predict a linear center, and this is one of those marginal cases. Is this prediction a spurious result from linear theory?

No! We have a conserved quantity, which we can exploit.

Note that

$$E = \frac{1}{2}\dot{x}^2 + V(x(t)) = \frac{1}{2}\dot{x}^2 + \frac{1}{4}x^4 - \frac{1}{2}x^2$$

is a conserved quantity.

If we plot $E(x, \dot{x})$ with a contour plot, we get the trajectories. The contours are where E is constant, so those are the trajectories. We just need to figure out which direction is forward in time.

We can immediately turn to our computer and calculate and plot E . We'd get something like this.

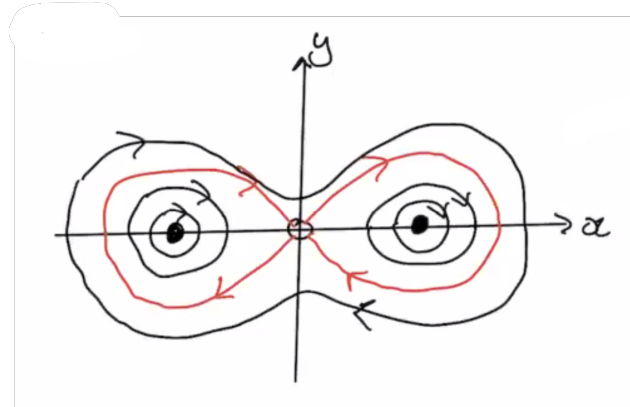


Figure 69: Contours of E .

There are **homoclinic loops or orbits** from the saddle – trajectories that leave the fixed point and then return it. Around the stable nodes we have centers. Outside the figure-eight loop, there are larger homoclinic loops.

The homoclinic loops satisfy $\vec{x}(t) \rightarrow \vec{x}_*$ as $t \rightarrow \pm\infty$. The unstable manifold of the saddle becomes the stable manifold.

Robustness of nonlinear centers.

If an isolated fixed point \vec{x}_* is a minimum (or maximum) of a conserved quantity $E(x)$, then all trajectories sufficiently close to \vec{x}_* are closed.

In other words, we have a nonlinear center that appears in these closed orbits, the same way linear theory would predict.

See the notes for what happens if we have non-isolated fixed points!

10.2 Reversible systems

These are systems with **time-reversal symmetry**.

Example.

Let's consider the Newtonian example again.

$$m\ddot{x} = F(x(t)) \rightarrow \begin{cases} \dot{x} = y \\ \dot{y} = \frac{1}{m}F(x) \end{cases}$$

Note that if we map $t \mapsto -t$, the chain rules tells us that $\frac{d}{dt} \rightarrow -\frac{d}{dt}$. So the system above is invariant (i.e, it has the same algebraic form) under the mapping $(t, x, y) \mapsto (-t, x, -y)$.

Therefore, if $(x(t), y(t))$ is a trajectory, then so is $(x(-t), -y(-t))$.

So all trajectories have a twin!

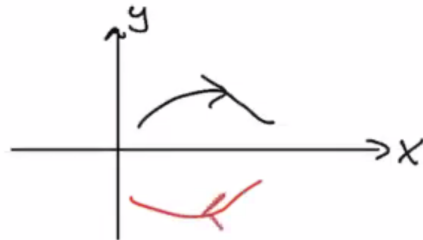


Figure 70: Flip the trajectory about $y = 0$ and reverse the arrow.

More generally, if we have a system

$$\begin{aligned} \dot{x} &= f(x, y) \\ \dot{y} &= g(x, y) \end{aligned}$$

and we map $t \mapsto -t$, $y \mapsto -y$, then

$$\begin{aligned} -\dot{x} &= f(x, -y) \\ \dot{y} &= g(x, -y) \end{aligned}$$

So we have invariance under this mapping if both of these hold:

1. f is odd in y , i.e $f(x, -y) = -f(x, y)$
2. g is even in y , i.e $g(x, -y) = g(x, y)$

Like conservative systems, centers are robust in reversible systems.

Suppose that $\vec{x}_* = 0$ is a linear center of a reversible system. We'll show that close to the origin, all trajectories are closed. So a trajectory that begins on one axis hits the axis again on the other side of the origin because of the swirling nature of the vector field. It also has a twin trajectory, because of time-reversal symmetry. This gives us closed orbits.

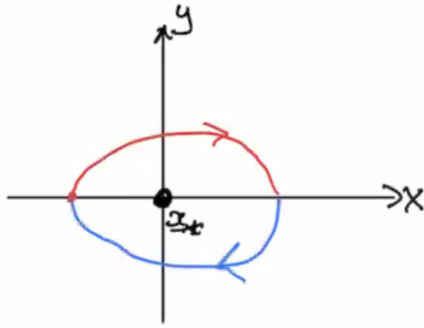


Figure 71: Closed orbits.

Example.

Consider the system:

$$\begin{aligned}\dot{x} &= y - y^3 = y(1 - y)(1 + y) \\ \dot{y} &= -x - y^2\end{aligned}$$

The fixed points here are $(0,0)$ and $(-1, \pm 1)$.

Note that we also have time-reversal symmetry. The \dot{x} function is odd in y , and the function for \dot{y} is even in y .

The Jacobian is

$$J(x, y) = \begin{pmatrix} 0 & 1 - 3y^2 \\ -1 & -2y \end{pmatrix}$$

At $(0, 0)$, the Jacobian is

$$J(0, 0) = \begin{pmatrix} 0 & 1 \\ -1 & 0 \end{pmatrix}$$

so the trace is 0 and the determinant is 1, and we have a linear center. But because time-reversal symmetry holds, we have a series of closed orbits about the origin, so this is a nonlinear center.

11 October 6, 2020

Linear stability analysis gave us information about the phase portrait in the vicinity of fixed points. But now we want global information about the phase portrait, and for that we'll use [index theory](#).

Question: does a closed orbit always contain a fixed point? If yes, what kind of fixed points? Can we rule out the existence of closed orbits in the phase portrait?

So far we've used intuition to say that trajectories will approach a saddle's unstable manifold as $t \rightarrow \infty$ and the stable manifold as $t \rightarrow -\infty$. But now we'll rigorously demonstrate this sort of thing.

11.1 The index of a closed curve

Let C be a simple closed curve (not necessarily a trajectory or orbit). This means it has no self-intersections.

Consider a vector field $\dot{\vec{x}} = \vec{f}(\vec{x})$ where everything is smooth. Take the vector field at some point on the curve and evaluate $\dot{\vec{x}}$ at that point. Repeat this for multiple points along the curve.

We want to quantify these vectors. Introduce an angle ϕ , the angle that each vector $\dot{\vec{x}}$ makes with the horizontal axis.

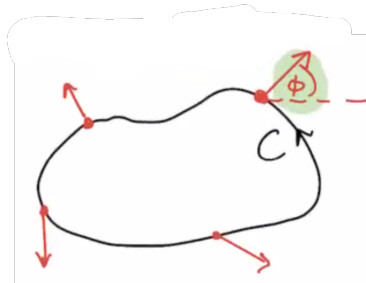


Figure 72: The curve C , labeled with vectors $\dot{\vec{x}}$ and ϕ .

How does ϕ vary as we traverse the closed curve C in the counterclockwise direction?

Note: we assume that \vec{f} is sufficiently smooth. This implies that the angle ϕ varies continuously. We will take $\phi \in \mathbb{R}$ so that it's not constrained to $(-\pi, \pi)$. This way we avoid jumps.

After one loop of C , we have that \vec{x} (so $\dot{\vec{x}}$) returns to the original value. So ϕ is the same, up to a factor of $2\pi n$.

The index allows us to describe the loops around C . If we wrap around once, we want the index to be one. If we wrap around twice, we want it to be two.

We define the **index** of a closed curve C to be

$$I_C = \frac{1}{2\pi}[\phi]_C$$

where $[\phi]_C$ means the change in ϕ over one loop of C .

Therefore I_C is the net number of counterclockwise revolutions as \vec{x} moves once along C in the counterclockwise direction.

For saddles, one loop around gives us an index of -1. This is a general feature of these. Nodes, spirals, etc have an index of 1. Some nonstandard cases can give us an index of 0.

Let's do this by hand.

Let's start with some curve C , and draw in the $\dot{\vec{x}}$ vectors.

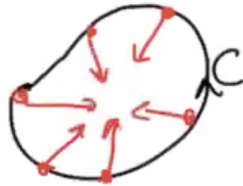


Figure 73: Starting curve.

We're going to label the arrows counterclockwise. Then we'll center them all on the same point.

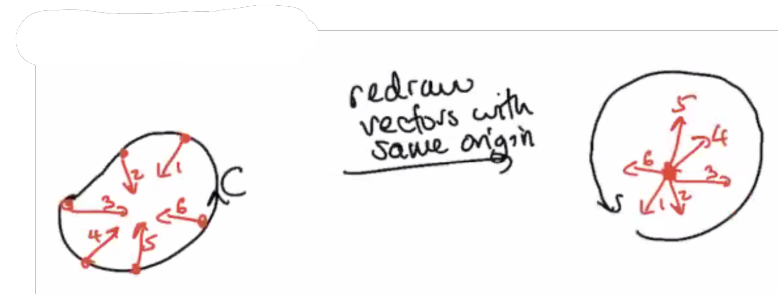


Figure 74: Vectors redrawn.

From this picture, you can see that going along C takes us on a 2π loop in the counterclockwise direction. So the index is $I_c = +1$.

This was a generic stable node shape (all $\dot{\vec{x}}$ vectors pointed inwards). Later,

we'll see that all nodes, centers, spirals, stars, and degenerate nodes have index curve $I_C = +1$.

What if we have a saddle? Some arrows will point inwards, others outwards. We label and recenter the arrows, and this is what we get.

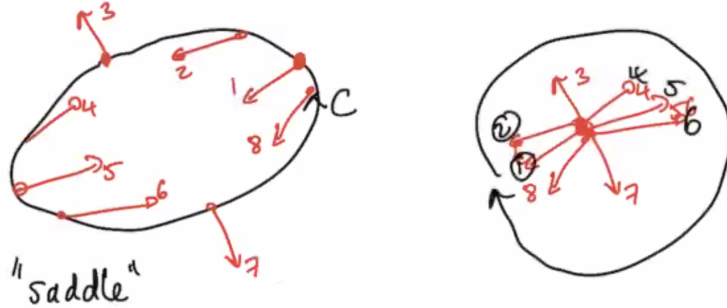


Figure 75: Index of a saddle.

It's a clockwise loop, so the index is -1.

11.1.1 Properties of the index of a curve

If we continuously deform a closed curve C without passing through any fixed points, the deformed curve C' has the same index, i.e $I_C = I'_C$.

A continuous change in C gives a continuous change in ϕ , so the index changes continuously. We know that the index must be an integer, by construction. So it can't jump from one integer to another. Therefore I_C must remain unchanged.

If C does not contain any fixed points, then $I_C = 0$.

Shrink C down to an infinitesimal curve. On this small curve, ϕ is approximately constant, by continuity of the vector field. Then $I_C = [\phi]_C = 0$.

If we map $t \mapsto -t$, then the index of the curve is unchanged.

This map means that the arrows on the vector field change direction by a factor of π . Mapping $t \mapsto -t$ means $\phi \mapsto \phi + \pi$. Therefore $[\phi]_C$ is unchanged, because every ϕ has a uniform π added to it. Then I_C is unchanged

Consider the case where the closed curve C is also a trajectory. Then $I_C = 1$.

As C is a trajectory, the vector field is tangential to C . As \vec{x} winds around C once, the tangent vector rotates in the same sense. So it also rotates once.

11.2 Index of a fixed point

Before, we were looking at the index of a curve.

Let \vec{x}_* be an isolated fixed point. Define the **index** of the fixed point x_* as I_C for any closed curve C that encloses \vec{x}_* and no other fixed points.

Note that for any such C , we can always deform it without changing I_C . So the index is independent of the particular choice of C . Therefore the index of the fixed point is a property only of \vec{x}_* , and not of any closed curves.

Here's a stable node-like example.

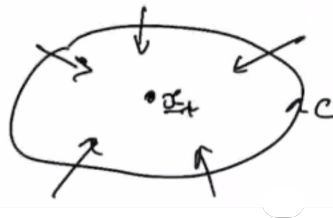


Figure 76: Index of a stable node.

We know the index of a such a curve is 1, so $I(x_*) = 1$ for this fixed point.

Here's an unstable node: If we send $t \mapsto -t$, the unstable node is sent to

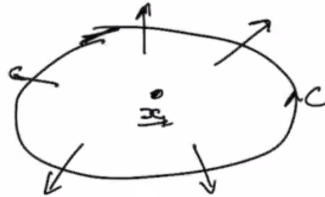


Figure 77: Index of an unstable node.

a stable node. The index is unchanged, so $I(x_*) = 1$ here as well.

Here's a saddle: We showed earlier that the index for any such curve is -1 , so $I(x_*) = -1$.

Note: stable/unstable nodes, spirals, degenerate nodes, stars, and centers all have an index of $+1$. Saddles have an index of -1 .

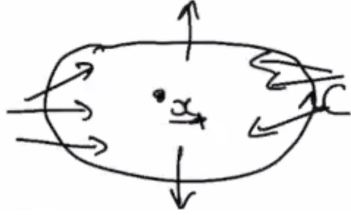


Figure 78: Index of a saddle.

Theorem.

If C is a closed curve that surrounds n isolated fixed points $(\vec{x}_1, \vec{x}_2, \dots, \vec{x}_n)$, then $I_C = I_1 + \dots + I_n$, where I_j is the index of the fixed point \vec{x}_j .

Proof sketch. Deform the closed curve C onto another closed curve Γ without passing through any fixed points. Then $I_C = I_\Gamma$.

We're going to "vacuum-pack" the fixed points by finding a Γ that encloses just the fixed points. See Figure 79.

Then Γ is a closed curve with infinitesimal circles γ_j about x_j , connected by two-way "bridges" of infinitesimal width.

By continuity of the vector field, the contributions over the bridges will cancel each other out. What remains are the circular orbits around the fixed points. Therefore, we're left with

$$I_\Gamma = I_{\gamma_1} + I_{\gamma_2} + \dots + I_{\gamma_n}$$

We also know that each I_{γ_i} is the index of \vec{x}_i . Thus

$$I_C = I_\Gamma = I_1 + \dots + I_n, \quad I_i = I_{\gamma_i}$$

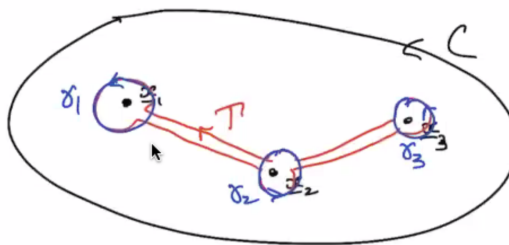


Figure 79: The deformed curve Γ .

Corollary.

A closed *orbit* must contain fixed points, where the sum of the indices of the fixed points is 1.

We know that the index of C , a closed orbit, is +1. The theorem above tells us that $I_C = \sum_k I_j$, so we must have at least one fixed point in the closed orbit, as otherwise the index would be 0. Therefore $\sum_j I_j = +1$.

Corollary.

A closed orbit always contains at least one fixed point.

Corollary.

If a closed orbit contains a saddle (index -1), then there must be some fixed points of index 1 (e.g nodes or spirals) also contained in the orbit.

Example.

Rabbits versus sheep (impossibility of closed orbits).

Recall the model for this scenario:

$$\begin{aligned}\dot{x} &= x(3 - x - 2y) \\ \dot{y} &= y(2 - x - y)\end{aligned}$$

where $x, y \geq 0$.

The fixed points were $(0,0)$, $(3,0)$, $(0,2)$, and $(1,1)$.

$(0,0)$ is an unstable node, so its index is +1.

$(3,0)$ and $(0,2)$ are stable nodes, so they have index +1.

$(1,1)$ is a saddle, so its index is -1.

Could we have a curve C_1 that is a closed orbit and trajectory? The phase portrait looks like Figure 80, with some sample curves drawn in.

C_1 doesn't work, because it contains no fixed points and has index 0. C_2 encloses a saddle, so its index would be -1 and not +1. This also fails. C_3

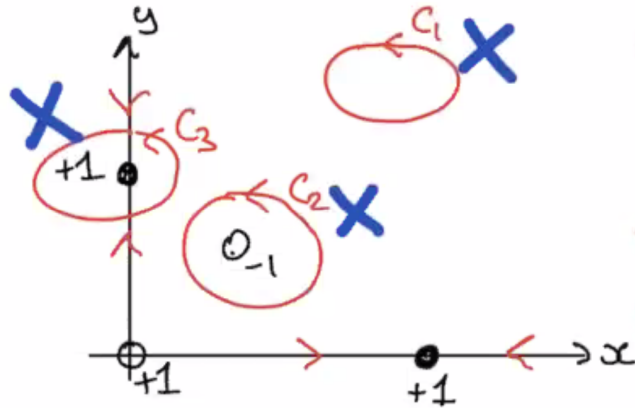


Figure 80: Rabbits and sheep phase portrait.

encloses one of the stable nodes. If it is an orbit, it is a trajectory. But then it would intersect the other trajectories going into the node, and then it's not valid at all.

Other candidate closed orbits all fail for similar reasons.

12 October 8, 2020

Today: **limit cycles**.

A **limit cycle** is an isolated closed trajectory or orbit. Because it's isolated, we preclude families of closed orbits, like centers.

Neighboring trajectories will spiral away or towards the closed orbit.

Like fixed points, limit cycles can be stable or unstable.

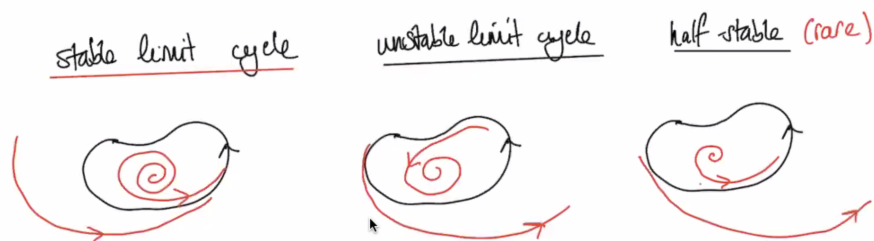


Figure 81: Types of limit cycles.

In a stable limit cycle, trajectories converge towards the limit cycle. For an unstable limit cycle, trajectories spiral outwards. Half-stable limit cycles exist, but they're quite rare. You can spiral into the limit cycle from one direction, and spiral away from the other side.

The form of the limit cycle does not depend on the initial condition (in contrast to centers). It depends purely on the form of the vector field. This gives it a specific “amplitude” and period.

Limit cycles arise in systems with self-sustaining oscillations, like heartbeats or some cases in seismology.

Example.

(In polar coordinates.)

$$\dot{r} = r(1 - r^2)$$

$$\dot{\theta} = 1$$

We have fixed points at $r = 0$ and $r = 1$ by looking at \dot{r} , plotted below.

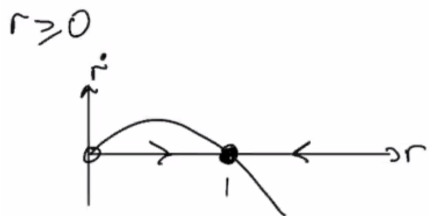


Figure 82: Plot of \dot{r} .

But $r = 1$ isn't a fixed point because $\dot{\theta}$ can never be 0. So $r = 1$ is an attractor but not a fixed point, and $r = 0$ is an unstable fixed point. What we actually end up having at $r = 1$ is a stable limit cycle.

Inside $r = 1$, we have a spiral outwards to an $r = 1$ circle. Outside $r = 1$, we have an inward spiral approaching the same circle. See Figure 83.

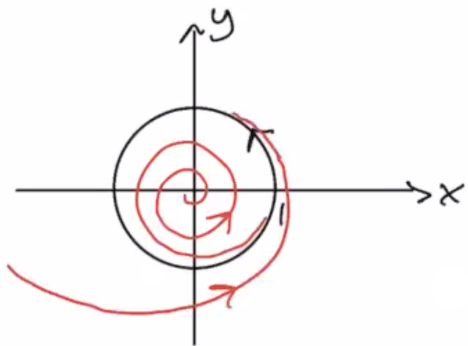


Figure 83: The stable limit cycle.

We can use this plot to find the evolution of x over time on the limit cycle. This is $x(t) = \cos(t)$, so a simple sinusoidal evolution. See Figure 84.

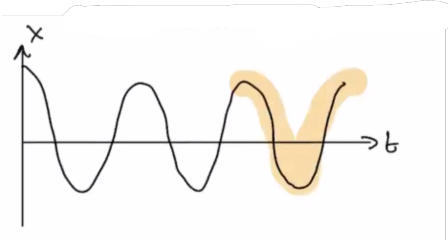


Figure 84: x evolution.

Example.

The van der Pol oscillator.

$$\ddot{x} + \mu(x^2 - 1)\dot{x} + x = 0$$

Here, $\mu \geq 0$ is a parameter.

If we set $\mu = 0$, it's just a harmonic oscillator. But the term gives us a nonlinear drag of sorts. When $(x^2 - 1) > 0$, i.e $|x| > 1$, we have large-amplitude oscillations decaying because the \dot{x} term has a positive coefficient. When $|x| < 1$, we have small-amplitude oscillations growing.

At $|x = 1|$, we have a stable limit cycle. Because of the nonlinearity, it's got a funky shape.

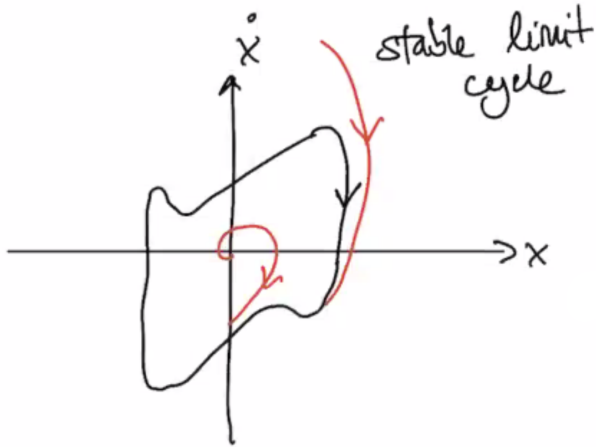


Figure 85: van der Pol stable limit cycle.

If you look at the evolution of $x(t)$, you see a transient followed by a

periodic cycle (not sinusoidal).

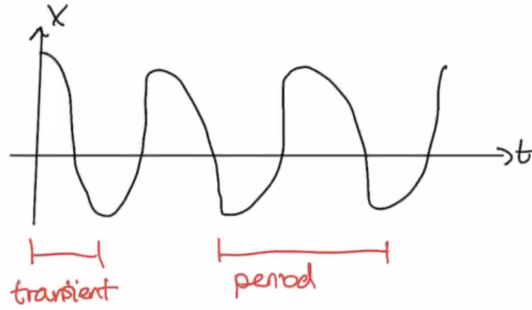


Figure 86: Time evolution of x .

It's a little harder to identify limit cycles than fixed points. If we can locate limit cycles, it's still quite difficult even after that to identify their stability. We're going to see some ways to rule out limit cycles.

12.1 Ruling out limit cycles

There are three common methods for doing this along with index theory.

Gradient systems. The goal here is to find a potential function $V(\vec{x})$ so that $\dot{x} = -\nabla V(\vec{x})$. This is different from before, where we had $\ddot{x} = -V'(\vec{x})$.

We want V to be continuously differentiable, single-valued, and scalar. Then this is called a **gradient system**. We will show that limit cycles are possible in gradient systems.

We'll proceed by contradiction. Suppose we have a limit cycle with period $T > 0$. Then $\Delta V = V(\vec{x}(T)) - V(\vec{x}(0)) = 0$. But we also have, using the fundamental theorem of calculus,

$$\Delta V = \int_0^T \frac{d}{dt} V(\vec{x}(t)) dt = \int_0^T \dot{x}(t) \cdot \vec{\nabla} V(\vec{x}(t)) dt$$

where in the second equality we have used the chain rule. We know $\dot{x} = -\nabla V(\vec{x})$, so we have

$$\int_0^T -|\dot{x}|^2 dt < 0$$

as $|\dot{x}| < 0$ for all t (if we do not have the trivial case of a fixed point). So we have a contradiction, because if there is a limit cycle the integral should be 0.

Therefore limit cycles cannot exist in gradient systems.

This is a nice formulation but it's a bit of a pain to find $V(x)$ that work for these.

Example.

$$\begin{aligned}\dot{x} &= \sin y = -\frac{\partial V}{\partial x} \\ \dot{y} &= x \cos y = -\frac{\partial V}{\partial y}\end{aligned}$$

If we integrate this, we get

$$V(x, y) = -x \sin y + \text{constant}$$

which shows there are no limit cycles.

Energy cycles. We'll create an energy-like function and show that it is always decreasing, so that then there can be no closed orbits.

Example.

We want to show closed orbits do not exist for this system:

$$\ddot{x} + \dot{x}^3 + x = 0$$

Consider the quantity

$$E(x, \dot{x}) = \frac{1}{2}x^2 + \frac{1}{2}\dot{x}^2$$

The first term here is a potential energy, and the second is a kinematic energy.

We want to show that along trajectories, E is decreasing. Then there can't be a periodic quantity, as is required for limit cycles and closed orbits.

Note the following result.

$$\frac{dE}{dt} = \frac{d}{dt}\left(\frac{1}{2}x^2 + \frac{1}{2}\dot{x}^2\right) = x\dot{x} + \dot{x}\ddot{x} = \dot{x}(x + \ddot{x})$$

From the ODE, $x + \ddot{x} = -\dot{x}^3$. So,

$$\frac{dE}{dt} = -\dot{x}^4 \leq 0$$

with equality only if $\dot{x} = 0$ for all time.

As with the potential, a periodic solution with period T requires $\Delta E = 0$.

But

$$\Delta E = \int_0^T \frac{dE}{dt} dt < 0$$

except at fixed points. So this is a contradiction, and closed orbits cannot exist in this case.

So if there's any energy dissipation, we can't have any periodic orbits.

12.1.1 Lyapunov functions

Our aim with this is to construct an energy-like quantity that decreases along trajectories. If we can find a **Lyapunov function**, then closed orbits do not exist.

Consider $\dot{\vec{x}} = \vec{f}(\vec{x})$ with a fixed point \vec{x}_* .

A Lyapunov function $V(\vec{x})$ is continuously differentiable and real. It must also satisfy two properties:

1. $V(\vec{x}) > 0$ for all $\vec{x} \neq \vec{x}_*$. ($V(\vec{x}_*) = 0$).
2. $\frac{d}{dt}V(\vec{x}(t)) < 0$ for all $\vec{x} \neq \vec{x}_*$. (It's 0 at $\vec{x} = \vec{x}_*$)

If you construct a Lyapunov function, you can show that the fixed point is not only a local attractor, but a *global attractor*. It turns out these functions have a bowl-like shape and \vec{x}_* lies at the bottom. Then we cannot have a closed orbit.

You can apply a similar argument as before to show that a system with a Lyapunov function cannot have closed orbits.

How do we construct one of these? We'll use sum of squares. Consider the system

$$\begin{aligned}\dot{x} &= -x + 4y \\ \dot{y} &= -x - y^3\end{aligned}$$

We have one fixed point at $(0, 0)$, and this is the only fixed point.

Let's try a Lyapunov function of the form $V(x, y) = x^2 + ay^2$. This is a paraboloid with a parameter a that we need to determine.

We need $a > 0$ if $V(x, y)$ is to have the bowl-like shape. Now we want, for $x, y \neq 0$,

$$\frac{dV}{dt} < 0$$

Differentiating, we get

$$\begin{aligned}\frac{dV}{dt} &= 2x\dot{x} + 2ay\dot{y} \\ &= 2x(4y - x) - 2ay(x + y^3) \\ &= -2[x^2 - 4xy + ay^4 + axy]\end{aligned}$$

We want to choose a so that the terms with xy cancel. If they remain in the expression, and if $x < 0$ and $y > 0$ for example, we might have that the overall derivative is positive, which means it can't be a Lyapunov function.

So we set $a = 4$. Then,

$$\frac{dV}{dt} = -2(x^2 + 4y^2) < 0$$

for $x, y \neq 0$.

So we have constructed a Lyapunov function, implying that $(0, 0)$ is globally stable and thus the system has no closed orbits.

12.1.2 Dulac's criterion

Dulac's criterion.

Let $\dot{\vec{x}} = \vec{f}(\vec{x})$ be a continuously differentiable vector field on a simply-connected subset R of \mathbb{R}^2 .

If there exists a continuously differentiable real-valued scalar function $g(\vec{x})$ such that $\vec{\nabla} \cdot (g\dot{\vec{x}})$ has one sign throughout R , then there are no closed orbits lying entirely within R .

Note that we're not looking at the entire plane here! Let's see why this is true.

Suppose a closed orbit C lies entirely within R . Define A as the region enclosed by C . By Green's Theorem,

$$\iint_A \vec{\nabla} \cdot (g\dot{\vec{x}}) dA = \oint_C g\vec{x} \cdot \vec{n}$$

where \vec{n} is the outward pointing normal vector.

If C is a closed orbit, it's a trajectory. Then $\dot{\vec{x}}$ lies tangential to the trajectory. Then it is perpendicular to \vec{n} . So the integral is

$$\oint_C g \times 0 dA = 0$$

So if $\vec{\nabla} \cdot (g\dot{x})$ is either > 0 or < 0 in A , the integral will not evaluate to 0.

This is a contradiction! Then C must not be a trajectory. A closed orbit cannot then exist in R . \square

There are some typical functions for $g(x, y)$ that often work.

$$\begin{aligned} g &= 1 \\ g &= x^{-a}y^b \\ g &= e^{ax} \\ g &= e^{by} \end{aligned}$$

Example.

Show that the following system has no closed orbits in the region R where $x, y > 0$.

$$\begin{aligned} \dot{x} &= x(2 - x - y) \\ \dot{y} &= y(4x - x^2 - 3) \end{aligned}$$

It's not immediately obvious looking at this what to pick for g . Let's try to find a g that will cancel the factors of x and y in front of the parenthetical terms.

Let's try $g(x, y) = \frac{1}{xy}$.

$$\begin{aligned} \vec{\nabla} \cdot (g\dot{x}) &= \frac{\partial}{\partial x} \left(g\dot{x} + \frac{\partial}{\partial y} (g\dot{y}) \right) \\ &= \frac{\partial}{\partial x} \left(\frac{2-x-y}{y} \right) + \frac{\partial}{\partial y} \left(\frac{4x-x^2-3}{x} \right) \\ &= -\frac{1}{y} < 0 \quad \text{for all } x, y > 0 \end{aligned}$$

The divergence is negative here, so it has the same sign everywhere. Then by Dulac's criterion, there are no closed orbits in this quadrant R .

12.2 Poincaré-Bendixson theorem

This is a result that proves that closed orbits do exist!

Suppose that

1. R is a closed, bounded subset of \mathbb{R}^2 (don't need simply-connected)

2. $\dot{\vec{x}} = \vec{f}(\vec{x})$ is a continuously differentiable vector field on an open set contained in R
3. R does not contain any fixed points
4. there is a trajectory C that is “confined” in R for all t

Then, either C is a closed orbit or approaches a closed orbit as $t \rightarrow \infty$. As a consequence, we conclude that R contains a closed orbit.

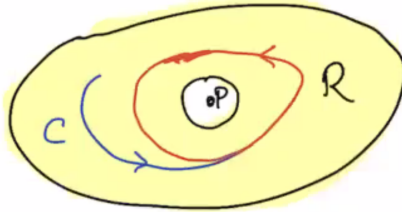


Figure 87: Visual representation of what's happening.

In the figure, P is a fixed point but not in R .

Next time we'll talk about how to construct a region R that works for this.

13 October 13, 2020

The take-home exam goes up today! You can either ask for clarification about a question, about material covered in lecture, or about material as it pertains to a question. No clever workarounds allowed!

Last time we were looking at methods of showing that limit cycles don't exist. A limit cycle exists when neighboring trajectories are not closed orbits – this is why centers don't count.

We went over gradient systems, Lyapunov functions, and Dulac's criterion. Today we'll look more into the Poincaré-Bendixson Theorem, which gives us conditions for the existence of limit cycles.

Let's restate the Poincaré-Bendixson theorem. Suppose that

1. R is a closed, bounded subset of \mathbb{R}^2 (don't need simply-connected)
2. $\dot{\vec{x}} = \vec{f}(\vec{x})$ is a continuously differentiable vector field on an open set contained in R
3. R does not contain any fixed points
4. there is a trajectory C that is “confined” in R for all t

Then, either C is a closed orbit or approaches a closed orbit as $t \rightarrow \infty$. As a consequence, we conclude that R contains a closed orbit.

We want R to be a “trapping” region, i.e. trajectories can enter but cannot leave. In the picture from last time, where we punctured a hole in R to hold the fixed point, we probably want that fixed point to be a repeller.

Example.

Polar coordinates, with $0 < \mu < 1$.

$$\begin{aligned}\dot{r} &= r(1 - r^2) + \mu r \cos \theta \\ \dot{\theta} &= 1\end{aligned}$$

Our aim is to find a trapping region where we can apply the Poincaré–Bendixson theorem. We try to find an annular trapping region.

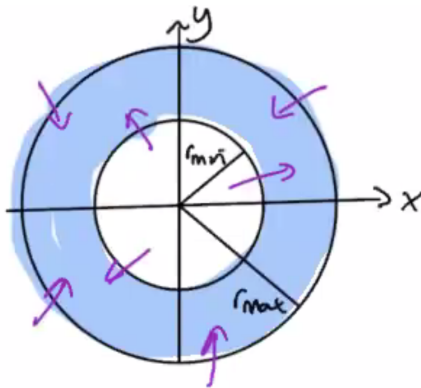


Figure 88: Annular trapping region.

There's one circle of radius r_{\max} and another of radius r_{\min} . We want the region between them to be a trapping region, so that $\dot{r} > 0$ for $r = r_{\min}$ and all θ . Similarly, we want $\dot{r} < 0$ for $r = r_{\max}$ and all θ .

We want to find the possible values of r_{\min} and r_{\max} .

Using the given equations, the first condition on \dot{r} and r_{\min} gives us

$$r_{\min}(1 - r_{\min}^2) + \mu r_{\min} \cos \theta > 0$$

We can put in the minimum value of $\cos \theta$ to give us a strict requirement.

$$(1 - r_{\min}^2) - \mu > 0$$

So as long as $0 < r_{\min} < \sqrt{1 - \mu}$, we have a satisfactory r_{\min} .

For r_{\max} ,

$$r_{\max}(1 - r_{\max}^2) + \mu r_{\max} \cos \theta < 0$$

So this is satisfied for all θ if we choose the maximum value for $\cos \theta$, which is 1. Then,

$$1 - r_{\max}^2 + \mu < 0$$

Thus $r_{\max} > \sqrt{1 + \mu}$.

For example, we have a trapping region where $0.99\sqrt{1 - \mu} < r < 1.01\sqrt{1 + \mu}$.

As $\dot{\theta} = 1$ everywhere, this region does not contain any fixed points. So we have satisfied the conditions for the Poincaré-Bendixson theorem, and a closed orbit exists in the trapping region.

Example.

The system

$$\begin{aligned}\dot{x} &= -x + ay + x^2y \\ \dot{y} &= b - ay - x^2y\end{aligned}$$

where $a, b > 0$ and $x, y > 0$.

Let's describe the phase portrait for this system.

The nullcline for $\dot{x} = 0$ is $y = \frac{x}{a + x^2}$.

The $\dot{y} = 0$ nullcline is $y = \frac{b}{a + x^2}$.

There's a fixed point where the two nullclines intersect. We can use the nullclines to identify the positive and negative flow directions for x and y as well. This indicates a swirling flow, suggesting orbits!

Trajectories that enter the region $x > 0, y > 0$ by crossing in from $x = 0$ or $y = 0$ satisfy the requirement for one side of the boundary: all trajectories come in and none go out.

Observe that $\dot{x} + \dot{y} = b - x$. Along trajectories,

$$\frac{dy}{dx} = \frac{\dot{y}}{\dot{x}} < -1 \iff \dot{y} + \dot{x} < 0$$

Note $\dot{y} + \dot{x} = b - x < 0$ for $x > b$, i.e for $x > b$, $\frac{dy}{dx} < -1$.

We can use this to define the other side of the region boundary with a diagonal line.

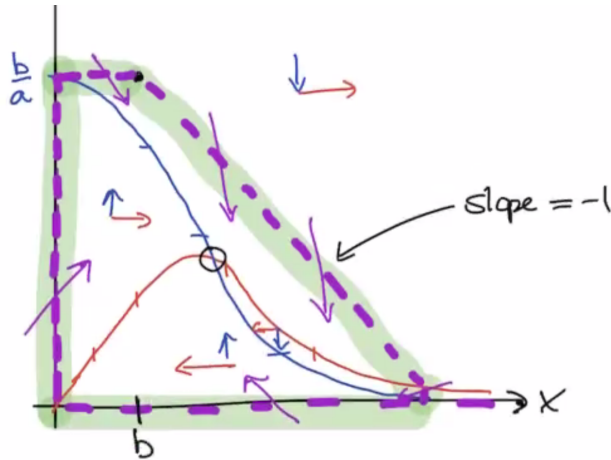


Figure 89: Trapping region.

Note that the region thus defined contains a fixed point! So we have to puncture an infinitesimal hole at the fixed point.

For parameters a, b such that the fixed point is a repeller (an unstable spiral, an unstable node, etc) we have defined a trapping region that does not contain a fixed point.

Then the Poincaré-Bendixson theorem states that there is a limit cycle in the trapping region.

It's critical that we choose the right a, b so that the fixed point is a repeller. Otherwise trajectories in the region will approach the fixed point, leaving the trapping region, so we wouldn't have limit cycles. This requires some linear stability analysis.

13.1 Liénard's theorem

A **Liénard system** has the canonical form

$$\ddot{x} + f(x)\dot{x} + g(x) = 0$$

We've seen this already with nonlinear damping and nonlinear spring forces, like the van der Pol oscillator where $f(x) = \mu(x^2 - 1)$ and $g(x) = x$.

Liénard's theorem. Consider the equation $\ddot{x} + f(x)\dot{x} + g(x) = 0$. Suppose that f and g satisfy the following conditions:

1. $f(x)$ and $g(x)$ are continuously differentiable for all x
2. $g(-x) = -g(x)$ for all x (i.e g is odd)

3. $g(x) > 0$ for all $x > 0$
4. $f(-x) = f(x)$ for all x (i.e f is even)
5. the odd function

$$F(x) = \int_0^x f(u) du$$

has exactly one positive zero at $x = a$, is negative for $0 < x < a$, is positive and nondecreasing for $x > a$, and $F(x) \rightarrow \infty$ as $x \rightarrow \infty$

Then the system has a unique stable limit cycle surrounding the origin in the phase plane.

A canonical $F(x)$ looks something like this.

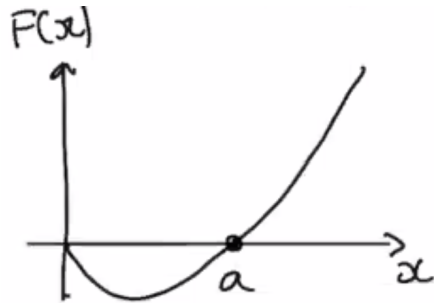


Figure 90: Canonical $F(x)$.

Example.

The van der Pol oscillator.

We have $f(x) = \mu(x^2 - 1)$ and $g(x) = x$.

f and g are clearly continuously differentiable. The conditions on g are satisfied: it is odd and positive for $x > 0$. We can see f is even. We just have to check the last condition.

$$F(x) = \mu \int_0^x u^2 - 1 du = \mu \left(\frac{1}{3}x^3 - x \right)$$

This is a positive cubic function. When $x > 0$, F is negative between 0 and $\sqrt{3}$. For $x > \sqrt{3}$, F is positive nondecreasing.

So the Liénard theorem conditions are satisfied, and we thus have a stable limit cycle about the origin. We simulated this on Problem set 4!

13.2 Relaxation oscillators

Our goal is now to analytically determine the approximate period and amplitude of a limit cycle.

Let's look at the van der Pol oscillator again, in the strongly nonlinear limit (when $\mu \gg 1$). If we were to simulate this and look at the dynamics of x and t , we would see something like this.

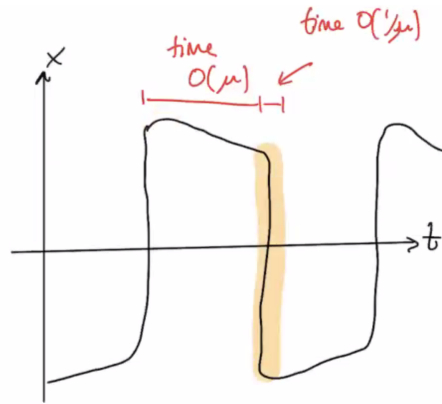


Figure 91: van der Pol x .

x changes slowly over a time of $O(\mu)$, and then rapidly changes over a time of $O(1/\mu)$.

This is called a **relaxation oscillator** because of the rapid change (highlighted in the figure).

Recall the full equation for the van der Pol equation.

$$\ddot{x} + \mu\dot{x}(x^2 - 1) + x = 0$$

Note that

$$\frac{d}{dt} \left(\dot{x} + \mu \left(\frac{1}{3}x^3 - x \right) \right) = \ddot{x} + \mu\dot{x}(x^2 - 1)$$

This is handy, because the differential equation tells us this whole thing is equal to $-x$. So let's define

$$w = \dot{x} + \mu \left(\frac{1}{3}x^3 - x \right)$$

Then we have a coupled system.

$$\dot{x} = w - \mu F(x) \quad \text{where } F(x) = \frac{1}{3}x^3 - x$$

$$\dot{w} = -x$$

Define $w = \mu y$. Now,

$$\begin{aligned}\dot{x} &= \mu(y - F(x)) \\ \dot{y} &= -\frac{x}{\mu}\end{aligned}$$

Let's draw the phase portrait now.

The $\dot{x} = 0$ nullcline is $y = F(x)$. The $\dot{y} = 0$ nullcline is $x = 0$. We can label the flow directions.

Note that μ determines time scales.

Observe that if $|y - F(x)| = O(1)$, then $\dot{x} = O(\mu)$ and $\dot{y} = O(1/\mu)$. So \dot{x} is large, and \dot{y} is small. Then \dot{y}/\dot{x} will be very small.

Also, when $|y - F(x)| = O(1/\mu^2)$, then $\dot{x} = O(1/\mu)$ and $\dot{y} = O(1/\mu)$. Then \dot{y}/\dot{x} is $O(1)$, so the trajectory moves slowly.

This gives us a limit cycle! (Note that it is about the origin.)

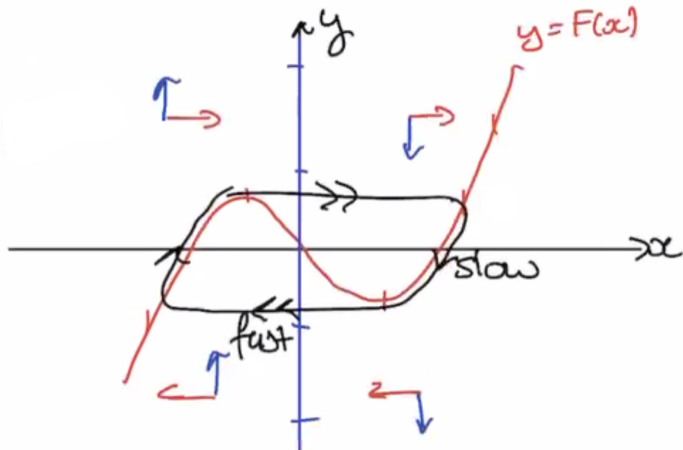


Figure 92: Limit cycle sketch.

Now we want to know how long it takes to complete a loop of the limit cycle. What is its period for $\mu \gg 1$?

We need to work out the start and end points geometrically. As the slow branches dominate the period, we have

$$T = 2 \times \text{time taken on each slow branch}$$

In other words,

$$T \approx 2 \int_{x_A}^{x_B} \frac{dt}{dx} dx$$

where x_A is where the trajectory crosses the nullcline, and x_B is where it rounds the corner on the slow branch.

Note that near the nullcline $\dot{x} = 0$, $y \approx F(x)$. Then $\dot{y} = \dot{x}F'(x) = (x^2 - 1)\dot{x}$.

Also, $\dot{y} = -x/\mu$. We can equate these two forms to get

$$-\frac{x}{\mu} \approx \dot{x}(x^2 - 1) \implies \dot{x} \approx \frac{-x}{\mu(x^2 - 1)}$$

So when μ is large, \dot{x} is small. This approximation is valid near $\dot{x} = 0$.

Then we have

$$T \approx 2 \int_{x_A}^{x_B} -\mu \frac{x^2 - 1}{x} dx$$

We need to find x_A, x_B . $F(x)$ has its minimum at $x_B = 1$. We can use geometry to find x_A . We want $F(x_A) = F(-x_B)$, so solving this, we get $x_A = 2$.

Then we have

$$\begin{aligned} T &\approx -2\mu \int_2^1 x - \frac{1}{x} dx \\ &\approx 2\mu \int_1^2 x - \frac{1}{x} dx \\ &= 2\mu \left[\frac{1}{2}x^2 - \log x \right]_{x=1}^2 \\ &\implies T \approx \mu [3 - 2\log 2] \end{aligned}$$

So the period grows linearly with μ .

We can also get the approximate maximum value of x . That's going to be approximately x_A , so its amplitude is about 2.

13.3 Weakly nonlinear oscillators

We consider equations of the form

$$\ddot{x} + x + \epsilon h(x, \dot{x}) = 0$$

for $0 < \epsilon \ll 1$ and a smooth function h .

For example, the van der Pol equation $\ddot{x} + x + \epsilon \dot{x}(x^2 - 1) = 0$.

Another example: the Duffing equation, $\ddot{x} + x + \epsilon x^3 = 0$.

These systems have a stable limit cycle. What is the period/amplitude?

To answer this, we need the method of multiple scales. Stay tuned for next time!

14 October 20, 2020

Last time we looked at the van der Pol oscillator in the limit of strong nonlinearity. Now we'll look at weakly nonlinear oscillators.

Recall that we're looking at systems of the form

$$\ddot{x} + x + \epsilon h(x, \dot{x}) = 0$$

We can look at the weak van der Pol oscillator, $\ddot{x} + x + \epsilon \dot{x}(x^2 - 1) = 0$.

Our goal is to use asymptotic techniques to determine the amplitude and period of the limit cycles in these systems.

Example.

Cautionary example! A damped oscillator where regular perturbation series fail.

$$\ddot{x} + 2\epsilon \dot{x} + x = 0 \quad x(0) = 0, \dot{x}(0) = 1$$

Power series in ϵ : $x(t) \sim x_0(t) + \epsilon x_1(t) + \epsilon^2 x_2(t) + O(\epsilon^3)$

We can substitute this ansatz into the differential equation.

$$\frac{d^2}{dt^2}(x_0 + \epsilon x_1 + O(\epsilon^2)) + 2\epsilon \frac{d}{dt}(x_0 + \epsilon x_1 + O(\epsilon^2)) + (x_0 + \epsilon x_1 + O(\epsilon^2)) = 0$$

Now we'll gather together powers of ϵ . If this holds for all values of ϵ , the coefficients on each such term should be 0.

$$(\ddot{x}_0 + x_0) + \epsilon(\ddot{x}_1 + 2\dot{x}_0 + x_1) = O(\epsilon^2)$$

Repeat this for initial conditions. The $O(1)$ terms give us the following equation.

$$\ddot{x}_0 + x_0 = 0 \quad x_0(0) = 0, \dot{x}_0(0) = 1$$

The $O(\epsilon)$ terms give the following.

$$\ddot{x}_1 + x_1 = -2\dot{x}_0 \quad x_1(0) = 0, \dot{x}_1(0) = 0$$

We hope to neglect the $O(\epsilon^2)$ terms as a small correction.

We can solve the $O(1)$ equation for x_0 . Then we can use that result to solve the $O(\epsilon)$ equation to get a result for x_1 . If we wanted to compute higher order corrections, we would just keep going like this.

The solution to the $O(1)$ equation is

$$x_0(t) = A \cos(t) + B \sin(t)$$

Adding the initial conditions gives us $x_0(t) = \sin(t)$.

Now it's time for the "cautionary" part of this example. Let's put this into the $O(\epsilon)$ equation. Then we get

$$\ddot{x}_1 + x_1 = -2 \cos(t)$$

This is resonant forcing on the RHS! We call it a **secular term**. If we solve, we get

$$x_1(t) = -t \sin(t)$$

But this blows up as $t \rightarrow \infty$!

Our ansatz was $x(t) \sim x_0(t) + \epsilon x_1(t) + O(\epsilon^2)$. Substituting,

$$x(t) \sim \sin(t) - \epsilon t \cos(t) + O(\epsilon^2)$$

There is an issue here! In creating the ansatz, we assumed that x_0 and x_1 were about the same size, because that's the only way ϵ acts as a small correction. Making x_1 blow up invalidates this – it only works at small t , where $\epsilon t \ll 1$. This means t is $O(1)$.

Clearly we're missing some physics that is necessary to describe the overall long-time dynamics of this system.

Recall that we're looking at the equation

$$\ddot{x} + 2\epsilon \dot{x} + x = 0 \quad \text{for } \epsilon \ll 1$$

Suppose there is no spring force. Then we have

$$\ddot{x} + 2\epsilon \dot{x} = 0$$

Then $x = 1$ and $x = e^{-2\epsilon t}$ are both solutions. In the second case, the damping timescale is $\frac{1}{2\epsilon}$, which is $O(1/\epsilon)$. This is *slow decay*.

If we have no damping, the equation is

$$\ddot{x} + x = 0$$

and the solutions are $x = \cos t$ or $x = \sin t$. The timescale here is $O(1)$.

So there are two timescales! A faster timescale for oscillations, and a slower timescale for the damping.

This brings us to the **method of multiple scales**. Let's define a fast timescale $\tau = t$, and a slow timescale $T = \epsilon t$. This is when $T = O(1)$ and $t = O(1/\epsilon)$.

We now try an expansion of the form

$$x(t) \sim x_0(\tau, T) + \epsilon x_1(\tau, T) + O(\epsilon^2)$$

The use of two timescales will allow us to come up with a solution that's valid over longer times!

Given our definitions of the timescales, we can use the chain rule to write

$$\frac{dx_0}{dt} = \frac{\partial x_0}{\partial \tau} \frac{\partial \tau}{\partial t} + \frac{\partial x_0}{\partial T} \frac{\partial T}{\partial t} = \frac{\partial x_0}{\partial \tau} + \epsilon \frac{\partial x_0}{\partial T}$$

So now we can write the derivatives in terms of these values.

Note though, that this takes us from ODEs to PDEs. But this does give us better results. The algebra becomes quite horrible because there are ϵ and time derivatives floating around, but eventually we get

$$[\partial_{\tau\tau}x_0 + x_0] + \epsilon[\partial_{\tau\tau}x_1 + x_1 + 2\partial_{\tau T}x_0 + 2\partial_Tx_0] = O(\epsilon^2)$$

At $\tau = T = 0$, we can use the initial conditions to get

$$\begin{aligned} 0 &= x_0 + \epsilon x_1 \\ 1 &= \partial_\tau x_0 + \epsilon[\partial_T x_0 + \partial_\tau x_1] \end{aligned}$$

This gives us (to leading order)

$$\partial_{\tau\tau}x_0 + x_0 = 0 \quad x_0(0, 0) = 0, \partial_\tau x_0(0, 0) = 1$$

The solution is then

$$x_0(\tau, T) = A(T) \sin \tau + B(T) \cos \tau$$

The initial conditions yield $A(0) = 1$ and $B(0) = 0$.

Now let's look at the piece that's $O(\epsilon)$. We get

$$\partial_{\tau\tau}x_1 + x_1 = -2(\partial_{\tau T}x_0 + \partial_Tx_0)$$

with initial conditions $x_1(0, 0) = 0$ and $\partial_\tau x_1(0, 0) = -\partial_T x_0(0, 0)$.

Substituting in the leading-order solution, we get

$$\partial_{\tau\tau}x_1 + x_1 = -2(A'(T) + A(T)) \cos \tau + 2(B'(T) + B(T)) \sin \tau$$

Note that we again have secular terms on the RHS! But this is where the second timescale gives us extra flexibility.

For the expansion to be valid, we set the coefficients to be zero.

$$A'(T) + A(T) = B'(T) + B(T) = 0$$

Remember we had $A(0) = 1$ and $B(0) = 0$. Then, solving,

$$A(T) = e^{-T} \quad B(T) = 0$$

So the leading order solution is

$$x_0(\tau, T) = e^{-T} \sin \tau$$

and the approximate solution is

$$x(t, \epsilon) = e^{-\epsilon t} \sin t + O(\epsilon)$$

This is a solution that is qualitatively and quantitatively accurate!

Note that we never actually solved for x_1 . We use the RHS of that equation, the secular terms, to complete the solution for x_0 . It's kind of a bootstrap process.

14.1 Weakly damped van der Pol oscillator

The $O(1)$ equation is

$$\partial_{\tau\tau} x_0 + x_0 = 0$$

and the $O(\epsilon)$ equation is

$$\partial_{\tau\tau} x_1 + x_1 = -2\partial_{\tau T} x_0 - (x_0^2 - 1)\partial_{\tau} x_0$$

The leading order solution from the first equation is

$$x_0(\tau, T) = A(T)e^{i\tau} + \bar{A}(T)e^{-i\tau}$$

Putting this into the next equation, we get

$$\partial_{\tau\tau} x_1 + x_1 = \{ie^{i\tau}[-2A' - A(|A|^2 - 1)] + \text{c.c.}\} + \text{non-secular terms}$$

This takes a bunch of algebra, but that's what we get.

We need to set the coefficient of the secular term to 0, so we get

$$2A' = A - A|A|^2$$

Here, $A' = dA/dT$. This is the Stewart-Landau equation. Relating this to real quantities, we can write

$$A(T) = r(T)e^{i\phi(T)}$$

Then

$$\frac{d}{dT}(re^{i\phi}) = \left(\frac{dr}{dT} + ir\frac{d\phi}{dT} \right) e^{i\phi(T)}$$

Then we get

$$2r' = r - r^3$$

$$\phi' = 0$$

So the phase must be constant. The stable fixed point here is $r = 1$ and $\phi = \phi_0$.

Then the solution is

$$x_0(\tau, T) = [e^{i(\tau+\phi_0)} + e^{-i(\tau+\phi_0)}] = 2\cos(\tau + \phi_0)$$

That's the leading-order part. Finally, then, we have

$$x(t) = 2\cos(t + \phi_0) + O(\epsilon^2)$$

14.2 Bifurcations in 2D systems

Here, we have topological changes in the phase space as a parameter is varied. “Topological change” means something like adding fixed points or closed orbits.

14.2.1 Saddle-node bifurcations

These occur when fixed points are created or destroyed.

For example,

$$\begin{aligned}\dot{x} &= \mu - x^2 \\ \dot{y} &= -y\end{aligned}$$

We can draw the phase portrait for $\mu > 0$. We get a stable node at $x = \sqrt{\mu}, y = 0$ and a saddle at $x = -\sqrt{\mu}, y = 0$.

As μ decreases, the “window” between the fixed points gets squashed until it vanishes. We end up with a half-stable fixed point when $\mu = 0$.

When $\mu < 0$, there are no fixed points. We have x and y always decreasing. We end up with a “ghost” of the fixed point near the origin when μ is small and negative.

In general, we have a saddle-node bifurcation when an $\dot{x} = 0$ nullcline and a $\dot{y} = 0$ nullcline intersect tangentially. Fixed points collide and annihilate each other at the tangential intersection.

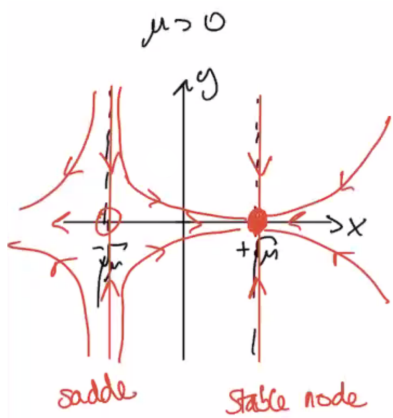


Figure 93: $\mu > 0$ phase portrait.

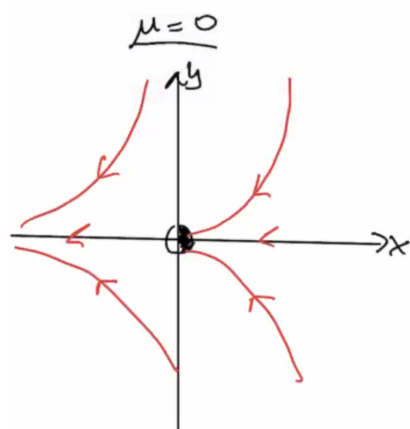


Figure 94: $\mu = 0$ phase portrait.

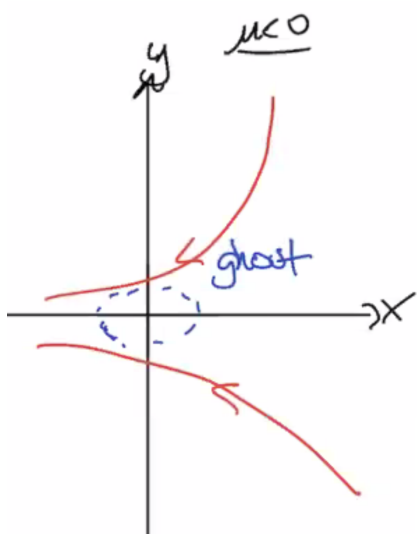


Figure 95: $\mu < 0$ phase portrait.

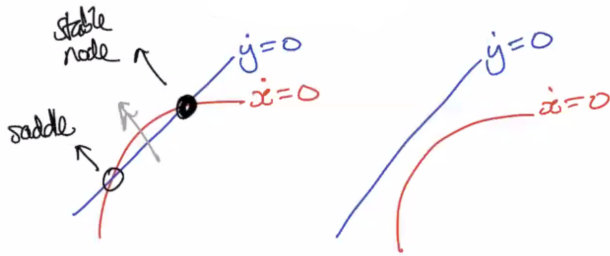


Figure 96: Tangential intersection for saddle-node bifurcations.

Example.

An example of such a bifurcation.

$$\begin{aligned}\dot{x} &= -ax + y \\ \dot{y} &= \frac{x^2}{1+x^2} - by\end{aligned}$$

where $x, y > 0$ and the parameters $a, b > 0$.

We can draw in the nullclines and do linear stability analysis to get that there's a stable node at the origin and at the outermost fixed point. There's a saddle in between.

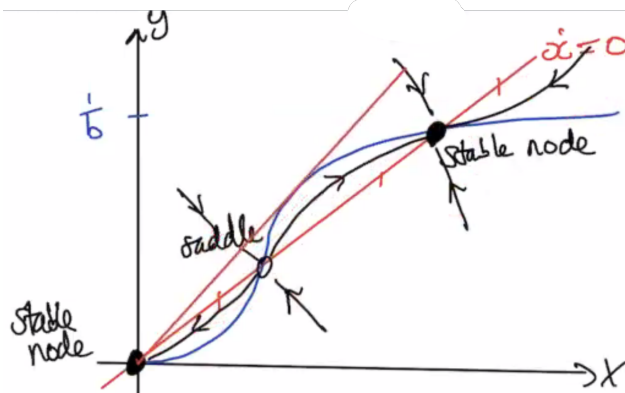


Figure 97: Collision of saddle and node as a increases.

From the figure, it's clear that as we vary a (keeping b fixed), we get a saddle node bifurcation. We go from 3 fixed points to 2 at the tangent point, and then to 1.

The fixed points satisfy

$$ax = \frac{1}{b} \frac{x^2}{1+x^2}$$

This implies that either $x = 0$, or

$$ab = \frac{x}{1+x^2}$$

So $abx^2 - x + ab = 0$.

The two fixed points collide when the discriminant vanishes here. This gives the condition $1 = (2ab)^2$. As $a, b > 0$, we have a saddle-node bifurcation when

$$a = \frac{1}{2b}$$

for b fixed.

See Central Manifold Theory for more on this method.

15 October 22, 2020

Today we'll look at other bifurcations in 2D.

Transcritical bifurcations are the exchange of a saddle and stable node. The canonical form is

$$\begin{aligned}\dot{x} &= \mu x - x^2 \\ \dot{y} &= -y\end{aligned}$$

We could also have supercritical pitchforks.

$$\begin{aligned}\dot{x} &= \mu x - x^3 \\ \dot{y} &= -y\end{aligned}$$

We go from a stable node to a saddle and the creation of a pair of stable nodes. This happens as $\mu < 0 \rightarrow \mu > 0$.

The subcritical pitchfork looks like

$$\begin{aligned}\dot{x} &= \mu x + x^3 \\ \dot{y} &= -y\end{aligned}$$

Here, we go from a stable node and a pair of saddles when $\mu < 0$ to just a saddle when $\mu > 0$.

Recall that a stable node has two negative eigenvalues, and a saddle has 1 negative eigenvalue and 1 positive eigenvalue. So when the stability changes, one eigenvalue passes through 0 at the bifurcation.

If we have a pair of complex-conjugate eigenvalues that destabilize as μ increases, we have a **Hopf** bifurcation. This describes oscillatory behavior,

like spirals. If $\mu < 0$, we have a stable spiral. When $\mu > 0$, it's an unstable spiral.

In a **supercritical Hopf bifurcation**, when $\mu < 0$, we have a stable spiral. When $\mu > 0$, we have an unstable spiral and *also* a small-amplitude, stable limit cycle that forms about the fixed point.

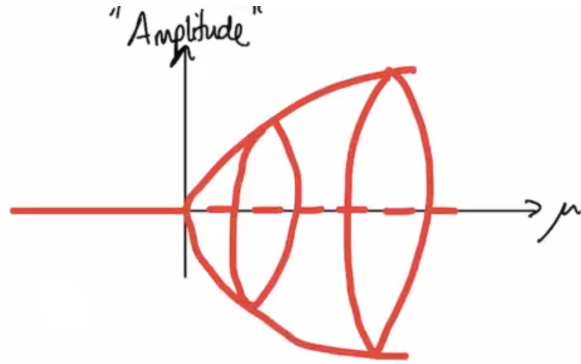


Figure 98: Bifurcation diagram.

For a **subcritical Hopf bifurcation**, when $\mu < 0$ there's a stable spiral and an unstable limit cycle. When $\mu > 0$, we have an unstable spiral.

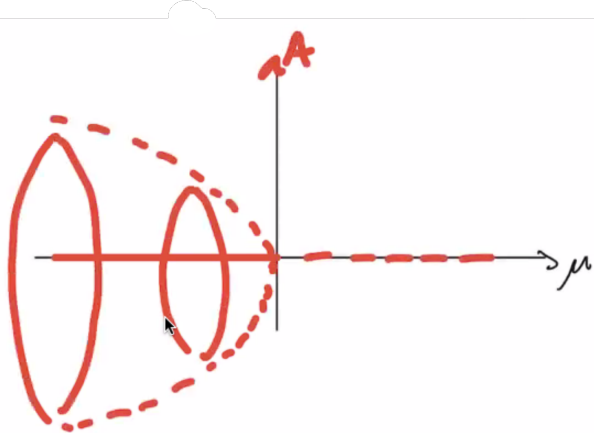


Figure 99: Bifurcation diagram.

Example.

Supercritical Hopf.

$$\begin{aligned}\dot{r} &= \mu r - r^3 \\ \dot{\theta} &= \omega + br^2\end{aligned}$$

What do the parameters mean? μ describes the growth rate away from

the origin, ω is the natural frequency, and b determines the change in frequency depending on the distance from the origin.

If we linearize about the origin, we get

$$\dot{r} \approx \mu r$$

$$\dot{\theta} = \omega$$

We can transform this using Cartesian coordinates, giving

$$\dot{x} \approx \mu x - \omega y$$

$$\dot{y} \approx \omega x + \mu y$$

We expect to have a bifurcation as μ goes from negative to positive, because the μr term determines whether the origin repels or attracts trajectories.

In the Cartesian system, we get that the eigenvalues are $\mu \pm i\omega$. So the spiral *destabilizes* as μ is increased through 0. For $\mu > 0$, we have an unstable fixed point at $r = 0$, and a stable limit cycle at $r = \sqrt{\mu}$. The limit cycle is small-amplitude for $0 < \mu \ll 1$.

This is quite a common form for Hopf bifurcations.

Now let's look at some **rules of thumb for the supercritical case**.

We have a stable spiral when $\mu < \mu_c$, and an unstable spiral when $\mu > \mu_c$.

1. When $\mu \gtrsim \mu_c$, the limit cycle amplitude $\sim \sqrt{\mu - \mu_c}$.
2. The frequency is $\omega + O(\mu - \mu_c)$, where $\omega = \text{Im}(\lambda(\mu_c))$, the imaginary part of the eigenvalues at the instability threshold. This approximation improves the closer you are to the bifurcation.
3. The limit cycle is approximately elliptical.

Example.

Subcritical Hopf bifurcation.

$$\begin{aligned}\dot{r} &= \mu r + r^3 - r^5 \\ \dot{\theta} &= \omega + br^2\end{aligned}$$

We can plot μ and r .

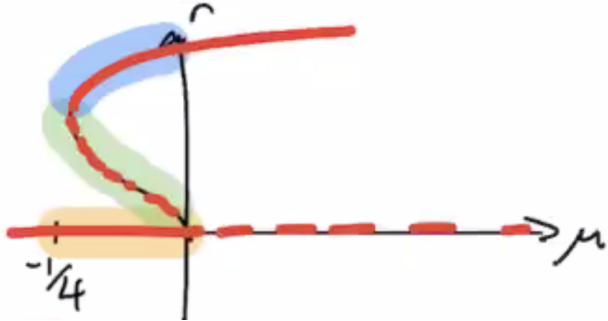


Figure 100: Bifurcation diagram.

In the range $-1/4 < \mu < 0$, the origin is a stable spiral (yellow). There is also an unstable limit cycle of intermediate amplitude (green), and also a stable limit of large amplitude (blue).

This gives us a somewhat complicated phase portrait.



Figure 101: Phase portrait.

When $\mu > 0$, the origin becomes an unstable spiral. We keep the large-amplitude stable limit cycle. So the phase portrait in this case looks like this.



Figure 102: Phase portrait.

Note that at $\mu = -1/4$, we have a saddle-node bifurcation when the two

limit cycles collide and annihilate.

There's one more type: **degenerate Hopf bifurcations**. These are pretty rare; Prof. Durey says he's never seen one appear in his research. This occurs when a nonconservative system becomes conservative at the bifurcation. For example,

$$\dot{x} + \mu x + \sin(x) = 0$$

Here, when $\mu < 0$, there's a stable spiral at $x = 0$. At $\mu = 0$, we lose the nonlinearity and are left with a nonlinear pendulum. This is a conservative system! There's a nonlinear center, so there's a family of closed orbits, not limit cycles. When $\mu > 0$, we have an unstable spiral at the origin.

Example.

Hopf bifurcation example.

$$\begin{aligned}\dot{x} &= a - x - \frac{4xy}{1+x^2} \\ \dot{y} &= bx \left[1 - \frac{y}{1+x^2} \right]\end{aligned}$$

where $a, b > 0$. Show there is a closed orbit in $x, y > 0$.

We're going to draw a phase portrait and create a trapping region so we can apply Poincaré-Bendixson.

Our $\dot{x} = 0$ nullcline is

$$y = \frac{(1+x^2)(a-x)}{4x}$$

This intersects the x -axis at $x = a$. As x gets very large, the cubic term dominates. At small x , it blows up. So we can sketch in the nullcline (in red). When we're above this curve, $\dot{x} > 0$.

The $\dot{y} = 0$ nullclines are

$$x = 0 \quad y = 1 + x^2$$

We can sketch this in (in blue). Above the parabola, \dot{y} is negative, and below, it's positive.

At the intersection of the x and y nullclines, we have a fixed point.

When trajectories cross the x -axis, they come up and to the right. When trajectories cross the y -axis, they come in to the right.

We can draw a line at $x = a$ until the parabola nullcline. Trajectories that cross this line go up and left. We can finish off this box – trajectories

crossing this final boundary go in and left. So all trajectories come into the trapping region.

If the fixed point is repelling, we can puncture it out and get a good trapping region. Then we can apply the Poincaré-Bendixson theorem for the punctured rectangle.

Doing linear stability analysis tells us that the fixed point is a repeller when

$$b < \frac{3}{5}a - \frac{25}{a} = b_c(a)$$

So this defines a trapping region!

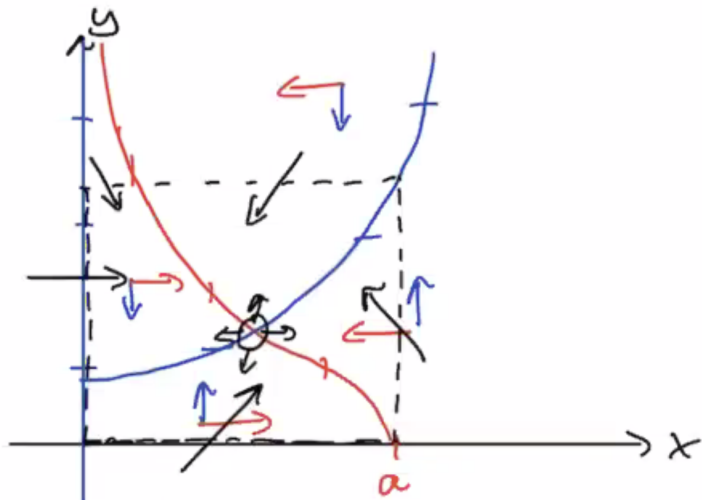


Figure 103: Phase portrait and trapping region.

Unfortunately, the Poincaré-Bendixson theorem doesn't tell us much about what type of closed orbits we have in the region.

We can use simulations, however, to plot trajectories, and then we see that we've got a *supercritical Hopf bifurcation*.

15.1 Global bifurcations

So far we've been looking at local bifurcations, when something changes in the vicinity of a fixed point. Now we'll talk about global bifurcations, where we have the creation/destruction of limit cycles via global changes in the phase portrait.

First, **saddle-node bifurcations of cycles**. Here, two limit cycles collide

and annihilate each other. For example,

$$\begin{aligned}\dot{r} &= \mu r + r^3 - r^5 \\ \dot{\theta} &= \omega + br^2\end{aligned}$$

This was our example from earlier!

For $\mu < -1/4$, we had a stable fixed point. At $\mu = -1/4$, we have a stable fixed point and a half-stable limit cycle. When $-1/4 < \mu < 0$, we have the two limit cycles (one unstable, one stable) and the same stable fixed point.

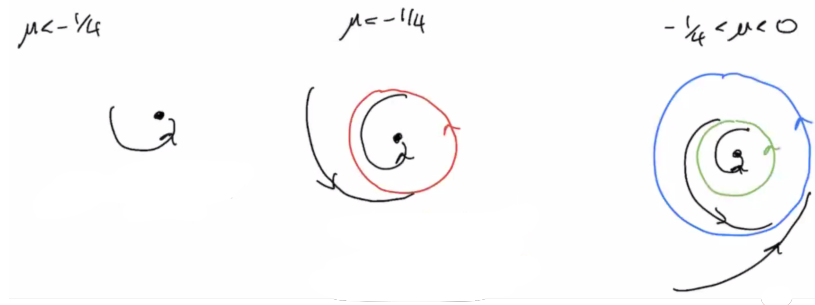


Figure 104: Global bifurcations.

Note that the limit cycle appears with an $O(1)$ amplitude.

Let's now look at **infinite period bifurcations**.

$$\begin{aligned}\dot{r} &= 1(1 - r^2) \\ \dot{\theta} &= \mu - \sin \theta\end{aligned}$$

Notice that the parameter $\mu \geq 0$ is now in the θ equation! This will lead to different dynamics.

When $\mu < 1$, there are two invariant rays. The $r = 1$ orbit is also stable. There's an unstable spiral from the origin, and the unstable ray is a saddle.

When $\mu > 1$, there's an unstable spiral at the origin and a stable limit cycle. There's also the ghost of the saddle-node bifurcation, where there's slow flow. So the period is

$$\sim \frac{1}{\sqrt{\mu - 1}}$$

for $0 < 1 - \mu \ll 1$ (i.e $\mu \gtrsim 1$).

One more type! In a **homoclinic bifurcation**, a limit collides with a saddle point and forms a homoclinic loop at $\mu = \mu_c$.

$$\begin{aligned}\dot{x} &= y \\ \dot{y} &= \mu y + x - x^2 + xy\end{aligned}$$

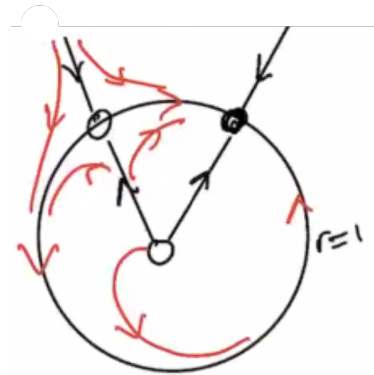


Figure 105: Phase portrait.

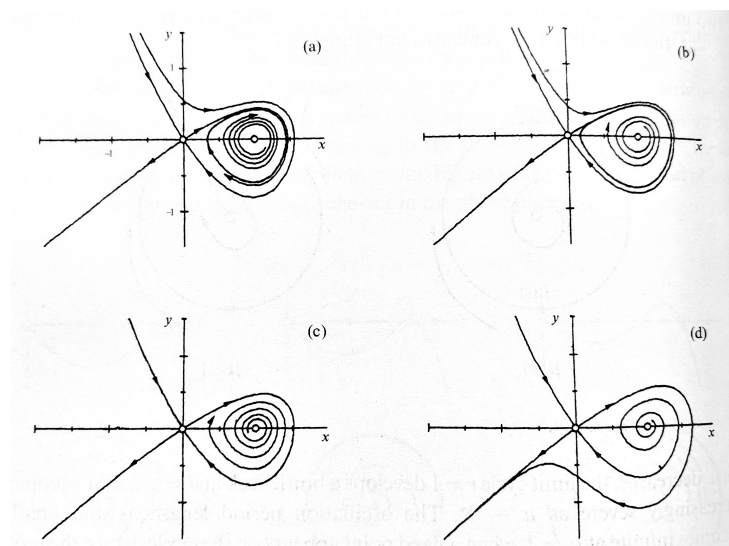


Figure 106: Phase portraits, Strogatz.

15.2 Generic scaling laws

If there's a bifurcation at $\mu = 0$, what are the amplitude and period of the limit cycle?

In the supercritical Hopf bifurcation, the amplitude is $O(\sqrt{\mu})$ and the period is $O(1)$.

In the saddle-node bifurcation of cycles, the amplitude is $O(1)$ and the period is $O(1)$.

In infinite period bifurcations, the amplitude is $O(1)$ and the period is $O(\mu^{-1/2})$.

In homoclinic bifurcations, the amplitude is $O(1)$, and the period is $O(|\log \mu|)$. You get this log scaling when trajectories pass near the fixed points.

16 October 27, 2020

Today we'll look at the [Lorenz equations](#).

$$\begin{aligned}\dot{x} &= \sigma(y - x) \\ \dot{y} &= rx - y - xz \\ \dot{z} &= xy - bz\end{aligned}$$

where $\sigma, r, b > 0$. Note that we have xz and xy , nonlinear terms. These offset the dissipation that might come from the other terms.

These equations were developed by Edward Lorenz at MIT, and published in a paper titled “Nonperiodic deterministic flow”. When he tried simulating them, he found that they exhibited some really unusual behavior.

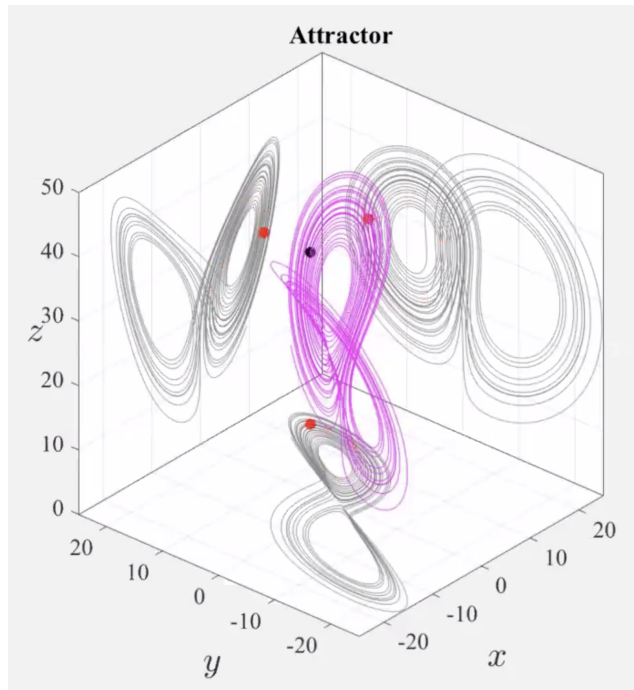


Figure 107: The Lorenz equations, with plane projections in grey.

It's really hard to predict which “wing” of the shape a point is on, as particles shoot from one wing to another.

The first thing to notice about this system is that we have symmetry. The equations are invariant under the mapping $(x, y, z) \mapsto (-x, -y, z)$.

Therefore, either solutions are symmetric or they have a symmetric pair. So if you have a fixed point, it has a paired point.

Note also that the trajectories in 3D seem to form a thin sheet – it's not a blob of possibilities. This brings us to the idea of **volume contraction**. We want to look at a family of solutions, and consider the solutions as a surface S that encloses a volume V . How do $S(t)$ and $V(t)$ evolve with small timesteps δt ?



Figure 108: $S(t)$ and $V(t)$.

The Lorenz equations are dissipative. How does the volume enclosed by trajectories change as we evolve the system? Consider the volume of a generic system $\dot{\vec{x}} = \vec{f}(\vec{x})$ where we're working in 3D, so $\vec{x} = \begin{pmatrix} x & y & z \end{pmatrix}$.

$V(t)$ is the volume enclosed by the surface $S(t)$ which is formed from the position of trajectories, with some initial condition $S(0)$. How does $V(t)$ evolve?

We're going to consider a small patch on the surface of the volume, of size δA . If everything is sufficiently smooth, we can find an outward-pointing unit normal vector \vec{n} from the volume. Enclosed within the patch δA is the vector $\dot{\vec{x}} = \vec{f}(\vec{x})$, as this is the direction of the flow. We want to know how changes in this patch affect the volume.

Note that as $\dot{\vec{x}} = \vec{f}(\vec{x})$, we have that $\vec{f} \cdot \vec{n}$ is the velocity projected onto the outward pointing normal.

The patch of area δA sweeps out a volume $(\vec{f} \cdot \vec{n})\delta A\delta t$ in an infinitesimal time increment δt .

We want to find the overall change in volume by summing over all infinitesimal patches δA . This is an integral!

$$V(t + \delta t) - V(t) = \int_{S(t)} (\vec{f} \cdot \vec{n}) \delta t dA$$

We're going to move δt to the LHS and take the limit where $\delta t \rightarrow 0$.

$$\frac{V(t + \delta t) - V(t)}{\delta t} = \int_{S(t)} (\vec{f} \cdot \vec{n}) dA = \int_{V(t)} \vec{\nabla} \cdot \vec{f} dV$$

where in the second equality, we've used the Divergence Theorem. Now

we take the limit $\delta t \rightarrow 0$.

$$\frac{dV}{dt} = \int_{V(t)} \vec{\nabla} \cdot \vec{f} dV$$

Cool! So this is how the volume subtended by the trajectories evolves.

For the Lorenz equations,

$$\begin{aligned}\dot{x} &= \sigma(y - x) \\ \dot{y} &= rx - y - xz \\ \dot{z} &= xy - bz\end{aligned}$$

what do we get?

$$\begin{aligned}\vec{\nabla} \cdot \vec{f} &= \frac{\partial}{\partial x}(\sigma(y - x)) + \frac{\partial}{\partial y}(rx - y - xz) + \frac{\partial}{\partial z}(xy - bz) \\ &= -\sigma - 1 - b \\ &= -(1 + \sigma + b)\end{aligned}$$

So the divergence of f in this system is constant, and negative. If we take our evolution equation for V , then we get

$$\frac{dV}{dt} = \int_{V(t)} -(1 + \sigma + b) dV = -(1 + \sigma + b) V(t)$$

So $V(t)$ decreases exponentially in time. This is what we saw in the plot of the Lorenz equations! It's a thin sheet in 3D, with essentially zero volume. This is a result of the contraction of all trajectories in phase space to a zero volume as $t \rightarrow \infty$.

This constrains our options a bit. We can have fixed points, limit cycles, and (this is new!) **strange attractors**. Strange attractors are a hallmark of chaotic systems.

As a consequence, we can't have quasi-periodic trajectories. These are trajectories that are nearly periodic but with a weak precession. Why not, exactly? These trajectories are incompatible with volume contraction.

We also can't have repelling fixed points or orbits. Then trajectories leaving the fixed point would go outwards, leading to a local increase in the volume. This isn't volume contraction, so it's also contradictory. But saddle-like structures may still arise.

16.1 Analyzing the Lorenz equations

The obvious fixed point is $x = y = z = 0$, for all σ, r, b .

A fixed point satisfies $y = x$ (in the first equation), $z = r - 1$ (the second equation), and $x^2 = b(r - 1)$ (the third equation). So for $r > 1$, we have a symmetric pair of fixed points.

$$c_1 = (+\sqrt{b(r-1)}, +\sqrt{b(r-1)}, r-1)$$

$$c_2 = (-\sqrt{b(r-1)}, -\sqrt{b(r-1)}, r-1)$$

Note that as $r \rightarrow 1^+$, we have $c_1, c_2 \rightarrow (0, 0, 0)$. This gives us a supercritical pitchfork bifurcation. This makes sense, because we're looking at a system with symmetry!

Now let's look at the stability of these fixed points. We'll use linear stability analysis to consider small perturbations about the origin. In this case, the nonlinear terms in the Lorenz equations are essentially 0.

$$\begin{aligned}\dot{x} &= \sigma(y - x) \\ \dot{y} &= rx - y - xz \approx rx - y \\ \dot{z} &= xy - bz \approx -bz\end{aligned}$$

This gives a linearization of the Lorenz equations. Note that this decouples the z term! Then $z \rightarrow 0$ as $t \rightarrow \infty$.

So we know that z decays. What about in the x, y plane? Consider the reduced system

$$\frac{d}{dt} \begin{pmatrix} x \\ y \end{pmatrix} = \begin{pmatrix} -\sigma & \sigma \\ r & -1 \end{pmatrix} \begin{pmatrix} x \\ y \end{pmatrix}$$

To determine the x, y -plane dynamics, we look at the eigenvalues of this matrix. The trace is $-(\sigma + 1)$, and the determinant is $\sigma(1 - r)$. So we notice that when $r > 1$, the determinant is negative and we have a saddle.

Also, $T^2 - 4D = (\sigma + 1)^2 - 4\sigma + 4\sigma r = (\sigma - 1)^2 + 4\sigma r > 0$. So we have a stable node for $r < 1$, because all three eigenvalues are real and negative.

How do we have flow towards the origin? In the z -direction, the flow is towards the origin. When we have a saddle at the origin, there's a stable manifold and an unstable manifold, so there's one outgoing direction and two total incoming directions.

How about global stability? For $r < 1$, we can construct a Lyapunov function, from which we conclude that the origin is a global attractor. Specifically, we use the following Lyapunov function.

$$\mathbb{V} = \frac{1}{\sigma}x^2 + y^2 + z^2 > 0 \quad \text{for } x, y, z \neq 0$$

(We're using a fancy V because we already used V for volume.) You can show that for $r < 1$, $d\mathbb{V}/dt < 0$ except at the origin. So we have a global attractor that's a stable node for $r < 1$.

At $r = 1$, the origin destabilizes and we end up with two new fixed points, which we will see are stable nodes. Let's look at the stability of c_1 and c_2 , as defined earlier.

These fixed points are linearly stable for

$$1 < r < r_H = \frac{\sigma(\sigma + b + 3)}{\sigma - b - 1}$$

for $\sigma > 1 + b$. We'll have to verify this on the upcoming problem set.

You can show that there's a Hopf bifurcation at r_H . We'll find that this is a subcritical Hopf bifurcation, in particular. This means there's an unstable limit cycle that contracts at reaches 0 at the moment that the stable fixed point at the origin destabilizes. Let's draw this out.

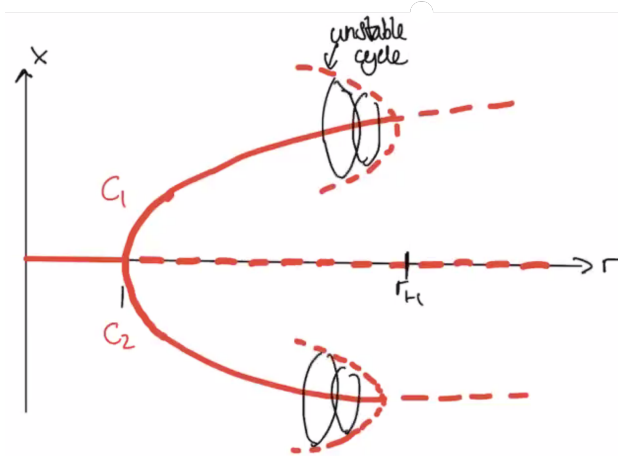


Figure 109: Bifurcation diagram.

These unstable cycles are actually called "saddle cycles". If you trace them back to where they come from, there's a "homoclinic bifurcation" (not drawn in here). We'll talk about those later.

What happens for $r > r_H$? There are no limit cycles appearing, but the trajectory settles on a very thin sheet in phase space of zero volume. There's fractal behavior! It's zero volume, but with infinite surface. We'll see this later in the course.

We'll see later that the dynamic that arises in the Lorenz system is very closely related to fractals.

16.2 Sensitivity to initial conditions

If you start the system with very close initial conditions, at large time, the trajectories diverge. There's behavior in which one trajectory is completely

on the other side as the first, and it becomes completely abnormal behavior after a while. What's happening here?

Small changes are amplified over time! Two trajectories that are initially close will end up on opposite sides of the attractor at a later time. (Weather changes are like this! This is why we can't trust long-term weather forecasts.)

How do we quantify this?

Let's start off with a trajectory that "lies on" the attractor. Call this $\vec{x}(t)$. Consider a perturbed trajectory $\vec{x}(t) + \vec{\delta}(t)$, where $\vec{\delta}(0) = \vec{\delta}_0$ and $|\vec{\delta}_0| \ll 1$.

How does $\vec{\delta}(t)$ evolve? If we do a log-log plot of $\vec{\delta}$ and t , we get something like this.

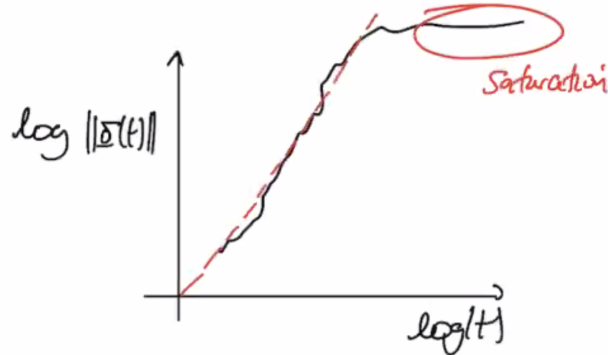


Figure 110: Log-log plot of δ and t .

There's exponential growth, so $|\delta(t)| = |\delta_0|e^{\lambda t}$. If $\lambda > 0$, the trajectories diverge as $t \rightarrow \infty$. This λ is called the **maximal Lyapunov exponent**. In the Lorenz system, we find that $\lambda \approx 0.9$.

After a while, the trajectories are on fully opposite ends of the attractor, and the system is saturated.

What are the other Lyapunov exponents? For an n -dimensional system, we have n Lyapunov exponents. To understand what's going on here, consider an n -dimensional sphere of initial conditions. As the system evolves, the growth of the trajectory will differ in different directions, and the sphere will be distorted over time into an ellipsoid.

We'll look at the length of the k -th principal axis of the hyperellipsoid, $\delta_k(t) > 0$. Because we're consider small perturbations, we can ignore the nonlinear terms and look at just the linear system. We then find that

$$\delta_k(t) \sim \delta_k(0)e^{\lambda_k t}$$

where λ_k is the k -th **Lyapunov exponent** for $k = 1, \dots, n$. We define the largest of these, λ , as the maximal Lyapunov exponent, i.e the one that dominates the evolution.

$$\lambda = \max_{k=1,\dots,n} \lambda_k$$

So it's these other Lyapunov exponents that give us a wobbly behavior in the plot sketched earlier, rather than straightforward exponential growth.

Note that the value of λ varies between trajectories – not hugely, but there's an appreciable difference. So we have to average over many trajectories to get a reliable answer. The larger the value, the faster the trajectories decay. This gives us a timescale for how quickly the trajectories become apart based on the initial conditions.

It becomes quite difficult to predict the dynamics deterministically. It's unfortunately computationally impossible to exactly determine much, either. But we can get quantitative information of what's going on nevertheless!

Next time, a real definition of chaos!

17 October 29, 2020

Chaos is aperiodic long-time behavior in a deterministic system that exhibits sensitivity to initial conditions.

Aperiodic long-time behavior means that there exist trajectories that do not approach a fixed point or periodic/quasi-periodic orbits. (Infinity may be thought of as a fixed point.)

Deterministic means that the system is not stochastic. There's no noise or model thereof.

Sensitivity to initial conditions means that there's a positive maximal Lyapunov exponent.

So these are the three properties we're looking for.

An **attractor** is a set to which all neighboring trajectories attract. More formally, a set A is an **attractor** if it satisfies all three of the following conditions:

- (1) A is invariant. A trajectory that starts in A remains in A for all time.
- (2) A attracts an *open* set of initial conditions.

- If $\vec{x}(0) \in U \supset A$ and U is open, then $\vec{x}(t)$ reaches A as $t \rightarrow \infty$.
- The largest such U is the basin of attraction of A .

(3) A is minimal – there is no proper subset of A that satisfies both (1) and (2).

Example.

The following system:

$$\begin{aligned}\dot{x} &= x - x^3 \\ \dot{y} &= -y\end{aligned}$$

We found that the fixed points are $(\pm 1, 0), (0, 0)$. The origin is a saddle and the other two are stable nodes.

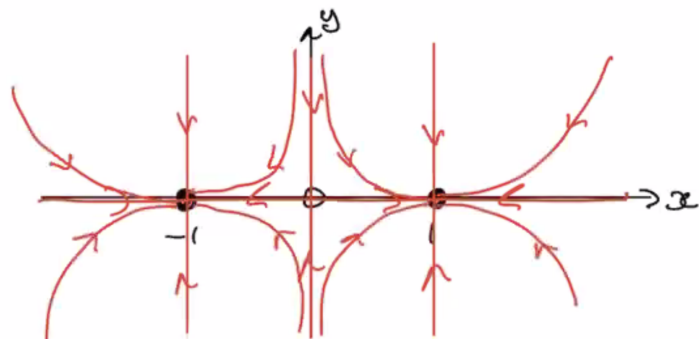


Figure 111: Phase portrait.

Consider $I = \{x, y \mid -1 \leq x \leq 1, y = 0\}$. This is a line that passes through the fixed points and includes them. Is I an attractor?

Let's check the attractor definition.

Does a trajectory that starts on I stay on I ? Yes, it is sent to one of the stable nodes and stays there. So I is an invariant set.

Can we find an open set in which we have trajectories that approach I as $t \rightarrow \infty$? From the phase portrait you can see that the entirety of the plane is a basin of attraction for I . Any trajectory, no matter where it starts, will approach some point along I (namely the two endpoints, or the saddle if you start on the stable manifold). So the basin of attraction $U \supset I$ is the entire plane.

Is I minimal? That is, are there are proper subsets of I that we can take that satisfy the other two properties? Yes! The single points $(1, 0)$ and $(-1, 0)$ are invariants, since they're fixed points. The basin of attraction for $(-1, 0)$ is everything where $x < 0$. The basin of attraction for $(1, 0)$ is everything where $x > 0$. So they have open sets as their basin of attraction.

So I is not an attractor as it is not minimal.

Next up, **strange attractors**. A **strange attractor** is an attractor that exhibits sensitivity to initial conditions.

If we're on a trajectory on this attractor and we take a tiny perturbation away from it, if we have a positive Lyapunov exponent, the two trajectories will end up on opposite sides of the attractor at some point.

An example of one of these is the Lorenz attractor.

If we plot z and t for the Lorenz attractor, we might get something like this.

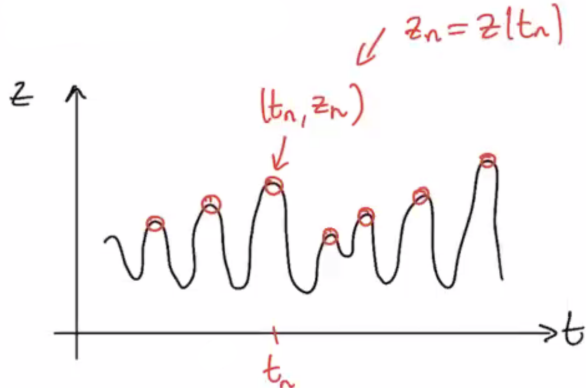


Figure 112: Time series.

Lorenz wanted to identify the times (t_n, z_n) when the time-series peaks. If you plot z_n and z_{n+1} , you get a very distinctive shape.

If you zoom in on it, it turns out it's not a curve. It has a fine-scale structure, or "thickness". It's some sort of fractal behavior. Looking closely at how this shape is formed, we see it's like Figure 114.

It turns out that when $z_n = z_{n+1}$, that's an unstable fixed point. It's also possible to show quite rigorously that this behavior isn't the consequence of wonky numerics, but the Lorenz attractor is indeed a strange attractor.

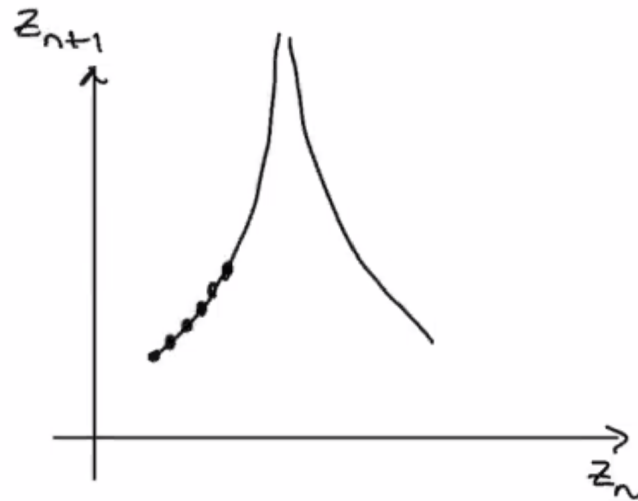


Figure 113: z_n and z_{n+1} .

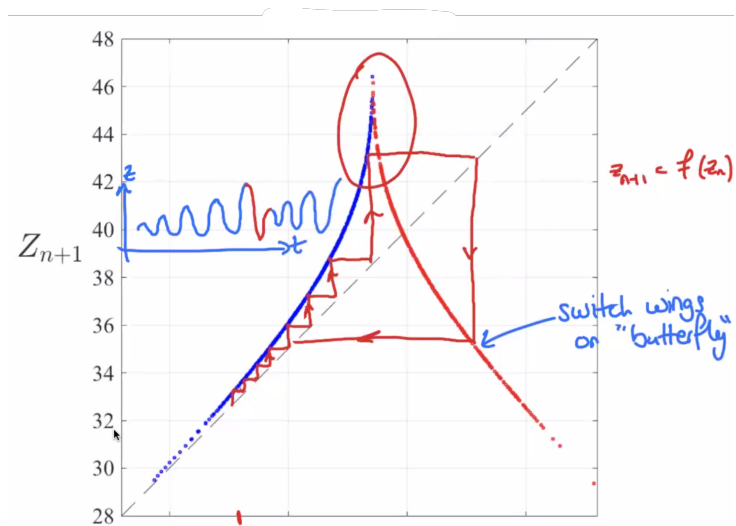


Figure 114: z_n and z_{n+1} data.

In any case, rather than trying to map out the continuous time evolution of the system, we can look at the maxima using this [Lorenz map](#).

Note: the cusp corresponds to the point where we switch from one wing to the other.

We can write an approximation for a curve $z_{n+1} = f(z_n)$. Note that $|f'(z)| > 1$, so there are no stable fixed points or periodic orbits. This comes from linear stability analysis.

17.1 Synchrony of chaotic systems

We're going to look at what happens when we let a chaotic system drive another system.

Two chaotic systems can synchronize. A receiver forced by a chaotic transmitter, for example.

Let's consider a circuit example. We'll have three voltages u, v, w that play the role of x, y, z in the Lorenz system.

$$\begin{aligned}\dot{u} &= \sigma(v - u) \\ \dot{v} &= ru - v - 20uw \\ \dot{w} &= 5uv - bw\end{aligned}$$

The numbers have been added to make the math a bit easier. We'll let this system be our transmitter.

The receiver system, with voltages u_r, v_r, w_r is

$$\begin{aligned}\dot{u}_r &= \sigma(v_r - u_r) \\ \dot{v}_r &= ru - v_r - 20uw_r \\ \dot{w}_r &= 5uv_r - bw_r\end{aligned}$$

Note that we're using u , not u_r in the last two equations. This is the transmitter u , so that's where the chaotic forcing in the system is coming from.

We'll show that the received will synchronize with the transmitter as $t \rightarrow \infty$. That is, that

$$\begin{aligned}e_1 &= u - u_r \rightarrow 0 \\ e_2 &= v - v_r \rightarrow 0 \\ e_3 &= w - w_r \rightarrow 0\end{aligned}$$

as $t \rightarrow \infty$. We can write out some differential equations.

$$\begin{aligned}\dot{e}_1 &= \sigma(e_2 - e_1) \\ \dot{e}_2 &= -e_2 - 20ue_3 \\ \dot{e}_3 &= 5ue_2 - be_3\end{aligned}$$

To show that things synchronize, we need to show that this system of differential equations has a global attractor at the origin. That is, that $(e_1, e_2, e_3) \rightarrow (0, 0, 0)$.

To show a global attractor exists, we try to find a Lyapunov function. Note that

$$e_2 \dot{e}_2 + 4e_3 \dot{e}_3 = -e_2^2 - 20ue_2 e_3 + 20ue_2 e_3 - be_3^2 = -(e_2^2 + be_3^2)$$

This gets rid of the factor of u that was floating around! We can write this as

$$\frac{d}{dt} \left(\frac{1}{2} e_2^2 + 2e_3^2 \right) = -(e_2^2 + be_3^2)$$

Notice that the RHS is negative unless $e_2 = e_3 = 0$.

Define the Lyapunov function

$$E = \frac{1}{2} \left(\frac{1}{\sigma} e_1^2 + e_2^2 + 4e_3^2 \right) \geq 0$$

where this is 0 only when $e_1 = e_2 = e_3 = 0$. We need to show that this decreases along trajectories.

$$\begin{aligned} \frac{dE}{dt} &= \frac{1}{\sigma} e_1 \dot{e}_1 + e_2 \dot{e}_2 + 4e_3 \dot{e}_3 \\ &= e_1(e_2 - e_1) - e_2^2 - be_3^2 && \text{from above} \\ &= -(e_1^2 - e_1 e_2 + e_2^2 + be_3^2) \\ &= - \left((e_2 - \frac{1}{2}e_2)^2 + \frac{3}{4}e_2^2 + be_3^2 \right) \\ &\leq 0 \end{aligned}$$

When is this equal to 0? This is a paraboloid. It's 0 only when each of $e_1 = e_2 = e_3 = 0$, i.e at the fixed point.

So we've verified that E is a Lyapunov function. This tell us that e_1, e_2, e_3 go to 0 as $t \rightarrow \infty$. As the e_i variables are the differences between the transmitter and received voltages, we can then conclude that the received will synchronize with the transmitter as $t \rightarrow \infty$.

This is pretty cool! You can use a chaotic system to add noise to something you're trying to transmit, and then use this to remove the noise afterwards. See "Using chaos to send secret messages" in Strogatz's book.

We've shown that the effect of putting a transmitted variable in the receiver system, which is *not* a Lorenz system, is that the receiver system replicates chaotic behavior.

As an aside, you can often look at a system where you have that the change in velocity can be given by a force plus a little bit of noise.

$$\begin{aligned} dX_t &= V_t \\ dV_t &= \sigma dW_t \end{aligned}$$

where dW_t is the noise. (This is stochastic differential equation notation.) What is the analog of this in deterministic systems? This means dV_t is equal to some chaotic forcing, u , where (u_1, u_2, u_3) evolve according to Lorenz. How does this influence the dynamics? That's one of the things Prof. Durey is currently looking into.

18 November 3, 2020

Today we're going to look at more 1D maps to understand the dynamics of chaotic systems.

The general form for a map is

$$x_{n+1} = f(x_n)$$

where $f : \mathbb{R} \rightarrow \mathbb{R}$ is some smooth function.

We use these maps to analyze differential equations (as we did for the Lorenz system), or as models for impulsively driven systems. They can also be used as a simple example of chaos.

A fixed point of the map f satisfies

$$x_* = f(x_*)$$

That is, $x_n = x_*$ for all n . This is analogous to the differential equation definition!

You can find a fixed point analytically, graphically, or numerically (using some root-finding techniques and things).

It's also interesting to consider the linear stability of a map. To study linear stability, we consider a small perturbation

$$x_n = x_* + \epsilon_n$$

where ϵ_n is the perturbation and $|\epsilon_n| \ll 1$ for all n . What happens to the perturbation? This will tell us about the stability of x_* .

So we can plug this into the map equation and Taylor expand.

$$\begin{aligned} x_{n+1} &= f(x_n) \\ x_* + \epsilon_{n+1} &= f(x_* + \epsilon_n) \\ &\sim f(x_*) + \epsilon_n f'(x_*) + O(\epsilon_n^2) \end{aligned}$$

Here we assume that the correction term remains negligible for all time.

Since $x_* = f(x_*)$, those terms cancel. We can linearize (ignoring the correct term) to obtain

$$\epsilon_{n+1} = \lambda \epsilon_n, \quad \lambda = f'(x_*)$$

where we call λ the multiplier.

Note that $\epsilon_{n+1} = \lambda \epsilon_n = \lambda(\lambda \epsilon_{n-1}) = \dots$. So,

$$\epsilon_n = \lambda^n \epsilon_0$$

where ϵ_0 is the initial perturbation.

Then, $\epsilon_n \rightarrow 0$ for $|\lambda| < 1$. Then, x_* is linearly stable.

Also, $\epsilon_n \rightarrow \infty$ for $|\lambda| > 1$. Here, x_* is linearly unstable.

The marginal case is $|\lambda| = 1$. Then $\epsilon_n = \epsilon_0$ for all n . In this case, we need to revisit the Taylor expansion.

$$\epsilon_{n+1} \sim \epsilon_n f'(x_*) + \frac{1}{2} \epsilon_n^2 f''(x_*) + O(\epsilon_n^3)$$

We've now included the quadratic term. If $f'(x_*) = \pm 1$, we can do a nonlinear analysis to rationalize the stability of x_* .

Or, we can use graphical techniques.

Example.

The map where $f(x) = x^2$, so $x_{n+1} = x_n^2$.

The fixed points x_* satisfy $x_* = x_*^2$. So we have fixed points at $x_0 = 0$ and $x_* = 1$.

For linear stability, we have $f'(x) = 2x$. So for $x_0 = 0$, $\lambda = f'(0) = 0$. This gives us a stable fixed point.

For $x_* = 1$, we have $\lambda = 2$. Then this is an unstable fixed point.

When λ is 0, we say that the fixed point is **superstable**. Why do we call it superstable? Let's take the logarithm of this map.

$$\log(x_{n+1}) = 2 \log(x_n)$$

We can define $y_n = \log(x_n)$. Then,

$$y_{n+1} = 2y_n$$

So we've gone from a nonlinear difference equation to a linear difference equation. Then, $y_n = 2^n y_0$. Converting back to x ,

$$\log(x_n) = 2^n \log(x_0) \implies \log(x_n) = \log(x_0^{2^n})$$

So, $x_n = x_0^{2^n}$. If $|x_0| < 1$, then $x_n \rightarrow 0$ very quickly, even faster than exponential decay.

We can use a graphical technique called "cobwebbing" to look at the evolution of this system.

We plot $f(x_n)$ and the line $x_{n+1} = x_n$ on a plot of x_n against x_{n+1} .

We identify x_0 on the x_n -axis, and use our plot of $f(x_n)$ to identify x_1 . We map onto the line $x_{n+1} = x_n$, giving us x_1 on the horizontal axis. Then we go vertically upwards, to find where x_2 is. We can keep doing this to obtain an evolution of x_n on the curve.

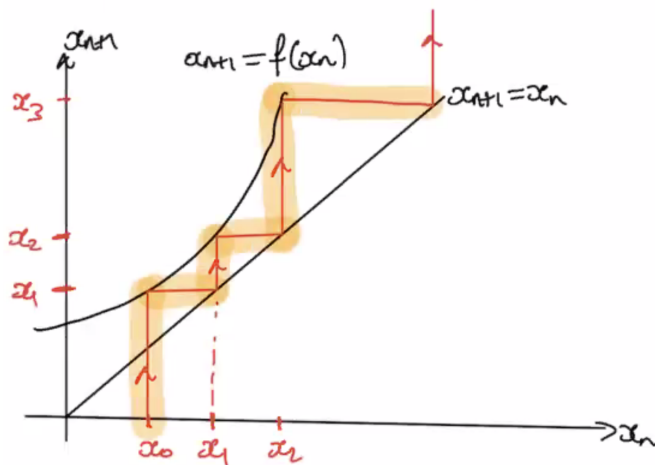


Figure 115: Cobwebbing.

Example.

$$x_{n+1} = \sin(x_n).$$

The fixed point here is $x_0 = 0$. Note that $\lambda = f'(0) = 1$. So then this is the marginal case, and we don't know if linear stability holds or not – we have to do a nonlinear analysis.

Rather than doing this analytically, we can do it graphically.

Here, the black curve is $x_{n+1} = \sin(x_n)$. Cobwebbing shows that we end up working our way down towards the origin, so $x_0 = 0$ is a linearly stable fixed point.

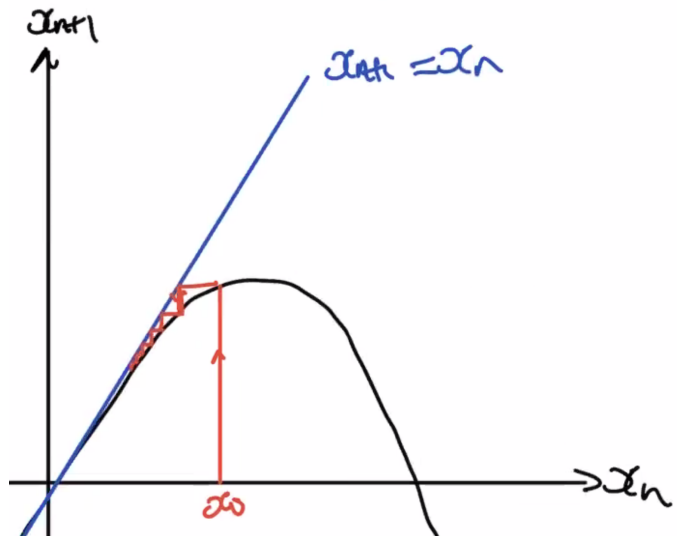


Figure 116: Cobwebbing with $\sin(x_n)$.

As an exercise, convince yourself that $x_0 = 0$ is *globally* stable.

Example.

$$x_{n+1} = \cos(x_n).$$

The fixed point x_* is the solution to the transcendental equation $x = \cos(x)$. We can plot $f(x_n)$ and the $x_{n+1} = x_n$ curve to identify fixed points.

We can start at a random point and cobweb to see what happens. We end up approaching the fixed point, but oscillating from above it to below it.

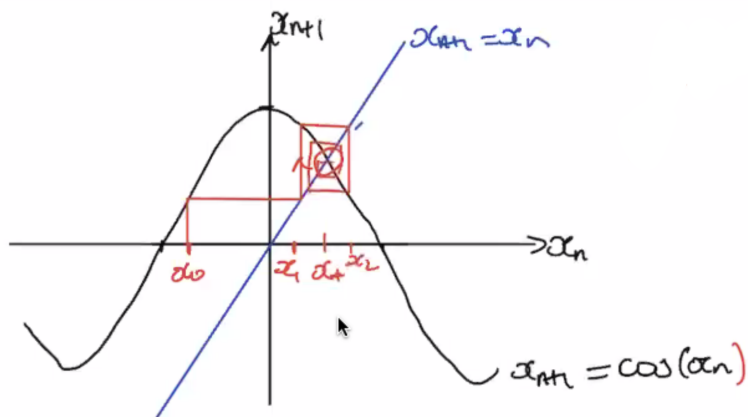


Figure 117: Cobwebbing to find stability.

So $x_n \rightarrow x_*$ as $n \rightarrow \infty$, but as $-1 < f'(x_*) = \lambda < 0$, we have a spiral-shaped cobweb.

So for $0 < \lambda < 1$, we have monotonic convergence. For $-1 < \lambda < 0$, we have oscillatory convergence. For $\lambda = 0$, we have superstable fixed points.

Example.

Logistic map. $x_{n+1} = rx_n(1 - x_n)$.

Here, $x_n \geq 0$ is the population, and $r \geq 0$ is a parameter.

We consider the range $0 \leq r \leq 4$. We guarantee that x_n satisfies $0 \leq x_n \leq 1$ if $0 \leq x_0 \leq 1$.

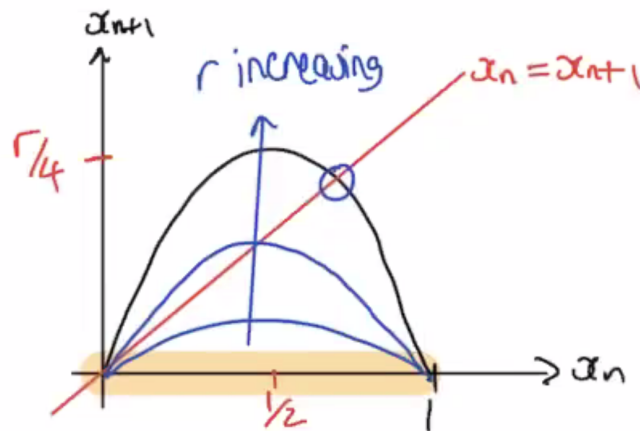


Figure 118: Logistic cobweb.

The fixed points x_* occur when

$$\begin{aligned} x_* &= rx_*(1 - x_*) \\ x_*(1 - r(1 - x_*)) &= 0 \end{aligned}$$

So one fixed point is $x_* = 0$ for all $0 \leq r \leq 4$. This is stable for $0 < r < 1$.

The other is $x_* = 1 - \frac{1}{r} \geq 0$, for $1 \leq r \leq 4$. This is stable for $1 < r < 3$.

So this other fixed point emerges at a bifurcation as r is increased. What happens for $r > 3$?

When $r < 3$, we get a steady state solution.

As you increase r past 3, you get cycles. At $r = 3$, a 2-cycle emerges. At $r = 3.449$, a 4-cycle is born. There's a period double cascade, where as

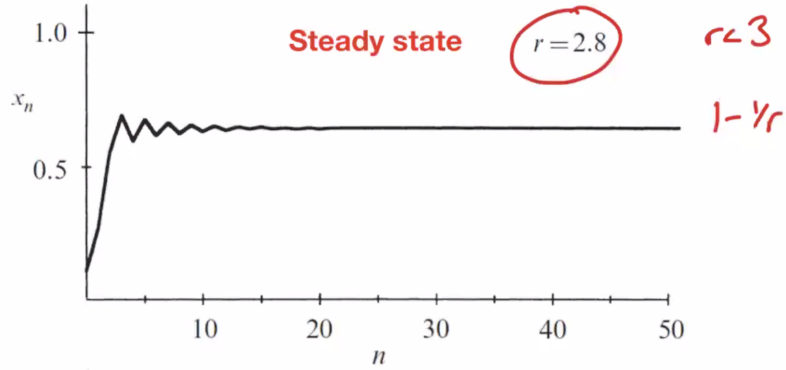


Figure 119: Steady state approaching $1 - 1/r$.

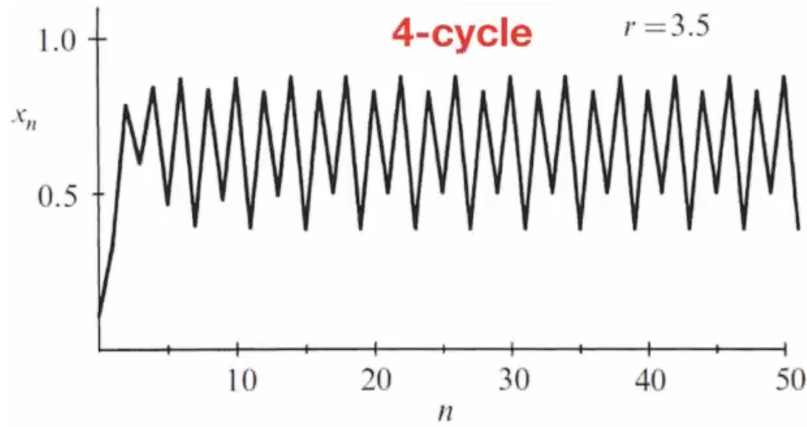


Figure 120: 4-cycle.

r increases, the number of points in the cycle doubles. There is a limiting value, though. At $r_\infty = 3.569946\dots$, we get chaotic behavior and an “ ∞ -cycle”. This is chaos.

We can look at plots of the map to try to look for patterns.

Let's look at the linear stability of the fixed points here.

For $x_0 = 0$, $\lambda = f'(0) = r$. So we have linear stability for $0 < r < 1$.

For $x_* = 1 - 1/r$,

$$\lambda = r - 2r \left(1 - \frac{1}{r}\right) = r - 2r + 2 = 2 - r$$

This is stable for $1 < r < 3$.

This gives us a bifurcation that's associated with the period doubling that begins at $r = 3$. This is called a **flip bifurcation**.

For the two cycle, we want to obtain $x_{n+2} = x_n$ for all n .

We want x_* to satisfy $x_* = f(f(x_*)) = f^2(x_*)$, where this is now a com-

posite map.

$$f^2(x) = f(f(x)) = f(rx(1-x)) = r[rx(1-x)](1-[rx(1-x)])$$

Then, doing some algebra,

$$f^2(x) = r^2x(1 - (r+1)x + 2rx^2 - rx^3)$$

This is a quartic. We can plot it. If we also plot $f^2(x) = x$, we can find the fixed points.

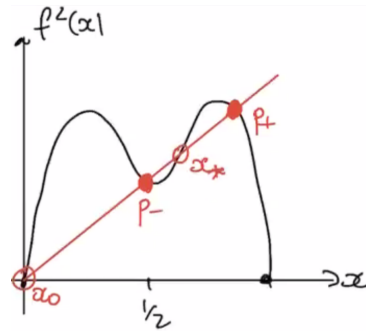


Figure 121: Quartic for f^2 .

There are 4 fixed points: x_0, x_*, P_+, P_- . The first two are unstable, and the latter two are stable. For $r \gtrsim 3$, we find that $f(P_+) = P_-$ and $f(P_-) = P_+$. Then, $P_+ = f^2(P_+)$ and $P_- = f^2(P_-)$.

What are P_+, P_- ? We can solve this.

$$\begin{aligned} x &= r^2x(1 - (r+1)x + 2rx^2 - rx^3) \\ 0 &= r^2x(1 - \frac{1}{r^2} - (r+1)x + 2rx^2 - rx^3) \\ \implies 0 &= r^2x \left(x - \left(1 - \frac{1}{r} \right) \right) \left(-rx^2 + (r+1)x - \left(1 + \frac{1}{r} \right) \right) \end{aligned}$$

So the first term here gives us $x_0 = 0$, then x_* , and then P_+, P_- . We can use the quadratic formula.

$$P_{\pm} = \frac{1}{2r} \left[r+1 \pm \sqrt{(r-3)(r+1)} \right]$$

This is real only for $r \geq 3$.

As $r \rightarrow 3^+$, $P_+ \rightarrow x_*^+ = \frac{2}{3}^+$. Similarly, $P_- \rightarrow x_*^- = \frac{2}{3}^-$.

So there's a supercritical flip bifurcation at $r = 3$, because these P_{\pm} are stable at small amplitude. But there do also exist subcritical flip bifurcations (just not in this example).

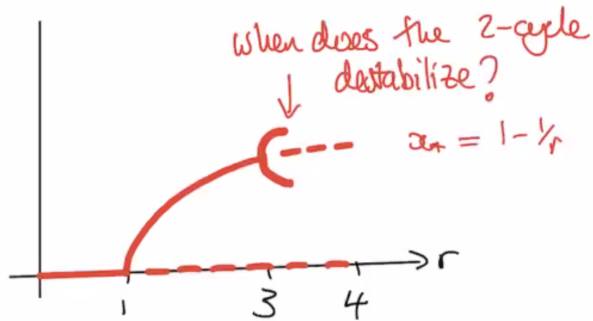


Figure 122: Bifurcation diagram.

19 November 5, 2020

Last time, we looked at the logistic map $x_{n+1} = f(x)$ with $f(x) = rx(1 - x)$.

We showed that for $r < 1$, $x = 0$ is a stable fixed point. For $r > 1$, $x = 0$ is unstable and $x = 1 - 1/r$ is stable.

For $3 < r < ?$ we showed that there was a stable 2-cycle in addition to $x = 0$ (unstable) and $x = 1 - 1/r$ (unstable).

To find the location of the 2-cycle, we looked at $f^2(x) = f(f(x))$. This gave us P_+ , P_- , with $f(P_+) = P_-$ and $f(P_-) = P_+$.

We found that

$$P_{\pm} = \frac{1}{2r} \left[(r + 1) \pm \sqrt{(r - 3)(r + 1)} \right]$$

for $r > 3$. These emerge at a “flip” bifurcation as r increases through 3.

Let's show the stability of the 2-cycle.

The multiplier λ of the composite map f^2 is

$$\lambda = \frac{d}{dx} f^2(x)|_{x=P_+} = f'(f(P_+)) f'(P_+)$$

Note that by the chain rule,

$$\frac{d}{dx} f(f(x)) = \frac{df}{dx} f(x) \frac{df}{dx}$$

Return to λ ,

$$\lambda = f'(P_-) f'(P_+)$$

This is the same value of λ as if we evaluated at $x = P_-$. So both P_+ and P_- destabilize simultaneously.

So we need to evaluate what the multiplier is using $f'(x)$.

$$f'(x) = r(1 - 2x)$$

So substituting this in,

$$\begin{aligned}\lambda &= r(1 - 2P_+)r(1 - 2P_-) \\ &= r^2(1 - 2(P_+ + P_-) + 4P_+P_-)\end{aligned}$$

From the definition of P_{\pm} ,

$$P_+ + P_- = \frac{1}{r}(r + 1)$$

Also,

$$P_+P_- = \frac{1}{4r^2} [(r + 1)^2 - (r - 3)(r + 1)]$$

Plugging this into the result for λ ,

$$\lambda = 4 + 2r - r^2$$

Recall that the 2-cycle is stable for $|\lambda| < 1$. Let's solve.

$$4 + 2r - r^2 = 1$$

$$4 + 2r - r^2 = -1$$

The first equation has a positive root at $r = 3$, and the second has a positive root at $r = 1 + \sqrt{6} \approx 3.45$.

So the 2-cycle is stable for $3 < r < 1 + \sqrt{6}$.

The cycle destabilizes with the multiplier passing through -1. At this point we expect another flip bifurcation, and a period-doubling.

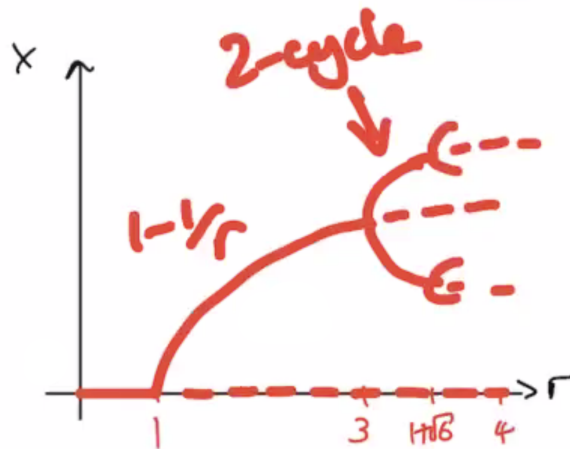


Figure 123: Bifurcation diagram.

19.1 Period doubling

The period-doubling cascades until we get to about $r \approx 3.57$, when we achieve chaos. We can draw an orbit diagram, where we plot r and the location of the points in the n -cycle.

The gaps in the orbit diagram are where we have chaos. Note that there's a big gap in there on the right where there are *three* points, not a power of two. If we zoom into what's happening there, we essentially see the same shape.

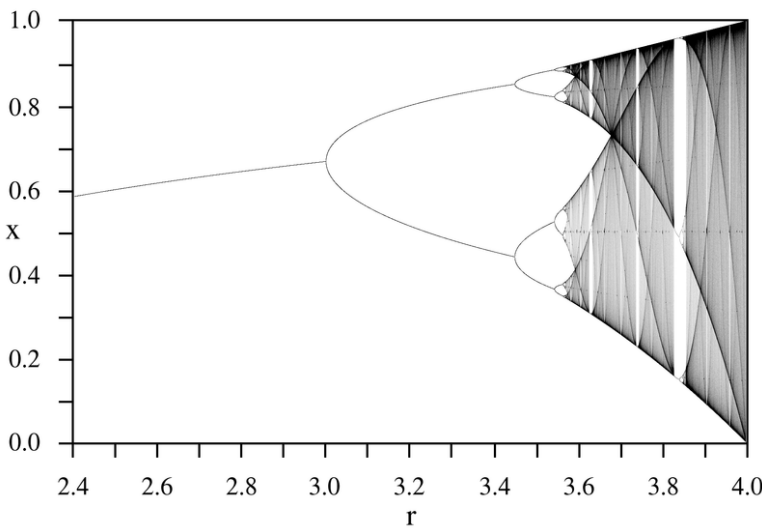


Figure 124: Orbit diagram.

Let's try to understand where these gaps and the 3-window come from. (The other two gaps are a 5-window and a 6-window.)

We want to understand why a 3-cycle emerges once we're in a chaotic regime. This requires us to find a fixed point of $f^3(x)$. We'll do this graphically. See Figure 125.

As r decreases, the curve shifts in the direction marked in blue, and we lose some fixed points. The points marked with an x are the fixed points of f . The points marked with a solid circle are part of a stable 3-cycle, and the open circles form the unstable 3-cycle. As we decrease r , these pairs of stable-unstable points collide and annihilate. This sounds like a saddle-node bifurcation, but this is in the context of a map. Here, it's called a **tangent bifurcation**.

The critical value of r for this is the smallest value of r at which the 3-cycle window arises. It should be about $1 + \sqrt{8}$.

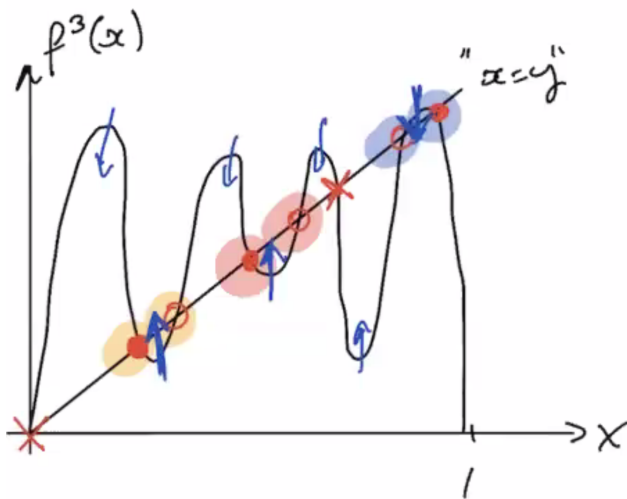


Figure 125: Finding fixed points.

Just before the periodic window emerges, we have lots of intermittents which appear in the very narrow channel before r increases past the tangent bifurcation.

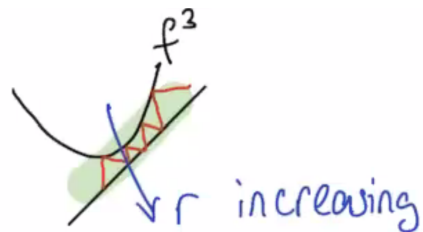


Figure 126: Cobwebbing visualization.

Many iterations are close to the ghost of the fixed point of f^3 . Once the system leaves this narrow channel at the critical r , chaotic behavior appears as it explores the map outside this region. So this explains intermittency in the system.

19.2 Lyapunov exponent

Consider the separation $|\delta_n| \ll 1$, of two trajectories. We want to define the Lyapunov exponent λ_e such that

$$|\delta_n| \approx |\delta_0| e^{\lambda_e n}$$

If $\lambda_e > 0$, we have sensitivity to initial conditions, and thus we have chaos.

Note that $x_n = f^n(x_0)$. Also, $x_n + \delta_n = f^n(x_0 + \delta_0)$.

We want an equation for δ_n in terms of x_0 . We obtain

$$\delta_n = f^n(x_0 + \delta_0) - f^n(x_0)$$

by simple subtraction.

Now we want to introduce λ_e . If we want

$$\left| \frac{\delta_n}{\delta_0} \right| \approx e^{\lambda_e n}$$

then we must have

$$\begin{aligned} \lambda_e &\approx \frac{1}{n} \log \left| \frac{\delta_n}{\delta_0} \right| \\ &= \frac{1}{n} \log \left| \frac{f^n(x_0 + \delta_0) - f^n(x_0)}{\delta_0} \right| \end{aligned}$$

Because $|\delta_0| \ll 1$, the argument of the logarithm is

$$\approx \frac{d}{dx} f^n|_{x=x_0}$$

Note that

$$\frac{d}{dx} f^n(x) = \frac{d}{dx} f(f^{n-1}(x)) = \frac{df}{dx}(f^{n-1}(x)) \frac{df^{n-1}}{dx}$$

by the chain rule. We can keep doing down the chain via induction to get

$$\frac{d}{dx} f^n(x) = \frac{df}{dx}(f^{n-1}(x)) \frac{df}{dx}(f^{n-2}(x)) \dots \frac{df}{dx}(x)$$

So that's the general expression but we want this at $x = x_0$. This gives us

$$\frac{d}{dx} f^n|_{x=x_0} = f'(x_{n-1}) f'(x_{n-2}) \dots f'(x_0) = \prod_{j=0}^{n-1} f'(x_j)$$

Plugging back into λ_e ,

$$\begin{aligned} \lambda_e &\approx \frac{1}{n} \log \left| \prod_{j=0}^{n-1} f'(x_j) \right| = \frac{1}{n} \log \left(\prod_{j=0}^{n-1} |f'(x_j)| \right) \\ &= \frac{1}{n} \sum_{j=0}^{n-1} \log |f'(x_j)| \end{aligned}$$

We then define

$$\lambda_e = \lim_{n \rightarrow \infty} \frac{1}{n} \sum_{j=0}^{n-1} \log |f'(x_j)|$$

Here, λ_e depends on x_0 . This should be the same for any x_0 in the basin of attraction of the attractor.

Note that when $\lambda_e < 0$, we have stable fixed points and cycles. When $\lambda_e > 0$, we expect to have chaotic attractors.

Let's calculate the Lyapunov exponent for a stable p -cycle containing the point x_0 .

Note that $x_0 = f^p(x_0)$. As the cycle is stable,

$$\left| \frac{d}{dx} f^p|_{x=x_0} \right| < 1$$

Then,

$$\log \left| \frac{d}{dx} f^p|_{x=x_0} \right| < 0$$

We can calculate λ_e .

$$\begin{aligned} \lambda_e &= \lim_{n \rightarrow \infty} \frac{1}{n} \sum_{j=0}^{n-1} \log |f'(x_j)| \\ &= \frac{1}{p} \sum_{j=0}^{p-1} \log |f'(x_j)| \\ &= \frac{1}{p} \log \left| \prod_{j=0}^{p-1} f'(x_j) \right| \\ &= \frac{1}{p} \log \left| \frac{d}{dx} f^p(x_0) \right| && \text{undoing chain rule} \\ &< 0 \end{aligned}$$

where in the last step we have used the result about the stability of the p -cycle.

Note: if the p -cycle is superstable, then $\frac{d}{dx} f^p(x_0) = 0$. Then, $\lambda_e = -\infty$.

The circled region is where the 2-cycle is superstable. The next big dip is where the 4-cycle is stable. We have chaos when $\lambda_e > 1$. The window around 3.8 marks the appearance of the 3-cycle.

These superstable circles and stable cycles give us a strong picture for what the Lyapunov exponent looks like, with these distinctive dips. The chaotic behavior occurs when the Lyapunov exponent is positive.

19.3 Universality

All this time we've been looking at the logistic map. Let's look at a more general class of maps.

Unimodal maps have only one peak.

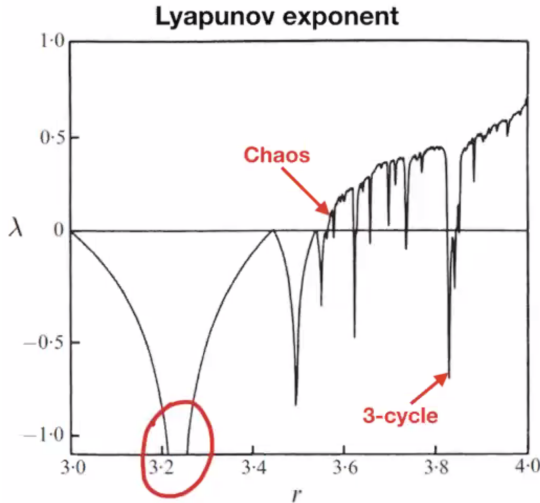


Figure 127: Lyapunov exponent.

A logistic map is unimodal when we look at $0 \leq r \leq 4$, $0 \leq x_n \leq 1$.

The sine map given by $x_{n+1} = r \sin(\pi x_n)$ with $0 \leq r \leq 1$, $0 \leq x_n \leq 1$ is also unimodal.

The maximum value of the logistic map occurs at $x = 1/2$. The maximum value is $r/4$.

The maximum value of the sine map also occurs at $x = 1/2$. The value there is r . This leads to similar, but not identical dynamics. The bifurcation locations are shifted, so while it's quantitatively different, the dynamics are qualitatively quite similar.

There's something called a u -sequence as well that both maps share. As r is varied, the order in which the stable periodic cycles emerge is the same.

Next time, we'll look at r_n , the value of r at which the 2^n -cycle appears. Then

$$\delta = \lim_{n \rightarrow \infty} \frac{r_n - r_{n-1}}{r_{n+1} - r_n}$$

It turns out that $\delta \approx 4.669\dots$ is a mathematical constant for unimodal maps. We'll show where this comes from.

20 November 10, 2020

Today our goal is to understand the structure of the orbital diagram for period-doubling cascades.

We can plot x against r , the bifurcation parameter. Let x_m be the value

of x that maximizes f . Here, f is unimodal with a quadratic peak.

If we have a period-doubling cascade, we get a series of branching bifurcations. We'll call each bifurcation point as r_n , so this is the value of r at which a 2^n -cycle appears.

Let R_n by the value of r at which the 2^n -cycle is superstable. This means that that's where λ , the multiplier, is 0. That means

$$\frac{df^{2^n}}{dx}|_{x_0} = 0 \iff \prod_{j=1}^{2^n} f'(x_j) = 0$$

This means the superstable cycle of a unimodal map always contains x_m , as $f'(x_m) = 0$. That's the only way we can ensure that the product of $f'(x_j)$ is 0.

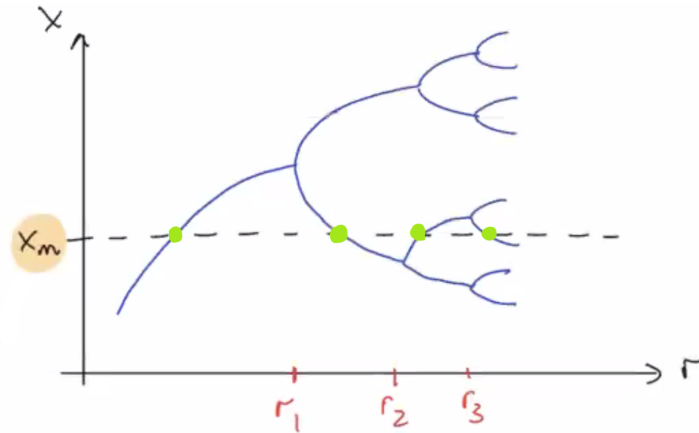


Figure 128: Bifurcation diagram.

So the points marked in green, where the blue curve intersects x_m , are R_0 , R_1 , R_2 , and R_3 . This is where the 1-, 2-, 4-, and 8-cycles are superstable.

20.1 Feigenbaum's observations

For any unimodal map f , we have that

$$\lim_{n \rightarrow \infty} \left[\frac{r_n - r_{n-1}}{r_{n+1} - r_n} \right] = \delta \approx 4.669\dots$$

This δ is called **Feigenbaum's constant**.

So what's going on here? What's this ratio?

The quantity $r_n - r_{n-1}$ is the distance in r between subsequent period-doubling bifurcations. The denominator is a similar quantity. So what

we're seeing is that the distance between the period-doublings gets closer and closer as we keep going.

There's a similar thing with the R_n values.

$$\lim_{n \rightarrow \infty} \left[\frac{R_n - R_{n-1}}{R_{n+1} - R_n} \right] = \delta \approx 4.669 \dots$$

So δ here is a mathematical constant, the same way that π and e are.

Define d_n to be the distance from x_m to the *nearest* point on a 2^n -cycle. The d_n values alternate in sign and shrink in size.

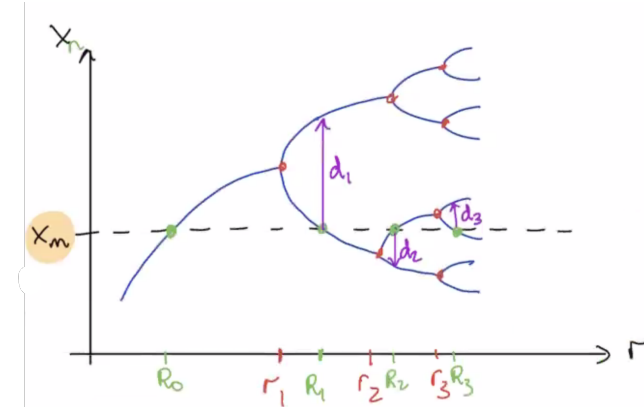


Figure 129: d_n values in purple.

$$\lim_{n \rightarrow \infty} \frac{d_n}{d_{n+1}} \rightarrow \alpha = -2.5029 \dots$$

Here, α is another constant.

Note that $\alpha < -1$ gives us the alternating result, and shrinks d_n as n gets larger, bringing us closer to x_m .

20.2 Feigenbaum's approach

We consider a unimodal map f with a parabolic maximum. That is, $f''(x_m) < 0$ and $f'(x_m) = 0$. Rather than worry about what happens as we vary r , we're going to focus on what happens at the values R_0, R_1, R_2, \dots .

At $r = R_0$, we can plot our map f against x . The fixed point is where f is maximized, because that's where we have our superstable fixed point. See Figure 130.

Next we can plot $r = R_1$. Here, since we've got a 2-cycle, we plot f^2 against x . Here, we have a superstable fixed point at the marked point in red. This is because x_m is contained in all superstable cycles.

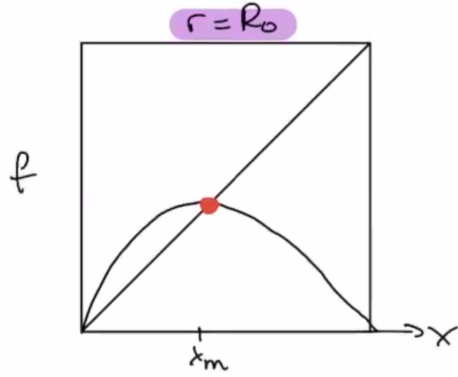


Figure 130: $r = R_0$.

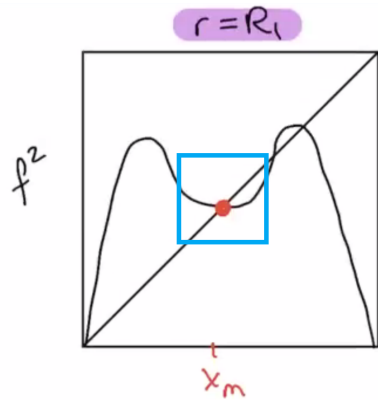


Figure 131: $r = R_1$.

We're going to draw a box around x_m . In that region, we get something that looks quite similar to Figure 130 flipped upside down and shrunk. The important thing is that the qualitative features of the curve inside this box are quite similar to those for f . So we can expect to have similar dynamics in the vicinity of x_m .

The fact that things are the wrong way around and shrunk points to the existence of α . Let's try to derive this.

Our first step is to translate the origin of x to x_m . Consider $x_{n+1} = f(x_n)$.

$$\begin{aligned} x_n &\mapsto x_n - x_m \\ f &\mapsto f - x_n \end{aligned}$$

Now we have $f'(0) = 0$ for our new map.

For $r = R_0$, we can plot $f(x; R_0)$ against x again but after this shift. Then the maximum appears at the origin (our axes are marked with dotted lines). So our fixed point is at the origin.

Now we can draw a smaller box for $r = R_1$, and consider the map

$f^2(x; R_1)$. We'll zoom in around the origin, and we have our superstable fixed point.

We want our second box to look like the first, so we rescale. To do this, we look at

$$\alpha f^2 \left(\frac{x}{\alpha}; R_1 \right)$$

We choose α so that the small box expands and is flipped. This requires $\alpha < -1$.

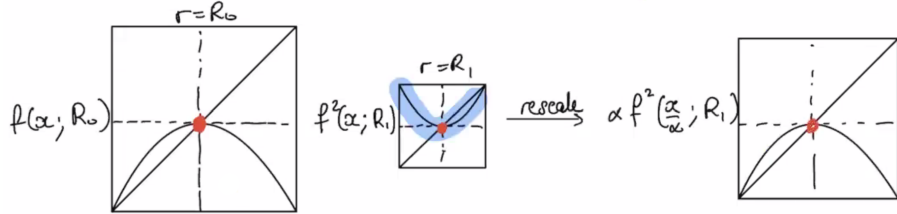


Figure 132: Rescaling.

So the second step is to figure out the rescaling so that

$$f(x; R_0) \approx \alpha f^2 \left(\frac{x}{\alpha}; R_1 \right)$$

where $\alpha \approx -2.5$.

We've gone from investigating superstable fixed points at R_0 to superstable fixed points at R_1 . We can use this same technique to look at 4-cycles.

The third step is to find out how

$$f^2 \left(\frac{x}{\alpha}; R_1 \right) \approx \alpha f^4 \left(\frac{1}{\alpha} \frac{x}{\alpha}; R_2 \right)$$

So here we're stepping from the superstable fixed point of f^2 to that of f^4 .

We can combine this with the first rescaling to link f and f^4 . Then,

$$f(x; R_0) \approx \alpha^2 f^4 \left(\frac{x}{\alpha^2}; R_2 \right)$$

So we can keep going like this. We get a feature that is wholly independent of f .

In the fourth step, we define the **universal function** $g_0(x)$ so that

$$g_0(x) = \lim_{n \rightarrow \infty} \left[\alpha^n f^{2^n} \left(\frac{x}{\alpha^n}; R_n \right) \right]$$

This limit exists for $\alpha = -2.5029 \dots$

Note that g_0 is independent of f , as long as f has a parabolic maximum. Note also that g_0 has a superstable fixed point.

The fifth step is to repeat this process starting at $f(x; R_m)$, which is where we have a superstable 2^m -cycle by definition. If we repeat this procedure, what we end up with is

$$g_m(x) = \lim_{n \rightarrow \infty} \left[\alpha^n f^{2^n} \left(\frac{x}{\alpha^n}; R_{n+m} \right) \right]$$

This is also a universal function, with a superstable 2^m -cycle.

The limiting case is what we look at in step 6, right at the onset of chaos. Let's look at $R_m = R_\infty$. Here, we no longer need to shift r when normalizing. This gives another universal function

$$g(x) = \alpha^2 g^2 \left(\frac{x}{\alpha} \right)$$

Solving this isn't immediately straightforward.

Note that we want $g'(0) = 0$. On the problem set, we'll show that $g'(0) = 1$ without loss of generality. You can then do a power series expansion of g near the origin. This gives the value of α .

This is what g looks like.

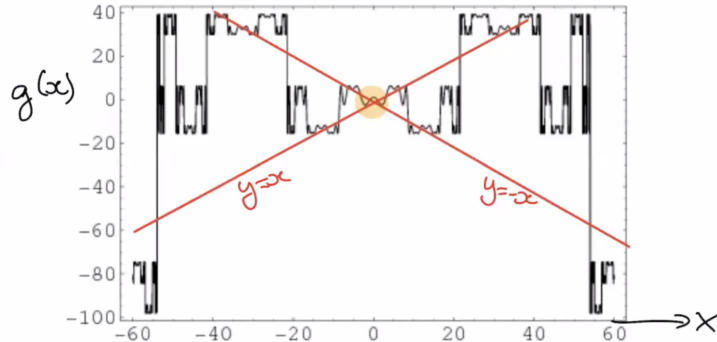


Figure 133: $g(x)$, universal function.

You can see that the parabolic feature at the origin is repeated elsewhere in the function as well. It's quite complicated.

The important takeaway is that there are lots of maps that exhibit similar behavior. If you work through these tests, you get α and δ .

People have done experiments on physical systems and reproduced some of these features and the Feigenbaum ratios. So this is a very robust mechanism for period-doubling.

Over the next few lectures, we're going to look at the fractal structure of chaotic attractors. First we'll look at fractals in general, and discuss

fractal dimension. Then we'll look at how strange attractors form, which has to do with stretching and folding. All of this deals with trying to quantify and characterize what strange attractors really are.

21 November 12, 2020

Fractals are complex geometric shapes with fine structure at arbitrarily small scales. Some fractals will exhibit self-similarity.

Our goal is to understand and describe the fractal nature of strange attractors, using fractal dimension for example.

First, a slight detour.

21.1 Countable and uncountable sets

We'll look at two sets, X and Y . They have the same **cardinality**, or number of elements, if there is an invertible mapping that pairs each element of X with precisely one element of Y . So there has to be a one-to-one correspondence.

If a set X can be put into one-to-one correspondence with the natural numbers $Y = \mathbb{N}$, then X is said to be **countable**. This means we can create a list of the elements of X , like so.

$$X = \{x_1, x_2, x_3, \dots\}$$

Otherwise, X is **uncountable**.

Example.

The set of positive even numbers is countable.

Let $E = \{2, 4, 6, \dots\}$. This is countable because there is an invertible mapping between E and \mathbb{N} – we simply double the elements of \mathbb{N} , or halve the elements of E . So if $n \in \mathbb{N}$, $2n \in E$.

Example.

The set of integers, \mathbb{Z} , is countable.

The fact that we can write \mathbb{Z} as a list $\{0, +1, -1, +2, -2, +3, -3, \dots\}$ means that it is countable.

Example.

The set of positive rationals, \mathbb{Q}^+ , is countable.

A number $p/q \in \mathbb{Q}^+$ if $p, q \in \mathbb{N}$. We're going to try to write down a list of elements in \mathbb{Q}^+ . You can't do this

$$\left\{ 1, \frac{1}{2}, \frac{1}{3}, \frac{1}{4}, \dots, 2, 1, \frac{2}{3}, \dots \right\}$$

because we never finish the fractions with numerator 1 before we get to numerator 2.

Instead, let's make a table where the (p, q) element is p/q .

$$\begin{bmatrix} 1/1 & 1/2 & 1/3 & 1/4 & \dots \\ 2/1 & 2/2 & 2/3 & 2/4 & \dots \\ 3/1 & 3/2 & 3/3 & 3/4 & \dots \\ \vdots & \vdots & \vdots & \vdots & \ddots \end{bmatrix}$$

In order to build our list, we'll weave ingeniously through the elements of this table.

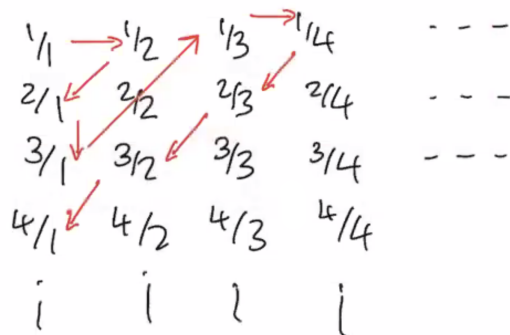


Figure 134: Ordering the rationals.

This process discards duplicates, giving us a list. So the positive rationals are countable.

Example.

The real numbers in the interval $[0, 1]$ form an uncountable set.

Suppose this set is countable. Then we have a list of elements $\{x_1, x_2, \dots\}$. In decimal form, we can write

$$\begin{aligned}x_1 &= 0.x_{11}x_{12}x_{13}\dots \\x_2 &= 0.x_{21}x_{22}x_{23}\dots \\x_3 &= 0.x_{31}x_{32}x_{33}\dots\end{aligned}$$

with $x_{ij} \in \{0, 1, 2, \dots, 9\}$.

Our aim (to show uncountability) is to construct a number $r \in [0, 1]$ not in our list. Then the list is incomplete.

Let $r = 0.\overline{x_{11}x_{22}x_{33}}\dots$. We choose $\overline{x_{nn}}$ to be any number in $\{0, 1, \dots, 9\}$ that is not equal to x_{nn} .

Hence $r \neq x_1$, as the first digits differ. Similarly, $r \neq x_2$ as the second digits differ. For any x_n , $r \neq x_n$ because it differs in the n -th digit.

Then r can't be in the list, so we have a contradiction. Therefore the set of reals in $[0, 1]$ is uncountable.

Note: $1 = 0.999\dots$ Why is this the case?

$$\begin{aligned}0.9 &= 1 - \frac{1}{10} \\0.99 &= 1 - \frac{1}{100} \\0.9999\dots &= 1 - \frac{1}{10^n} \quad \text{if we have } n \text{ 9's}\end{aligned}$$

So $0.999\dots$ recurring is

$$\lim_{n \rightarrow \infty} \left(1 - \frac{1}{10^n}\right) = 1$$

This validates our representation of $x_n \in [0, 1]$ as $0.x_{n1}x_{n2}x_{n3}\dots$

21.2 The Cantor set

Consider the interval $[0, 1]$. We're going to repeatedly break this interval into smaller pieces.

We start with $S_0 = [0, 1]$.

We're going to define S_1 next. To do this, we take S_0 and remove its middle third. This gives us

$$S_1 = \left[0, \frac{1}{3}\right] \cup \left[\frac{2}{3}, 1\right]$$

For S_2 , we'll do the same.

$$S_2 = \left[0, \frac{1}{9}\right] \cup \left[\frac{2}{9}, \frac{1}{3}\right] \cup \left[\frac{2}{3}, \frac{7}{9}\right] \cup \left[\frac{8}{9}, 1\right]$$

We keep going until we get to S_∞ , which is C , the **Cantor set**.

The Cantor set contains infinitely many infinitesimal pieces, separated by different gaps.

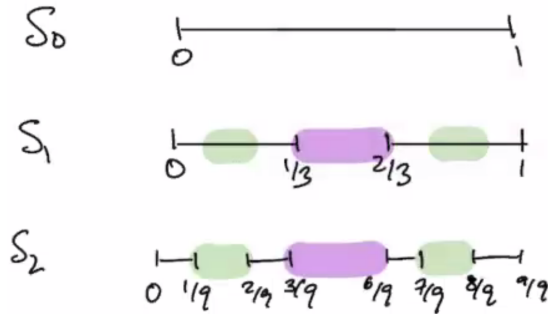


Figure 135: Generating the Cantor set.

What are properties of the Cantor set?

1. *Structure at arbitrarily small scales.* As we zoom in on C , we see more and more structure.
2. *Self-similarity.* Each interval has the middle third removed, so C contains smaller copies of itself (by construction). The left portion of S_{n+1} looks like S_n scaled down by a factor of 3.
3. *Non-integer dimension.* We'll talk about this later!

Other properties of C :

1. C has measure zero. This means we can cover C with intervals whose length is arbitrarily small.
2. C is uncountable.

Why does C have measure 0? $C = S_\infty$ can be covered by S_n for all n . But the length of S_n is $(2/3)^n$, which goes to 0 as $n \rightarrow \infty$.

To show why C is uncountable, note that it contains all points $c \in [0, 1]$ that do not have a 1 in their base-3 (ternary) expansion. If $x \in [0, 1]$, we can write

$$x = \frac{a_1}{3} + \frac{a_2}{9} + \frac{a_3}{27} + \dots = 0.a_1a_2a_3$$

where $a_j = \{0, 1, 2\}$.

In S_1 , the elements between 0 and $1/3$ all have $a_1 = 0$. The elements between $2/3$ and 1 all have $a_1 = 2$. The chunk we remove has $a_1 = 1$. Similarly, for S_2 , we remove the elements with $a_2 = 1$. So the $a_n = 1$ entries are deleted at the S_n stage of constructing C .

Suppose we can list the elements of C as $\{c_1, c_2, c_3, \dots\}$ with

$$c_i = 0.c_{i1}c_{i2}c_{i3}\dots$$

in ternary.

Define $\bar{c} = 0.\bar{c}_{11}\bar{c}_{22}\bar{c}_{33}\dots$. Here, $\bar{c}_{nn} \neq c_{nn}$ and also $\bar{c}_{nn} \neq 1$. This just toggles between 0 and 2.

So \bar{c} is not in our list but is in the Cantor set. Therefore the list is incomplete, and thus C is uncountable.

21.3 Dimension of self-similar fractals

The minimal number of coordinates required to describe every point in the set is the **dimension**. This breaks down for fractals.

Example.

The von Koch curve.

We construct this curve as shown below.

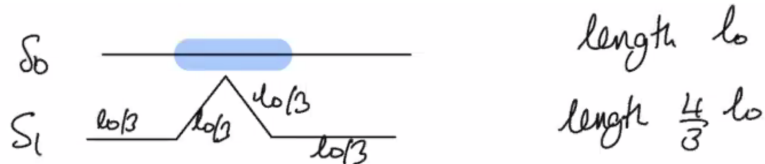


Figure 136: Constructing the von Koch curve.

We replace the middle third of each line segment with an equilateral triangle. $S_\infty = K$, the von Koch curve.

The total arc length is ℓ_∞ .

$$\ell_1 = \frac{4}{3}\ell_0 \quad \ell_2 = \frac{16}{9}\ell_0 \quad \ell_n = \frac{4^n}{3^n}\ell_0$$

So $\ell_n \rightarrow \infty$ as $n \rightarrow \infty$ – the curve has infinite arclength.

The length between any two points on K is infinite, so we expect K to be of dimension greater than 1.

21.4 Similarity dimension

Construct a square of length ℓ . We can reconstruct the square using $m = 4$ squares of length $\ell/2$, where $r = 2$. We can do the same with $m = 9$ and $r = 3$.

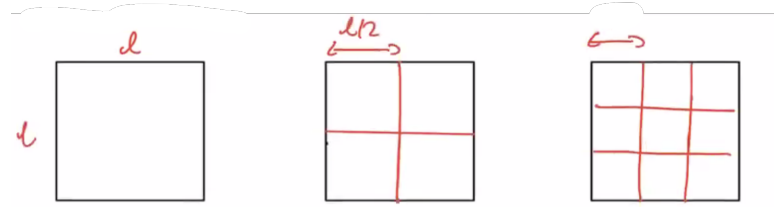


Figure 137: The square.

Note that $m = r^d$, where $d = 2$. The square is composed of m copies of itself and each copy is scaled down by a factor of r .

For a cube, we can construct it from $m = r^d$ copies of itself where $d = 3$.

In general, we consider a self-similar set that is composed of m copies of itself when each copy is scaled down by a factor of r .

The **similarity dimension** d satisfies $m = r^d$.

$$d = \frac{\log m}{\log r}$$

Example.

The Cantor set.

In going from S_n to S_{n+1} , we duplicate and scale down by a factor of 3. So C is composed of $m = 2$ copies of itself, each scaled down by a factor of $r = 3$.

$$d = \frac{\log 2}{\log 3} \approx 0.63$$

Example.

The von Koch curve.

S_{n+1} is comprised of 4 copies of S_n , each scaled down by a factor of 3. Then for K ,

$$d = \frac{\log 4}{\log 3} \approx 1.26$$

$1.26 > 1$, which supports the observation that we end up with infinite length.

Next time we'll look at fractals that aren't self-similar.

22 November 17, 2020

Last time we defined the **similarity dimension**. If a self-similar set is composed of m copies of itself scaled down by a factor of r , then the similarity dimension d satisfies $m = r^d$. Then,

$$d = \frac{\log m}{\log r}$$

22.1 Cantor set – abstraction

A closed set S is called a **topological Cantor set** if the set S satisfies the following two properties.

1. S is *totally disconnected*. All points in S are separated from each other (no intervals).
2. S has no “isolated” points. For any $p \in S$ and for all $\epsilon > 0$, there exist $q \in S$ ($q \neq p$) such that q lies within ϵ of p .

This gives us a paradox – points are spread apart but packed together!

Note that these are topological properties, not geometric – so we can't assume self-similarity here.

22.2 Box dimension

This is used for non-self-similar fractals. Here, we measure the set in a way that ignores irregularities of size less than $\epsilon \rightarrow 0$ and then considers the dependence as $\epsilon \rightarrow 0$.

Let S be a subset of a D -dimensional Euclidean space. Let $N(\epsilon)$ be the *minimum* number of D -dimensional cubes of length ϵ needed to cover S .

We define the **box dimension** d so that we have $N(\epsilon) \propto \epsilon^{-d}$ as $\epsilon \rightarrow 0$.

Then,

$$d = \lim_{\epsilon \rightarrow 0} \frac{\log N(\epsilon)}{\log 1/\epsilon}$$

If we have a smooth curve of length L , $N(\epsilon) \sim L/\epsilon \propto \epsilon^{-1}$ as $\epsilon \rightarrow 0$. So $d = 1$.

If we have an area A , $N(\epsilon) \sim A/\epsilon^2$, so we have $d = 2$.

Example.

The Cantor set.

Note that the set S_n consists of 2^n intervals of length 3^{-n} each. This gives us our N and ϵ – if $\epsilon = 3^{-n}$, we need $N = 2^n$ intervals to cover S_n .

We take the limit $n \rightarrow \infty$ to get the limit $\epsilon \rightarrow 0$.

$$\begin{aligned} d &= \lim_{\epsilon \rightarrow 0} \frac{\log N(\epsilon)}{\log 1/\epsilon} \\ &= \lim_{n \rightarrow \infty} \frac{\log 2^n}{\log 3^n} \\ &= \lim_{n \rightarrow \infty} \frac{n \log 2}{n \log 3} \\ &= \frac{\log 2}{\log 3} \end{aligned}$$

So this agrees with the similarity dimension we calculated last time! We broadened our decision to include non-self-similar sets, but it still works for self-similar ones too.

Example.

A non-self-similar fractal.

We're going to start with a box. We'll take the box and split it up into 9 smaller boxes. Then we'll randomly delete one of them.

Note that S_1 is covered minimally by 8 squares of length $1/3$. Similarly, S_2 is covered by 8^2 squares of length $(1/3)^2$.

So S^n is covered minimally by $N = 8^n$ squares of size $\epsilon = (1/3)^n$. Then the box dimension is

$$d = \lim_{\epsilon \rightarrow 0} \frac{\log N}{\log(1/\epsilon)} = \lim_{n \rightarrow \infty} \frac{\log 8^n}{\log 3^n} = \frac{\log 8}{\log 3}$$

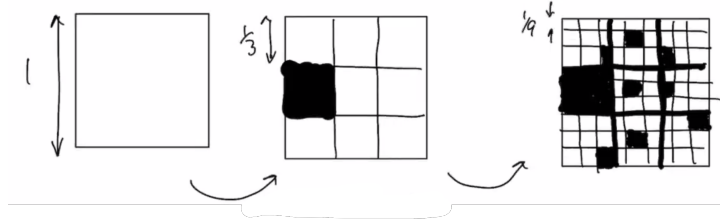


Figure 138: S_0, S_1, S_2 for this fractal.

Note $\log 3 < \log 8 < \log 9 = 2 \log 3$, so $1 < d < 2$. This means we have a non-integer dimension.

There are some downsides to the box dimension. It's difficult to find a minimal covering, and computation often takes a lot of storage space.

An alternative is the **Hausdorff dimension** – this gives us different box sizes and allows overlaps.

22.3 Pointwise and correlation dimension

This has to do with characterizing strange attractors. We can simulate the dynamics on a chaotic attractor and look at the fine structure, and then try to find the fractal dimension.

We pick a point \vec{x} on the attractor A .

Let $N_{\vec{x}}(\epsilon)$ denote the number of points \vec{x}_i on A that lie within a ball of radius ϵ about \vec{x} . The \vec{x}_i points are sampled from the simulation, after we discard the initial transient.

Most of the points in the ball will come from earlier or later portions of the trajectory. Then $N_{\vec{x}}(\epsilon)$ gives a measure of how frequently the trajectory passes within ϵ of \vec{x} .

Then we can find a power law $N_{\vec{x}}(\epsilon) \propto \epsilon^{d_p}$, where d_p is the pointwise dimension of \vec{x} .

To account for variations in $d_p(\vec{x})$ with \vec{x} , we average $N_{\vec{x}}(\epsilon)$ over many \vec{x} . Then we get that the average is

$$C(\epsilon) \propto \epsilon^d$$

where d is the **correlation dimension**.

We can make a plot here. When it plateaus for larger ϵ , we engulf the attractor. At lower ϵ , the only point in the ϵ -ball is \vec{x} itself, so it just approaches 1.

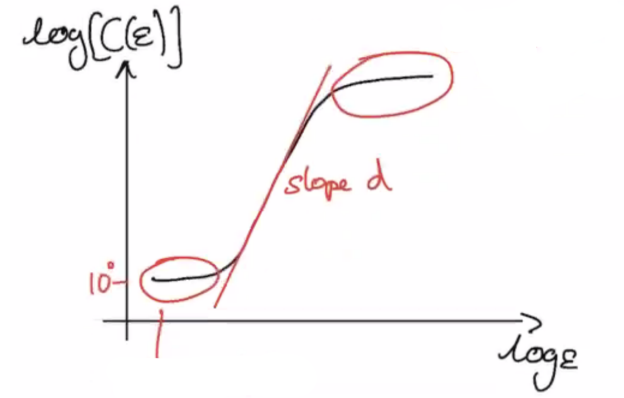


Figure 139: Finding d .

We can find d using a scaling law in the middle region.

The correlation dimension takes account of the density of points on the attractor, whereas in the box dimension all occupied boxes are weighted equally. In general, $d_{\text{correlation}} \leq d_{\text{box}}$.

Example.

Lorenz attractor.

$d_{\text{corr}} = 2.05 \pm 0.01$ in this case. This is a non-integer dimension! This converges rapidly as the number of sampling points \vec{x}_i is increased.

Example.

Logistic map, $x_{n+1} = rx_n(1 - x_n)$.

Recall that we had period-doubling in this map. Consider $r = R_n$, where the 2^n -cycle is superstable. We take all the values on these cycles, and as $n \rightarrow \infty$, they form a topological Cantor set!

The actual fractal emerges at R_∞ , when we have chaos. We can calculate the correlation dimension, and we get $d_{\text{corr}} = 0.500 \pm 0.005$ at $r = r_\infty$.

This is pretty close to 0.5! Recall that $d_{\text{box}} \approx 0.538$, so we have $d_{\text{corr}} \leq d_{\text{box}}$.

Now the question is *why* we get such fractal properties in the first place.

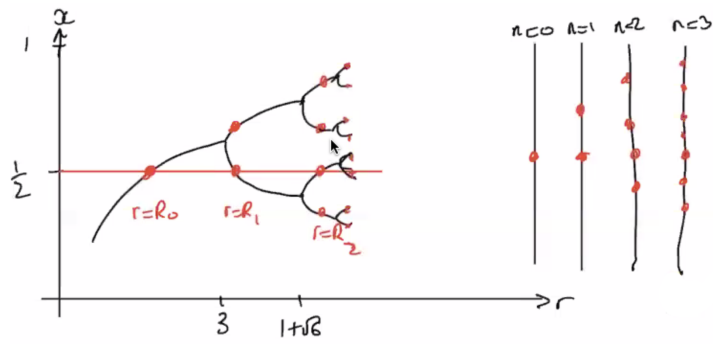


Figure 140: The fractal emerges at the onset of chaos.

22.4 Strange attractors

Why do systems become chaotic? The basic mechanism at play is stretching and folding.

If we start with a blob of initial conditions, stretching (via a positive Lyapunov component) and flattening (via dissipation), changes the shape of the blob.

But there are constraints on this – you can't keep stretching to infinity. This is where folding comes in, because trajectories must remain in a bounded region.

What we end up with after repeating this is a topological Cantor set.

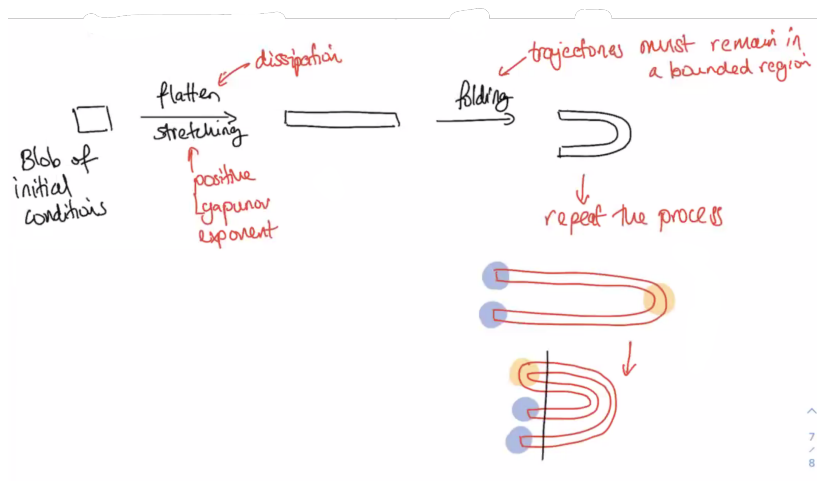


Figure 141: Stretching and folding.

23 November 19, 2020

Today we'll look more at how strange attractors form.

We talked about stretching and folding last time. Stretching occurs due to dissipation and having a positive maximal Lyapunov exponent, and the folding occurs due to confinement of trajectories.

As this repeats, we get a layered fractal structure.

Example.

Baker's map.

$$(x_{n+1}, y_{n+1}) = \begin{cases} (2x_n, ay_n) & 0 \leq x_n \leq 1/2 \\ (2x_n - 1, ay_n + 1/2) & 1/2 \leq x_n \leq 1 \end{cases}$$

Here we have a parameter $a \in (0, 1/2]$. The map transforms $x, y \in [0, 1]^2$ to itself.

We can rewrite

$$(x_{n+1}, y_{n+1}) = (2x_n, ay_n) + \begin{cases} (0, 0) & 0 \leq x_n \leq 1/2 \\ (-1, 1/2) & 1/2 \leq x_n \leq 1 \end{cases}$$

Ignoring the cases, what's happening is that x is getting stretched by 2 and y is getting squeezed by a . The cases shift things by $(-1, 1/2)$. Let's draw a picture and transform it using these rules.

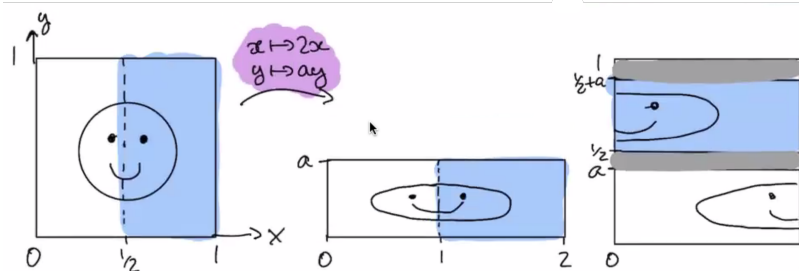


Figure 142: Stretching x and squeezing y , then shifting.

Note that there is a “forbidden region”, marked in grey. As a gets smaller, the forbidden region gets bigger. As we keep iterating, we get more and more grey strips.

Let's consider S as the unit square, and define B as the Baker's map.

Going from S to $B(S)$ gives us the forbidden regions we found in the smiley face example.

When we apply B , again, the whole thing is squished into the region $[0, a]$ and then duplicated on top into the region $[1/2, 1/2 + a]$. Now we have stripes of height a^2 .

$B^3(S)$ has eight strips of height a^3 . It keeps going like this.

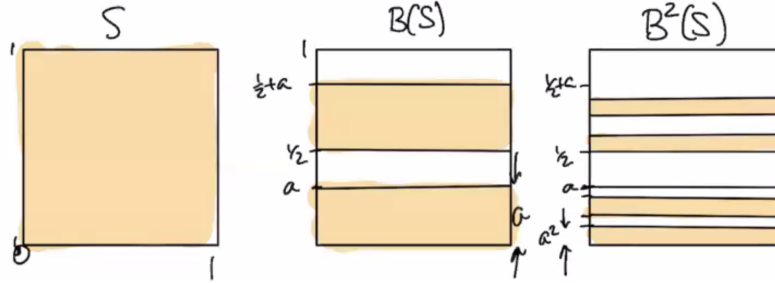


Figure 143: Applying B to S .

$B^n(S)$ consists of 2^n strips each of height a^n . The limit set $A = B^\infty(S)$ is a fractal.

What is the box dimension of A ? For $B^n(s)$, each strip may be covered by $N \sim a^{-n}$ boxes of size $\epsilon = a^n$.

We have 2^n strips, so the total number of boxes $N \sim 2^n a^{-n} \sim (2/a)^n$.

Then the box dimension is

$$d = \lim_{\epsilon \rightarrow 0} \frac{\log N(\epsilon)}{\log 1/\epsilon} = \lim_{n \rightarrow \infty} \frac{\log(2/a)^n}{\log a^{-n}} = \frac{\log(a/2)}{\log a}$$

We can rewrite this as

$$d = \frac{\log a + \log 1/2}{\log a} = 1 + \frac{\log 1/2}{\log a}$$

As $a \rightarrow 1/2$, $d \rightarrow 2$. As $a \rightarrow 0$, $d \rightarrow 1$.

What is the dissipation of this map? For this we look at area contraction. For any region R contained within the unit square,

$$\text{Area}[B(R)] = 2a \times \text{Area}[R] < \text{Area}[R]$$

when $2a < 1$, i.e $a < 1/2$.

If we were to look at the attractor $A = B^\infty(S)$, $\text{Area}[A]$ is $\lim_{n \rightarrow \infty} (2a)^n$. This limit is 0 when $a < 1/2$.

So we have a constant area contraction, which recalls constant volume contraction in the Lorenz system. A consequence of this is that we can't

have any unstable nodes or spirals, because then we would be creating volume. So we cannot have any repelling fixed points of the map B .

Note that area is conserved when $a = 1/2$.

Example.

The Hénon map is a map that has the essential features of the Lorenz system.

$$x_{n+1} = y_n + 1 - ax_n^2$$

$$y_{n+1} = bx_n$$

Here, $-1 < b < 1$ and $a > 0$. The typical parameter values are $a = 1.4$ and $b = 0.3$.

Let's start with a rectangular region. To see the effect of the x_{n+1} mapping, we look at the map $x' = x$, $y' = 1 + y - ax^2$. This turns the horizontal edges of the triangle into parabolas, and leaves the vertical edges unchanged.

Now let's look at the y_{n+1} map. We'll look at $x'' = bx'$, $y'' = y'$. This gives us a contraction.

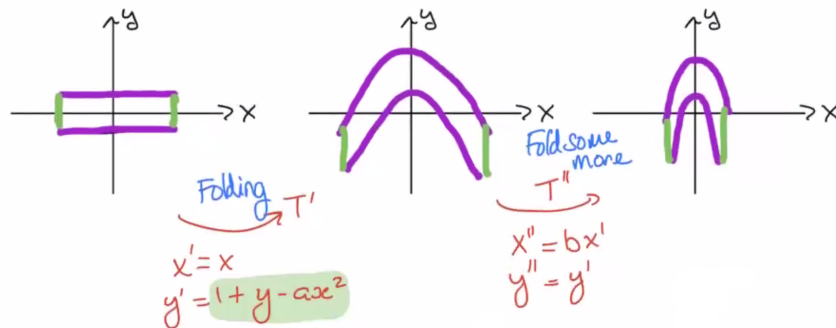


Figure 144: Breaking the map down into pieces.

The final step is to swap the orientation, so that we've done the correct thing to both x and y . For this we use the map $x''' = y''$, and $y''' = x''$. This gives us the result in Figure 145.

So if $(x, y) = (x_n, y_n)$, then $(x''', y''') = (x_{n+1}, y_{n+1})$. So the composition of these three maps is the Hénon map.

Some properties of the map are as follows.

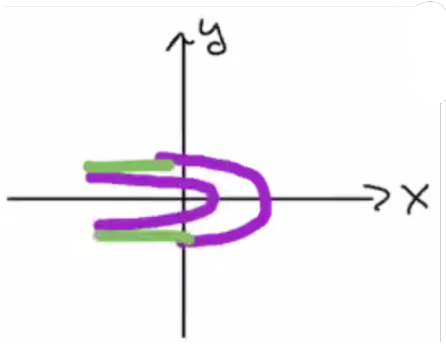


Figure 145: Result.

1. *Invertible.* Given (x_{n+1}, y_{n+1}) , we can find a unique (x_n, y_n) . For $b \neq 0$, the inverted map is

$$x_n = y_{n+1}/b$$

$$y_n = x_{n+1} - 1 + a \left(\frac{y_{n+1}}{b} \right)^2$$

Not all maps are invertible, for example the 1D logistic map.

2. *Dissipative for $-1 < b < 1$.* This means there's a uniform dissipative rate, as in the Lorenz map. If we start with an area $\delta x \delta y$, after applying the map we have an area $|\det J| \delta x \delta y$.

Area contraction happens if $|\det J| < 1$, where J is the Jacobian matrix of the map. For this map,

$$J = \begin{pmatrix} -2az & 1 \\ b & 0 \end{pmatrix}$$

Then, $|\det J| = |b|$, so we have contraction for $-1 < b < 1$, and for all x, y .

3. In certain parameter regimes, there is a trapping region. That is, there exists R so that $T(R) \subset R$, where T represents the Hénon map.
4. Some trajectories can escape to infinity for certain parameter values, due to the quadratic term $-ax_n^2$.

What are the “best” parameter values?

If b is too close to 0, then contraction is too strong and the fine structure becomes invisible. If b is too close to ± 1 , then we do not have sufficient folding. So taking $b = 0.3$ works.

If a is too small or large, then some trajectories can escape to infinity. For intermediate a , there is a period-doubling cascade as a is increased and a

chaotic attractor forms. It turns out that $a = 1.4$ is in the chaotic region for $b = 0.3$.

If we plot the strange attractor, we see self-similarity and fractal structure. Slicing through the curves gives us topological Cantor sets.

24 December 1, 2020

Today we're going to look at attractor reconstruction. What happens when you can't collect data on every variable, and the data you have has noise? Your time series might *look* aperiodic and chaotic, but how can you make a falsifiable argument that it really is?

For example, the Belousov-Zhabotinsky reaction. There's a lot of things we could measure here, but say we look at the bromide ion potential over time. It seems aperiodic, but is it? Can we visualize what the attractor looks like?

24.1 Attractor reconstruction

The aim here is to infer the existence and form of a strange attractor based on limited (and potentially noisy) experimental data. So this is getting into practical applications of dynamical systems.

Suppose we have a time series of just one variable, $B(t)$, in a high-dimensional system. We also have imperfect control over the parameters and actual readings.

We don't want to try taking derivatives of $B(t)$, because taking accurate derivatives of noisy data is incredibly hard. So we can't take the data and plot the usual phase portrait.

But there are embedding theorems that we can use. Instead of looking at $B(t)$, $\dot{B}(t)$, we can look at $B(t)$ and $B(t - T)$. Here, $B(t - T)$ is a time-delayed version of the series by T . We can plot the phase space generated by time delays.

Why does this work instead of the derivative? We can write the derivative as

$$\frac{dB}{dt} \simeq \frac{B(t) - B(t - \delta t)}{\delta t}$$

where δt is small. So \dot{B} is a linear combination of $B(t)$ and a time-delayed version $B(t - \delta t)$, but it's wonky because of noisy data. For very powerful

mathematical reasons, we can extrapolate to $B(t)$ and $B(t - T)$ where T is *not* small, but appreciable – and get more reliable results.

We could also look at multiple delays, so the space

$$\begin{pmatrix} B(t) \\ B(t - T) \\ B(t - 2T) \end{pmatrix}$$

This would be described by an “embedding dimension of 3”.

Aside: For mathematical details of why time delays work, see the Embedding Theorems of Whitney and Takens.

So what happens if you plot these? If you choose T correctly, you get something which, in 2D phase space, looks like an unraveling attractor shape.

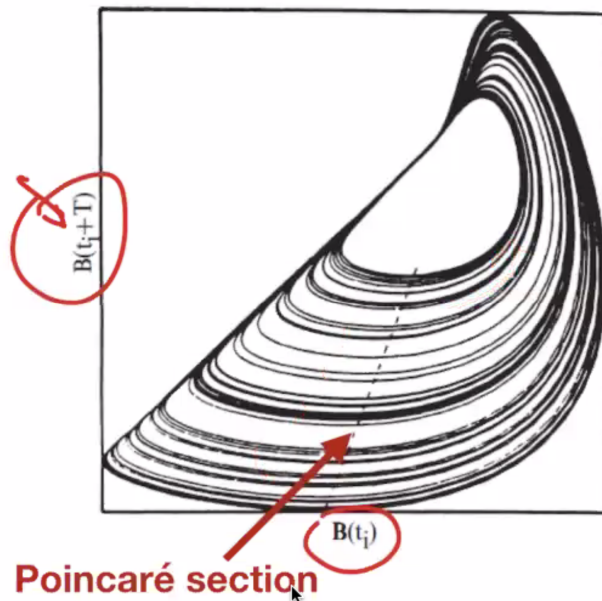


Figure 146: Plotting $B(t)$ and $B(t + T)$.

We've got a **Poincaré section** here (marked with a dotted line). The idea here is that we can choose a line or a plane in our phase space that trajectories pass through. It's good for the Poincaré section to be orthogonal to the trajectories. We can look at the change in the value of $x = B(t + T)$ each time the trajectory passes through the plane. If we had a periodic orbit, it would always be the same. But if it's aperiodic, the value moves. We can plot these x_n values. This gives us something that looks like a unimodal one-dimensional map.

How can we use this to convince a skeptic that we have a chaotic system in

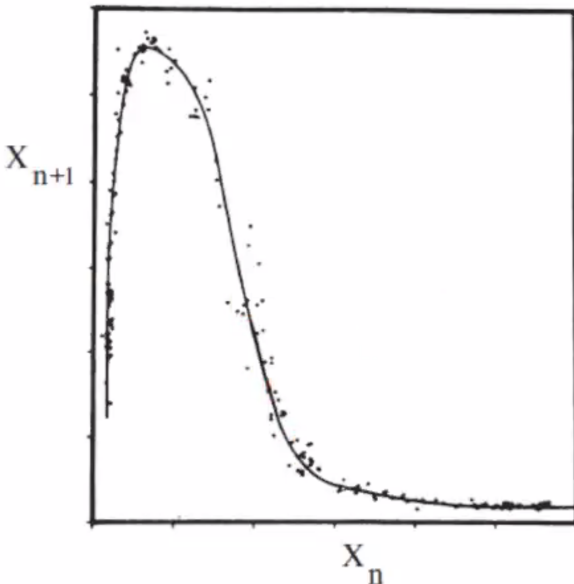


Figure 147: A 1D map?

our data? Can we add any extra evidence? Thirty years ago, people found that varying control parameters created periodic windows like we saw in orbital diagrams earlier. This provided really strong evidence that we were looking at chaotic dynamics, not just super noisy systems or systems with very long periods.

24.2 Practical issues

How do you choose the number of time delays (mathematically speaking, the embedding dimension)? We need enough time delays for the underlying attractor to disentangle itself in phase space.

We don't want to take too many time delays and not be able to visualize the system. So how do you know when you've got enough? To do this, compute the correlation dimension for each embedding dimension. So you can make a plot of these two quantities, and you might get saturation.

On the plot in Figure 148, it looks like 3 is a good value to go with. This is a methodical search, and it relies on the crucial scientific principle of hope.

Once we've picked the number of time delays, we want to pick the actual time delays. We can find the time it takes to go around the attractor. The rule of thumb is to take 10-50% of the mean orbital period around the attractor as T .

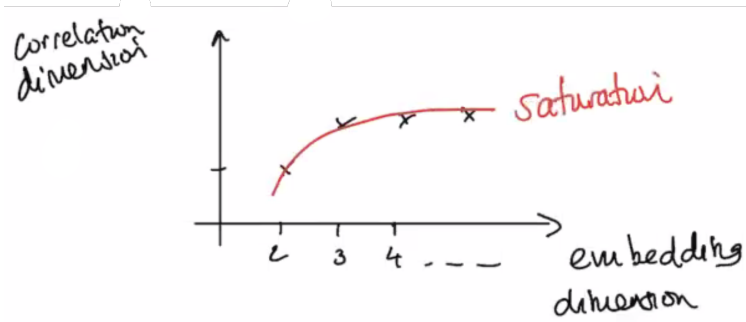


Figure 148: Saturation of correlation dimension.

Example.

Choice of delay time for the time series $x(t) = \sin(t)$.

Our goal is to find the “best” time delay for disentangling the trajectory in phase space

$$\begin{pmatrix} \sin(t) \\ \sin(t+T) \end{pmatrix}$$

If we set $T = 0$, in phase space we lie on the line $y = x$. This is bad, because if we have any noise, we’ll get a narrow band of scattering and we won’t see any structure.

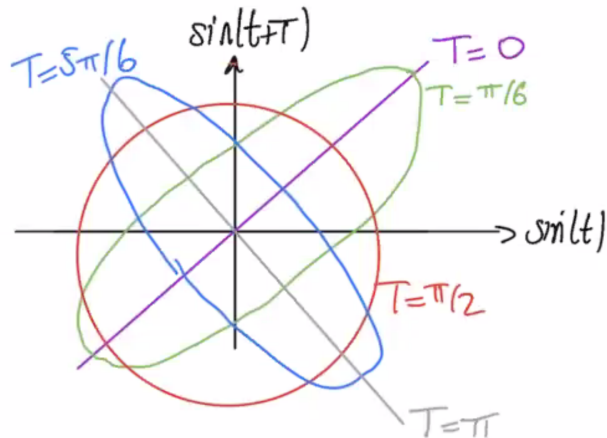


Figure 149: Testing T in phase space.

Let’s try $T = \pi/6$. In this case, we end up getting an ellipse. This is slightly more stretched out, so if we have any noise, the distance means that things overlap less and we can still see structure.

If we take $T = \pi/2$, we get a circle in phase space. This is the ideal case!

We've disentangled so much that we've maximally reduced the effects of one noisy measurement on other measurements.

If we take $T = 5\pi/6$, we're back to an ellipse. We've compressed again, so this isn't good – we're looking at something less open so we're more susceptible to noise.

If we take $T = \pi$, then we're looking at $y = -x$, which is not helpful either.

Note: the period around the attractor is 2π . For this time series, the optimal time delay for the most “open” attractor is $\pi/2$. So our time delay is 25% of the mean orbital period.

24.3 Non-autonomous systems

So far we've been looking at time-autonomous systems, with no explicit time dependence. What about non-autonomous systems? If you run the experiment on Monday, it looks different than on Tuesday. Or there's some sort of periodic driving. In any case, there's explicit time dependence, as below.

$$\frac{dx}{dt} = x(t) + \sin(t)$$

To rewrite this as an autonomous system, we can define two variables.

$$x_1(t) = x(t) \quad x_2(t) = t$$

Then we can write

$$\begin{aligned}\dot{x}_1 &= x_1 + \sin(x_2) \\ \dot{x}_2 &= 1\end{aligned}$$

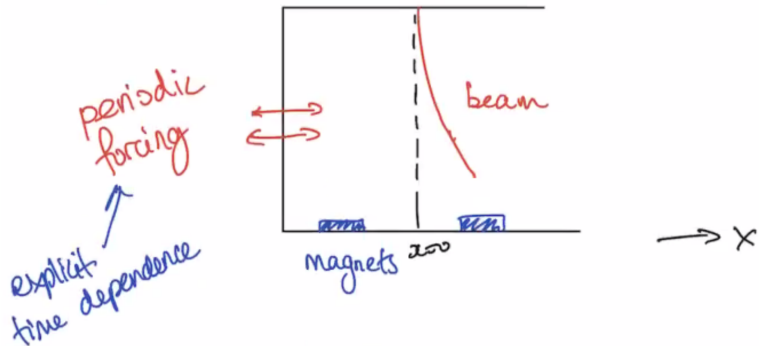
Now we can apply the theory we've been developing all semester. Note, though, that there are no fixed points because $\dot{x}_2 = 1$. So we're always marching on through time, but we could have periodic behavior.

The key thing here is that we're increasing the dimension of our system by 1 in order to make it autonomous again. You can't have chaos in an autonomous 2D system, but if you have explicit time dependence, you *can* have non-autonomous 2D systems that do exhibit chaos.

Example.

Forced double-well oscillator.

We have the setup below with a periodic forcing – this is where the explicit time dependence comes in.



The chaotic behavior is likely to occur when the forces are balanced and the beam is bent through the energy barrier at $x = 0$.

Let's write a mathematical model, using a double-well potential. The magnets are located at the minima of the potential. At $x = 0$, we have a local maximum, and this is a saddle. A slight perturbation either way will send us to one of the minima.

We can write a dimensionless equation.

$$V(x) = \frac{1}{4}x^4 - \frac{1}{2}x^2$$

Recall $m\ddot{x} = -dV/dx$, so we can write

$$\ddot{x} + b\dot{x} + x^3 - x = F \cos(\omega t)$$

We've written our equations in the vibrational frame of reference. Above, the first term is the beam deflection, then a drag term, then the magnets. On the RHS we have an inertial force due to a change of reference. The amplitude of the force is F and its frequency is ω .

This isn't too bad to simulate. We can plot things in the x, \dot{x} plane. But since we've got explicit time dependence, we've also got t as a third dimension. If we only look at two dimensions, we get spaghetti – but if we take advantage of the third dimension, trajectories no longer cross. We'd like to disentangle the dynamics and try to find some structure.

We can ask what our system looks like after evolving over one period of the forcing. This is effectively strobing the system. We can take a series of Poincaré sections along the t axis, spaced $2\pi/\omega$ apart, each parallel to the $x-\dot{x}$ plane.

We end up getting some pretty cool fine-scale structure in the Poincaré section.

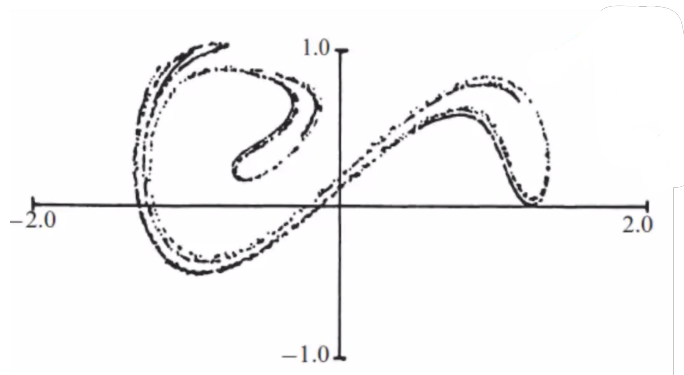


Figure 150: Structure in Poincaré section.

Here's another question – could we have transient chaos in a non-autonomous system?

Yes! It's possible to have erratic behavior before approaching a periodic state near one of the magnets. It appears that whether we end up near one magnet or the other depends on the initial conditions. You could explore the 2D parameter space of initial conditions and color code each point in the plane based on where it ends up in long-term behavior.

This essentially draws the basins of attraction, and you get something very cool like this.

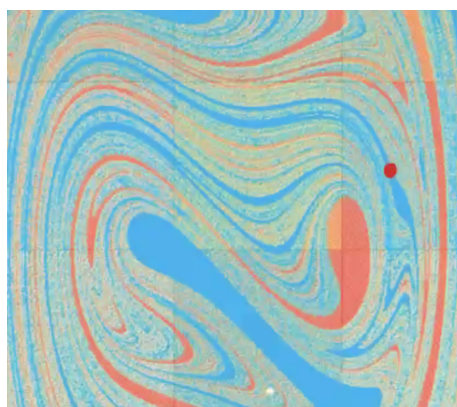


Figure 151: Basins of attraction.

This has fractal structure! Some other interesting systems with this behavior are the forced van der Pol and forced Duffing equations.

25 December 3, 2020

Today we talked about cool things that Matt works on in the intersection of fluid mechanics and dynamics.

1. subcritical Faraday waves
2. bouncing droplets on vertically vibrating baths
3. pilot wave systems